Aus dem

Department für Augenheilkunde Tübingen

Forschungsinstitut für Augenheilkunde

Investigation of complement system dependent inflammatory pathways in retinal pigment epithelium (RPE) cells

Inaugural-Dissertation
zur Erlangung des Doktorgrades
der Medizin

der Medizinischen Fakultät
der Eberhard Karls Universität
zu Tübingen

vorgelegt von

Schmidt, Tiziana Luisa

2022

Dekan:	Professor Dr. B. Pichler
1. Berichterstatter:	Professor Dr. M. Ueffing
2. Berichterstatter:	Professor Dr. K. Schulze-Osthoff
3. Berichterstatter:	Professor Dr. O. Strauß
Tag der Disputation:	26.04.2022

Table of contents

List of figures

List of tables

Abbreviations

µg	microgram
µl	microliter
µM	micromolar
A.U.	arbitrary units
Akt	protein of PI3K/Akt pathway (synonym: protein kinase B)
AMD	age-related macular degeneration
AP	alternative pathway of the complement system
APOE	apolipoprotein E (gene)
ARMS2	age-related maculopathy susceptibility protein 2 (gene)
ARPE19	cell line of retinal pigment epithelium cells
BrM	Bruch's membrane
BSA	bovine serum albumin
C2	complement component 2
C3, C3a, C3b	complement component 3, 3a (anaphylatoxin), 3b
C5, C5a, C5b	complement component 5, 5a (anaphylatoxin), C5b
CAPE	caffeic phenylethyl ester
CCL2	c-c motif chemokine ligand 2 (gene), associated protein: MCP-1
CCP	complement control protein
cDNA	complementary DNA
CETP	cholesteryl ester transfer protein (gene)
CFB	complement factor B (gene)
CFH	complement factor H (gene)
CFI	complement factor I (gene)
CNV	choroidal neovascularization
CO_2	carbon dioxide
COL8A1	collagen type VIII alpha 1 chain (gene)
CP	classical pathway of the complement system
CRP	C-reactive protein
CS	complement system
Ctrl	control
CXCL8	C-X-C motif chemokine ligand 8 (gene), associated protein: IL-8
ddH_2O	ultra-pure water
dH_2O	deionized water
DMEM	Dulbecco's Modified Eagle Medium
DMSO	dimethyl sulfoxide
DNA	deoxyribonucleic acid
dNTP	deoxynukleosidtriphosphate
e.g.	exempli gratia, for example
ECM	extracellular matrix
ERK1/2	extracellular signal-regulated kinases
FB	complement factor B (protein)
FCS	fetal calf serum
FGF	fibroblast growth factor

FH	complement factor H (protein)
FI	complement factor I (protein)
GA	geographic atrophy
GAG	glycosaminoglycans
GM-CSF	granulocyte-macrophage stimulating factor (protein)
GPX1	glutathione peroxidase 1 (gene)
GROα	C-X-C motif chemokine ligand 1 (protein)
GWAS	genome-wide association studies
H_2O_2	hydrogen peroxide
HCS	human complement serum
HS	heparan sulfate
hTERT-RPE1	cell line retinal pigment epithelium cells
HUVEC	human umbilical vein endothelial cells
IGF	insulin-like growth factors
IKK	IκB kinase
IL-1β	interleukin 1β (protein)
IL-18	interleukin 18 (protein)
IL-1a	interleukin 1a (protein)
IL-21	interleukin 21 (protein)
IL-6	interleukin 6 (protein), associated gene: IL6
IL-8	interleukin 8 (protein), associated gene: CXCL8
IL1-ra	interleukin 1 receptor antagonist (protein)
IL6	interleukin 6 (gene), associated protein: IL-6
INFγ	interferon gamma
IRI	renal ischemia reperfusion injury
IκBα	inhibitor of κB
JNK	c-jun N terminal kinase
κB	transcription factor κB (heterodimer of p50/p65)
kDa	kilodalton
LIPC	lipase C (gene)
LP	lectin pathway of the complement system
MAC	membrane attack complex (also known as: C5b-9)
MAPK	mitogen-activated protein kinase
MCP-1	monocyte chemoattractant protein 1, associated gene: CCL2
mCRP	membrane complement regulatory proteins
MDA	malondialdehyde
mg	milligram
MIF	macrophage migration inhibitor (protein)
MIP-1α/-1β	macrophage inflammatory protein 1 alpha/beta, gene: CCL3/CCL4
ml	milliliter
mM	millimolar
mRNA	messenger RNA
mTOR	mechanistic target of rapamycin kinase
MTT	3-(4,5-dimethylthiazol-2-yl)-2,5-diphenyltetrazolium bromide
NF-κB	nuclear factor kappa-light-chain-enhancer of activated B-cells

p	value of probability
p-Akt	phosphorylated Akt
p-ERK	phosphorylated ERK
p-NF-κB	phosphorylated NF-κB (= p-p65)
p38	p38 mitogen-activated protein kinases
p65	subunit of κB transcription factor (see κB)
PARKIN	E3 ubiquitin-protein ligase parkin
PBS	phosphate-buffered saline
PDGF	platelet derived growth factor
PEDF	pigment epithelium derived factor
PGC1α	peroxisome proliferator-activated receptor gamma coactivator 1α
PI3K	phosphatidylinositol-3-kinase
POS	photoreceptor outer segments
PRPL0	ribosomal protein lateral stalk subunit P0
(q-RT)-PCR	(quantitative real-time) polymerase chain reaction
RAGE	receptor of advanced glycation end products
RAP	RAGE antagonist peptide
RELA	nuclear factor NF-κB p65 subunit (gene)
RNA	ribonucleic acid
ROS	reactive oxygen species
RPE	retinal pigment epithelium
RT	room temperature
SCR	short consensus repeats
SDS-PAGE	sodium dodecyl sulfate polyacrylamide gel electrophoresis
SEM	standard error of the mean
Serpin E1	plasminogen activator inhibitor-1 (PAI-1) (protein)
SFM	serum free medium
siCFH	knock-down of *CFH* gene
siNeg	negative control
siRELA	knock-down of RELA gene
siRNA	silencing RNA
SNP	single nucleotide polymorphism
STAT3	signal transducer and activator of transcription 3
TBS (TBST)	tris-buffered saline (with Tween20)
TGF-β	transforming growth factor beta
TIMP3	tissue inhibitor of metalloproteinases 3 (gene)
TNF-α	tumor necrosis factor alpha
V	volt
VEGF	vascular endothelial growth factor
WB	Western blot
Wnt	wingless-related integration site
Y402H	*CFH* polymorphism (base exchange tyrosine Y to histidine H)

1 Introduction

Losing sight constitutes a huge incision in a person's life, its quality and can restrict daily life enormously. A very common disease, which is one of the leading causes of blindness worldwide, is the age-related macular degeneration (AMD). AMD affects mainly the elderly population, as age related changes by themselves represent a risk. It is characterized by a progressive central vision loss, since the macula, the site of sharpest vision, is affected. The exact pathogenesis of this disease is not yet fully understood and is the subject of intense ongoing research. Various risk factors, such as age, lifestyle and genetics are currently stated as possible influencers. So far, therapeutic options are limited, especially with regard to curative approaches. Estimates suggest that by 2040 more than 300 million people worldwide will suffer from AMD (Wong et al. 2014), which once again emphasizes the necessity of suitable therapeutic options.

The following sections are intended to first provide a short, general overview of anatomical structures and physiological conditions in the eye, especially regarding the retinal pigment epithelium (RPE) cell layer, followed by background information on AMD and the current state of knowledge concerning its pathophysiology, with special focus on the topics of inflammation and the complement system.

1.1 Anatomic background of the retina and RPE cell functions

For visual perception in the eye, a complex interplay of different retinal cells is required. The retina is a multi-layered tissue located in the eye's posterior. Under normal conditions, the incoming light stimulus is directly conducted through all the other retinal layers to the photoreceptors, the retinal part that consists of rods and cones and that is responsible for visual phototransduction (Salesse 2017). Although the layer structure of the retina is consistent, there exist some local peculiarities. One of these peculiar regions is the macula, a circular retinal area temporal of the optic nerve, which itself consists of a central region, the fovea,

and is surrounded by a parafoveal and perifoveal zone (Kolb et al. 1995). The fovea of the macula is the region with the highest cone density and thus responsible for central and sharp vision (Kolb et al. 1995).

The photoreceptor cells themselves are located above a single cell layer, called retinal pigment epithelium (RPE), followed by a thin extracellular matrix (ECM), the Bruch's membrane (BrM), which both form the blood-retina barrier and separate the retina from the choriocapillaris layer, containing multiple blood vessels (Curcio and Johnson 2013). Figure 1.1 illustrates this architecture schematically and provides an overview of the main functions of RPE cells.

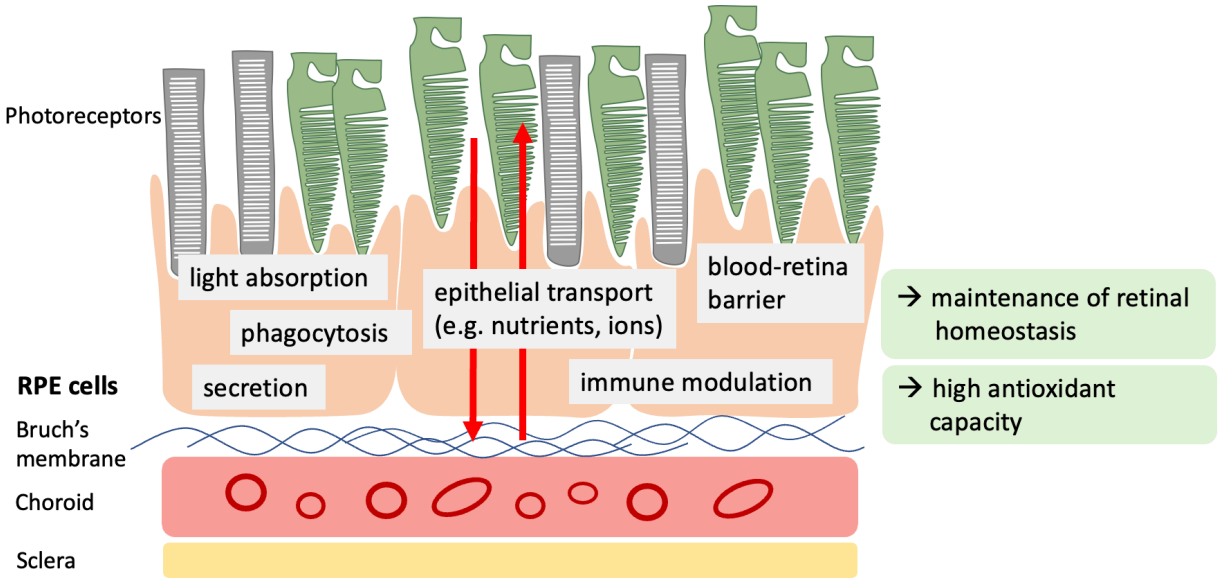

Figure 1.1: **Schematic on RPE cell functions**
Graphical illustration of the different layers of the eye: sclera, choroid (containing blood vessels), Bruch's membrane, RPE cell layer and photoreceptors (=part of the retinal layers). The most important functions of RPE cells are highlighted.

For the maintenance of the retinal homeostasis the RPE cells play a decisive role: forming a blood-retina barrier, RPE cells assume an important function for the supply of the retina (e.g. with oxygen) (Strauss 2005). Further, they are involved in controlling the exchange of molecules in both directions, besides nutrients also for ions and metabolic waste products (Strauss 2005). Moreover, RPE cells are stated to be involved in the visual cycle, light absorption, phagocytosis of the photoreceptor outer segments (POS) and secretion of e.g. growth factors like

FGF, TGF-β, IGF, PDGF, VEGF, PEDF and several interleukins (Strauss 2005). Due to their function and localisation, RPE cells are continuously exposed to high-energy light and photo-oxidative stress and therefore need protective mechanisms against e.g. light-induced reactive oxygen species (ROS). For this purpose, RPE cells are able to absorb and filter the light: this can be achieved through their pigmentation and due to their possession of enzymatic as well as non-enzymatic antioxidant capacities (e.g. superoxide dismutase, carotenoids etc.) (Boulton and Dayhaw-Barker 2001). Moreover, the eye constitutes an immune privileged organ, which is ensured by various features, like e.g. the blood-retina barrier function, the presence of soluble immunomodulatory factors in the aqueous humor, antigen-presenting cells, etc. (Streilein 2003) and enables tight regulatory mechanisms regarding the inflammatory and immune response (Zhou and Caspi 2010). RPE cells seem to participate in this process as well and to possess immunomodulatory functions by creating an immunosuppressive and anti-inflammatory microenvironment (Holtkamp et al. 2001) (Detrick and Hooks 2020). From all the aspects mentioned above, it can be summarized that RPE cells under normal conditions are essential for the functionality of visual processing and the stabilization of the retinal homeostasis.

1.2 Age-related macular degeneration (AMD)

1.2.1 Clinical disease's overview

There are many diseases of the eye that can arise from the structures described above. A particularly common disease, that will be subject of this work, is the age-related macular degeneration (AMD). AMD is a chronical, progressive and degenerative disease, affecting the macula, the cone-dominated, central retinal area that is responsible for high resolution and color vision (Mitchell et al. 2018). Worldwide many people are affected by AMD, especially in the elderly population in industrialized countries: together with cataract, glaucoma and diabetic retinopathy, AMD has become the leading cause of blindness (Bourne et al. 2014; Kocur and Resnikoff 2002).Typical symptoms patients describe are a progressive central visual loss, a decreased visual acuity and contrast perception, as well as

a distorted vision (Mitchell et al. 2018). Clinically, AMD can be divided in early, intermediate and late stages. A hallmark of the disease is the appearance of drusen, protein and lipid rich deposits between the RPE cell layer and BrM (Toomey, Johnson, and Bowes Rickman 2018). Advanced forms of AMD can manifest in two ways: non-neovascular ("dry") and neovascular ("wet") AMD. Whereas dry AMD goes along with an irreversible loss of retinal cells, called geographic atrophy (GA), the neovascular form is characterized by the proliferation of new blood vessels from the choriocapillaris layer (= choroidal neovascularization CNV), which can cause oedema, retinal bleedings and cell damage (Campochiaro 2013). Neovascular forms are often associated with a rapidly progressing course, whereas early AMD stages often occur asymptomatically and progresses gradually (Mitchell et al. 2018). About 10 to 25% of AMD patients are affected by the neovascular form: in these cases, patients may benefit from the injection of VEGF inhibitors, whereas no effective, therapeutic approaches are available for the "dry" form yet (Nowak 2014), implying a great potential with regard to the evaluation of new therapeutic options.

1.2.2 Morphological changes and pathophysiology

With the advancement of age, physiological changes occur in the structure and function of RPE cells, BrM and the choroidal layer, that may be involved in the development of AMD. Concerning the RPE cell layer, pigmentary changes due to an increase in lipofuscin and a decrease in melanin granules were described (Boulton and Dayhaw-Barker 2001). Further, alterations in mitochondrial function and energy metabolism were implicated, potentially making the RPE cells more susceptible towards oxidative stress and leading to a reduced antioxidant capacity (Boulton and Dayhaw-Barker 2001). Bruch's membrane is subject to age related changes as well: BrM is a thin layer of extracellular matrix composed of five layers and consists mainly of collagen, fibronectin and proteoglycans, respectively glycosaminoglycans like heparan sulfate and dermatan sulfate (Curcio and Johnson 2013). With increasing age, BrM thickens (Okubo et al. 1999) and lipids accumulate (Pauleikhoff et al. 1990). The permeability

decreases (Hussain et al. 2010), which on one side negatively affects the nutrient supply of the retina and on the other side impairs the discard of metabolic waste products from the retina to the choroid (Fig. 1.2 C). The main pathophysiological changes are visualized in figure 1.2: while A-B show a healthy retinal structure and physiological conditions of the eye, C-F show the transition from age-related changes in the retina (C) to the development of advanced AMD forms (E, F) (schema of retinal changes with corresponding fundoscopy images). Within the choroid layer, age-related changes appear the following way: the choroid thins out and loses flexibility (Wakatsuki et al. 2015), accompanied by a decreased blood flow (Chirco et al. 2017), which additionally affects the nutrient supply of the retina and RPE cell layer. Furthermore, an increased number of inflammatory cells, such as leukocytes and macrophages, was implied in the choroid (Armento, Ueffing, and Clark 2021) (Ogura et al. 2020).

Besides the changes in the aforementioned cell layers, in the aging process as well as in AMD it also comes to the deposition of extracellular debris between BrM and RPE cells, so-called drusen deposits. Drusen can be found in people without disease value or diagnosed with early AMD (Fig. 1.2D), but a correlation between increasing numbers, distinct variations in size, shape, distribution and advanced forms of AMD has been drawn (Heesterbeek et al. 2020). Drusen thus represent a major hallmark of AMD. The "soft" drusen, which are particularly typical for AMD, consist largely of lipids, but also contain proteins: it has been shown that the protein proportion consists mainly of components of the complement system (FH, FB, C3, C5, C5b-9,), but also of C-reactive protein (CRP) and various immunoglobulins (Toomey, Johnson, and Bowes Rickman 2018), suggesting a role for inflammation and complement system involvement in AMD. It seems that the physiological function (e.g. transport function) of the stated structures is already strongly impaired by age-related changes. Moreover, chronic inflammation and involvement of the complement system seem to occur in the context of AMD: further evidence for these factors playing a major role in AMD’s pathogenesis from a genetic and molecular point of view is provided in separate chapters (see 1.3 and 1.4). In addition, other influencing factors are

discussed: oxidative stress is considered another key factor in the pathogenesis of AMD (Beatty et al. 2000). Due to the high-energy light and the high oxygen consumption, the retina is physiologically exposed to high levels of reactive oxygen species (ROS): with increasing age, however, the protective mechanisms against oxidative stress decline (e.g. decrease in antioxidant capacity), which renders the eye more susceptible towards oxidative injury and thus may contribute to retinal dysfunction (Jarrett and Boulton 2012). Recently, a link between long-term oxidative stress and the induction of inflammation in ARPE19 cells has been implicated (Macchioni et al. 2020) (Datta et al. 2017). However, the impact of the different drivers, like the complement system, inflammation and oxidative stress, on each other still needs to be further clarified: for example, it is still not fully determined which mechanism is altered first and to what extent these factors interact.

With increasing progression, the number of RPE cells declines, which can result in an irreversible vision loss, called geographic atrophy (GA) (Fig. 1.2 E). In the wet form of AMD, there may also be sprouting of new blood vessels from the choroid (= CNV) (Fig. 1.2 F).

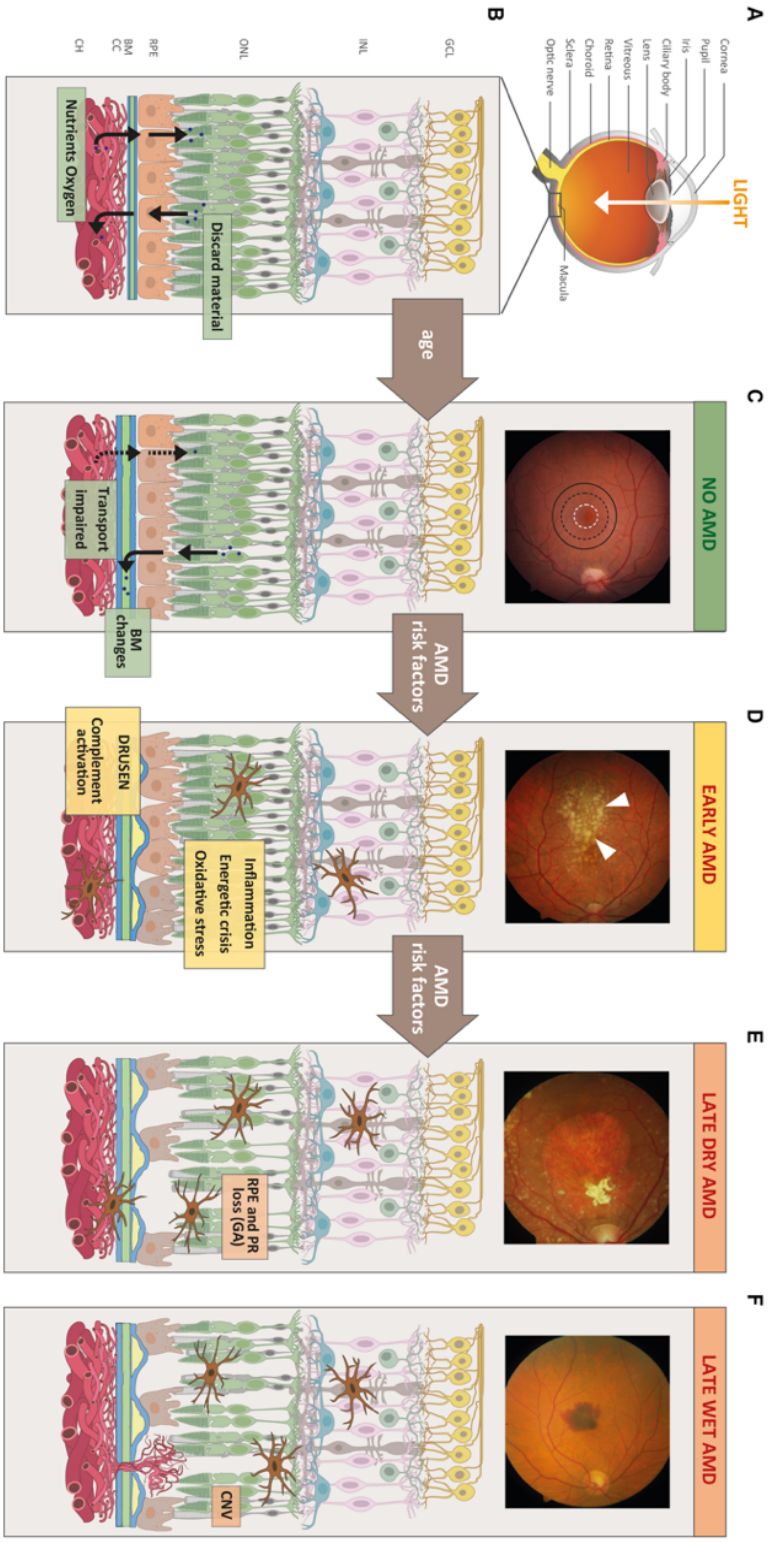

Figure 1.2: Disease stages of AMD with changes in retinal structure and fundoscopy pictures
Reference: Armento, A., Ueffing, M. & Clark, S.J. The complement system in age-related macular degeneration. *Cell. Mol. Life Sci.* (2021). For detailed description see chapter 1.2.2.

1.2.3 Risk factors

So far, many different risk factors are considered to be associated with the appearance and the progression of AMD. The spectrum of the previously identified risk factors includes individual and environmental factors as well as lifestyle and genetic aspects. The influence that these factors have with regard to the individual predisposition to AMD, has not yet been conclusively clarified. The most frequently considered factors are shortly summarized below.

1.2.3.1 Ageing, smoking and lifestyle factors

Already included in the disease's name, a major risk factor is **ageing**. It has been shown that the prevalence of early AMD is strongly increased by age, especially > 70 years old with an overall prevalence of 13.2% (Colijn et al. 2017). **Smoking** constitutes an important environmental risk factor, that - in contrast to aging - is modifiable and preventable: it was shown that active smokers had a higher risk for early AMD as well as for its progression (Klein et al. 2008). Furthermore, it has been investigated, that **obesity** measured in form of a higher body mass index (BMI), a higher waist circumference and a higher waist-hip ratio was associated with an increased risk for AMD progression, whereas physical activity tendentially had beneficial effects (Seddon et al. 2003). Dysbalanced blood lipid levels, such as cholesterol, are also discussed in association with increased risk of AMD (Jonasson et al. 2014). Although obesity can't be equated with an unhealthy, unbalanced and high-fat diet, **nutrition** seems to influence AMD progression: the Mediterranean diet - rich in fruits, vegetables, legumes and fish - has been identified to reduce the risk of developing AMD (Merle et al. 2019).

1.2.3.2 Genetic risk factors

An increased family incidence has been reported in association with AMD, suggesting genetic components to be involved: patients with first-degree relatives suffering from AMD had a lifetime risk of 50% to develop AMD in comparison to controls with a risk of 12% (Klaver et al. 1998). In the past, genome-wide association studies (GWAS) revealed multiple **genetic variants** that are related to AMD. In 2016 researchers identified 34 susceptible loci with 52 common and

rare genetic variants (Fritsche et al. 2016): with this study, already known variants were confirmed and novel variants were designated. Two particularly strongly to AMD linked variants have been identified in genes of *ARMS2/HTRA1* and complement factor H (*CFH*), the latter being examined in more detail below (chapter 1.3). Beside these two, further risk variants were detected in genes involved in the complement system (e.g. *CFB, CFI, C2, C3*), remodeling of the extracellular matrix (e.g. TIMP3, COL8A1) and lipid/cholesterol metabolism (e.g. APOE, CETP, LIPC) (Fritsche et al. 2016) (Armento, Ueffing, and Clark 2021). As can be seen, genetic aspects may constitute a determining role in AMD's context, since several genetic risk variants, distributed over almost all chromosomes, have been identified, which underlines the complex character of this disease (van Lookeren Campagne et al. 2014). However, it is noticeable that many of these alterations have been located in genes of the complement system, pointing it out as a potential and important driver.

1.3 Complement system and the role of FH

1.3.1 Complement system

The complement system is part of the human's humoral innate immune system and represents an important first-line defense mechanism against pathogens (Ricklin et al. 2010). It consists of a proteolytic cascade of more than 30 proteins and can be activated in three different ways. These are shown in figure 1.3: the lectin pathway (LP) is depicted on the left, the classical pathway (CP) in the middle and the alternative pathway (AP) on the right. The LP can be activated by recognition of specific bacterial surface moieties, whereas the CP is initiated by antibody-pathogen immune complexes (Sarma and Ward 2011). In contrast, the AP can be activated spontaneously by hydrolysis of C3 to C3(H_2O) (Pangburn and Müller-Eberhard 1983). This leads in several steps to the formation of the C3(H_2O)Bb complex, which cleaves C3 to C3b, that in turn can associate with factor B (FB) and create more C3 convertase (= C3bBb). This constitutes a significant amplification loop (see also Fig. 1.3). Since this branch can be activated without external stimulus and is active constitutively, continuous control

and tight regulation is mandatory. One of the major regulators and inhibitors of the AP of the complement system, is the complement factor H (FH) protein (van Lookeren Campagne, Strauss, and Yaspan 2016), that will be examined in more detail below. However, all three pathways - once initiated - lead to the activation of a proteolytic cascade with the formation of C3 and C5 convertases, that cleave the complement components into their active forms, C3b and C5b. Graphically, this is presented in figure 1.3 by the convergence of all three pathways to the terminal pathway down below. C3b, besides its amplification function, tags cells for phagocytosis (opsonization) (Thau, Asuka, and Mahajan 2021), whereas the components C3a and C5a function as anaphylatoxins chemoattracting immune cells and amplify inflammatory processes (Peng et al. 2009). The terminal pathway of the complement cascade includes the association of factor C5b with C6-C9, forming the membrane attack complex (MAC), that leads to lysis of the target cells (Morgan 2016).

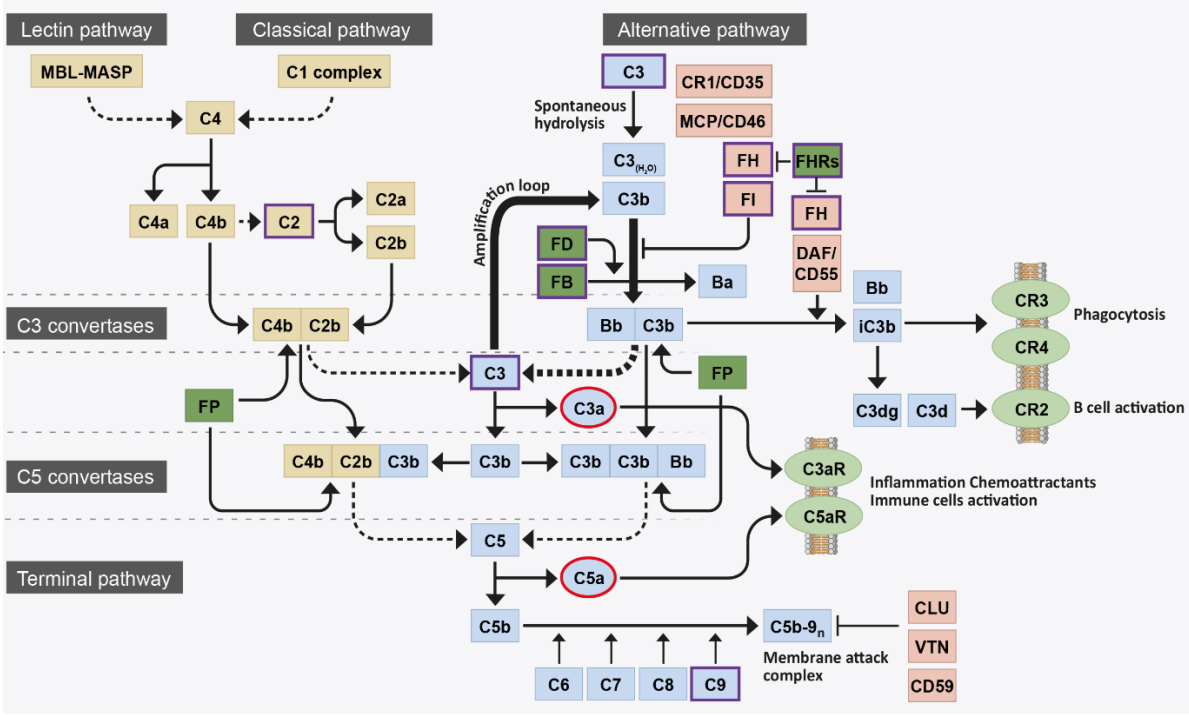

Figure 1.3: Overview on human complement system (CS)
The lectin, classical and alternative pathway are illustrated. Once initiated, the different complement components become cleaved (=cascade). In the end, a membrane attack complex (MAC) C5b-9 is formed, leading to cell lysis of the target cells. CS is part of the human's innate immune system.
Reference: Armento, A., Ueffing, M. & Clark, S.J. The complement system in age-related macular degeneration. *Cell. Mol. Life Sci.* (2021).

1.3.2 Complement factor H (CFH)

Under normal conditions, the *CFH* gene, located on chromosome 1, encodes for factor H (FH), a plasma protein with a molecular weight of 155 kDa, that is an important regulator of the AP and prevents an uncontrolled, excessive activation due to the natural *tick over* mechanism (Toomey, Johnson, and Bowes Rickman 2018). Thereby, the complement regulatory functions of FH can be summarized as follows: (1) FH binds C3b (FH-C3b complexes) and acts as a cofactor for factor I (FI), that can bind to this complex and inactivate C3b by cleavage, (2) FH accelerates the decay of C3 convertase (C3bBb) and (3) prevents C3 convertase assembly (Wu et al. 2009). FH consists of 20 domains, known as complement control protein (CCP) modules or short consensus repeats (SCR) (Ripoche et al. 1988). Over the years, distinguished activities were attributed to the different CCPs: thus, the CCPs 1-4 were found to mediate the above-mentioned complement regulatory activity by binding C3b and FI (Gordon et al. 1995). Other CCPs, 6-8 and 19-20, are known to be involved in binding various other ligands like glycosaminoglycans (GAG), sialic acid, C-reactive protein (CRP) and the oxidative stress marker malonyl dialdehyde (MDA) (Parente et al. 2017). These bonds, especially to GAG and sialic acids, might also contribute to the protection of host tissues from self-induced damage and attack (Wu et al. 2009) (Schmidt et al. 2008), as they are involved in the recognition and the distinction between *self* and *non-self* patterns (Meri and Pangburn 1990).

1.3.3 CFH Y402H polymorphism

In 2005, several research groups identified a variant in the complement factor H gene (*CFH*) to be highly associated with a predisposition for AMD (Edwards et al. 2005) (Haines et al. 2005) (Klein et al. 2005): this variant comprises a non-synonymous single nucleotide polymorphism (SNP) within the *CFH* gene, in which at position 402 the base tyrosine (Y) is exchanged to histidine (H) (“Y402H polymorphism”). Interestingly, this polymorphism is located within CCP7, that is not directly linked to the regulation of the complement system (AP), but associated with the binding sites to several surface proteins and inflammatory

mediators (see 1.3.2.). It could be shown that a binding domain to heparan sulfate (HS), belonging to the GAG family, is located in CCP7 (Blackmore et al. 1996), and that the Y402H polymorphism is linked to a reduced binding affinity to these HS structures (Clark et al. 2006). Further, Clark et al. proposed that the binding of FH to GAG structures like HS and dermatan sulfate (DS) within Bruch's membrane is impaired for the Y402H polymorphism and that this could lead to a dysregulation/overactivation of the complement system and local inflammation, possibly contributing to the development of AMD (Clark et al. 2010) (Clark, Bishop, and Day 2010). Moreover, within the Y402H variant also the binding of FH to CRP (Laine et al. 2007) (Molins et al. 2016) and the oxidative stress marker malondialdehyde (MDA) (Weismann et al. 2011) is affected, which are associated with a decreased binding affinity. For both of these binding partners the impaired binding affinity is discussed to be linked to chronic inflammation, as CRP and MDA unbound both can increase proinflammatory effects (Molins et al. 2016) (Weismann et al. 2011).

1.4 Inflammation in AMD

In previous chapters it has been pointed out that AMD is a multifactorial disease, however, inflammation plays a major role in its pathogenesis. There is evidence of inflammatory processes in a number of locations: RPE cells have been shown to be competent producers of a variety of cytokines due to various stimuli, like TNFα (Elner et al. 1992) or oxidative stress (Macchioni et al. 2020).

In addition, the accumulation of innate immune cells could be shown in subretinal areas (Fletcher 2020). Further, mast cells in the choroid layer have been implicated to be continuously stimulated in the context of RPE cell degeneration and thus may contribute to AMD's progression (Ogura et al. 2020). Moreover, proinflammatory factors have been found in drusen's composition (see 1.3.3).

An important factor that contributes to inflammation is also the complement system, that builds up a link between the innate and adaptive immune system (Walport 2001): complement activation among others can lead to the stimulation and attraction of further immune cells (see 1.3.1). The anaphylatoxins C3a and

C5a for example are known to provide chemoattracting properties and moreover to participate in the modulation of the adaptive immune response (Klos et al. 2009). C3a and C5a have also been described to stimulate monocytes and dendritic cells and are thereby considered to be involved in T cell regulation (Li et al. 2012). In summary, inflammation represents an important part of AMD's pathogenesis, however, it is closely linked to other influencing factors such as oxidative stress and the complement system.

1.5 Signaling pathways involved in AMD

Investigations of signaling pathways in databases, using e.g. microarray gene expression data containing information of RPE/choroid or retinal tissue samples from AMD patients and controls, have revealed multiple pathways to be altered in the context of AMD (Makarev et al. 2014) (Saddala et al. 2020). Signaling pathways involved in inflammatory response, cell survival and proliferation were particularly affected: this comprised for example activation of AKT, MAPK/ERK, STAT3 pathway in RPE/choroid and retinal tissue of AMD patients compared to controls (Makarev et al. 2014). Besides these, also other pathways were identified to be activated, like the mTOR, glucocorticoid signaling pathway (Makarev et al. 2014) or the Wnt pathway in APRE19 cells (Zhou et al. 2010). In association with the Y402H *CFH* polymorphism the NF-κB pathway was discussed to be affected in ARPE19 cells (Cao et al. 2016). In this study, the role of FH dysregulation regarding the activation of the NF-κB, Akt and ERK pathways was investigated in RPE cells. The main focus of this work hereby was on NF-κB signaling: for this reason, this pathway will be described in more detail below. The other signaling pathways (Akt and ERK) will be introduced at the respective result and discussion chapters.

1.5.1 NF-κB signaling pathway

The nuclear factor kappa-light-chain-enhancer of activated B-cells (NF-κB) pathway is known to be an important pathway mediating inflammation and is described in the context of many inflammatory diseases (Tak and Firestein 2001). Besides, NF-κB takes part in the promotion of cell survival, differentiation and

proliferation (Hayden and Ghosh 2008). It can be divided into two branches: canonical and non-canonical NF-κB signaling. Here, the focus will be on the canonical pathway. As illustrated in figure 1.4, there are a number of possible receptors and different stimuli that can activate NF-κB: these include cytokines such as IL-1 or TNFα, but also physical or oxidative stress (Oeckinghaus, Hayden, and Ghosh 2011). Once activated, the IκB kinase (IKK), which consists of three components, phosphorylates the inhibitor of κB (IκBα). As a result, phosphorylated IκBα is ubiquitinated and degraded in the proteasome: this in turn leads to the release of the transcription factor κB, the heterodimer of p50/p65, which translocates into the nucleus and initiates the transcription of NF-κB target genes (Hayden and Ghosh 2008).

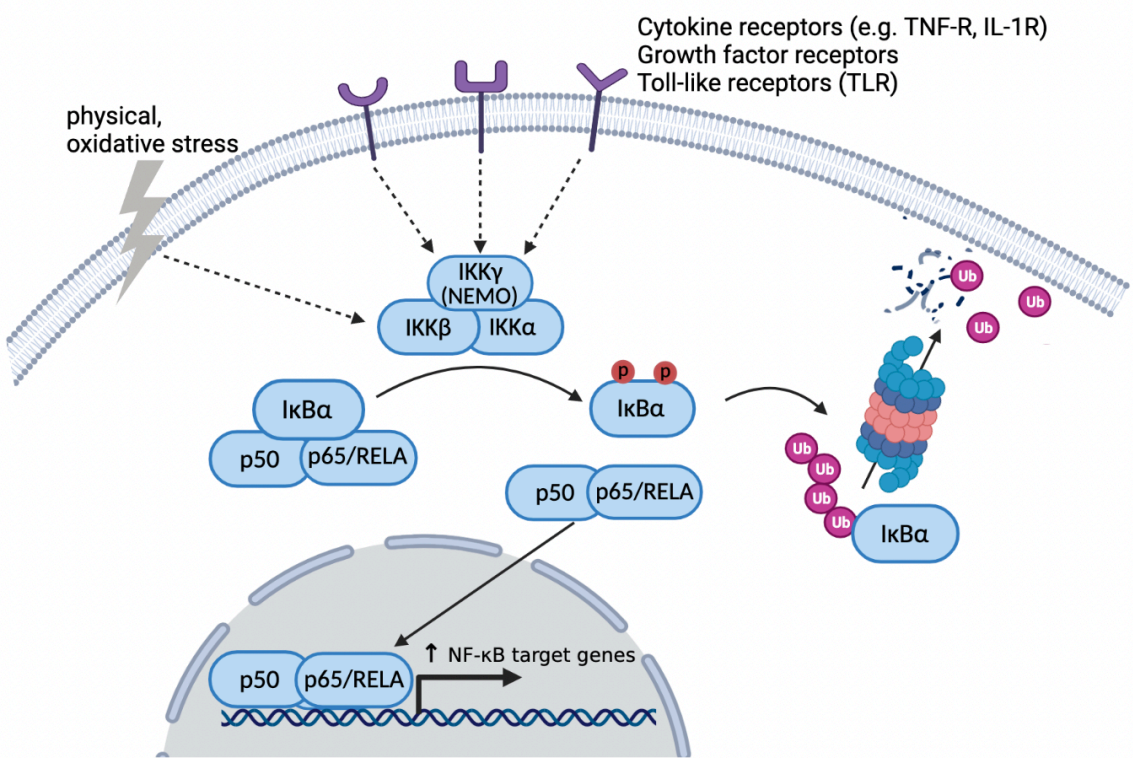

Figure 1.4: NF-κB signaling pathway – simplified schema on the canonical branch
The canonical NF-κB signaling pathway can be activated by different stimuli *via* several receptors (selection shown). Once activated (dotted arrow = multistep process), this leads to an activation of the IκB kinase (IKK), that phosphorylates the inhibitor of κB (IκBα), which consequently is ubiquitinated and degraded in the proteasome. Subsequently, the transcription factor κB, in form of the heterodimer of p50/p65, is released, and can initiate the transcription of typical NF-κB target genes.

1.6 Role of FH in RPE cells – recent studies

In recent studies the role of FH on the antioxidant capacity and on the energy metabolism in RPE cells was investigated (Armento et al. 2020). Therefore, the *CFH* gene was knocked-down in hTERT-RPE1 cells. Under FH loss an increase of C3 at gene and at protein levels was found, which may indicate increased complement activation. Figure 1.5 visualizes the effects of FH (left panel), as well as the alterations detected under FH loss (right panel) in regard to RPE cell metabolism. In order to mimic oxidative injury, the cells were stimulated with hydrogen peroxide (H_2O_2). Peroxide exposure combined with FH loss led to metabolic changes in RPE cells: glycolysis and mitochondrial respiration were reduced, whereas the lipid peroxidation was increased (right panel of Fig. 1.5) (Armento et al. 2020). Transcriptional levels of genes involved in the glucose metabolism and in mitochondrial stability were altered upon H_2O_2 stimulation + *CFH* knock-down.

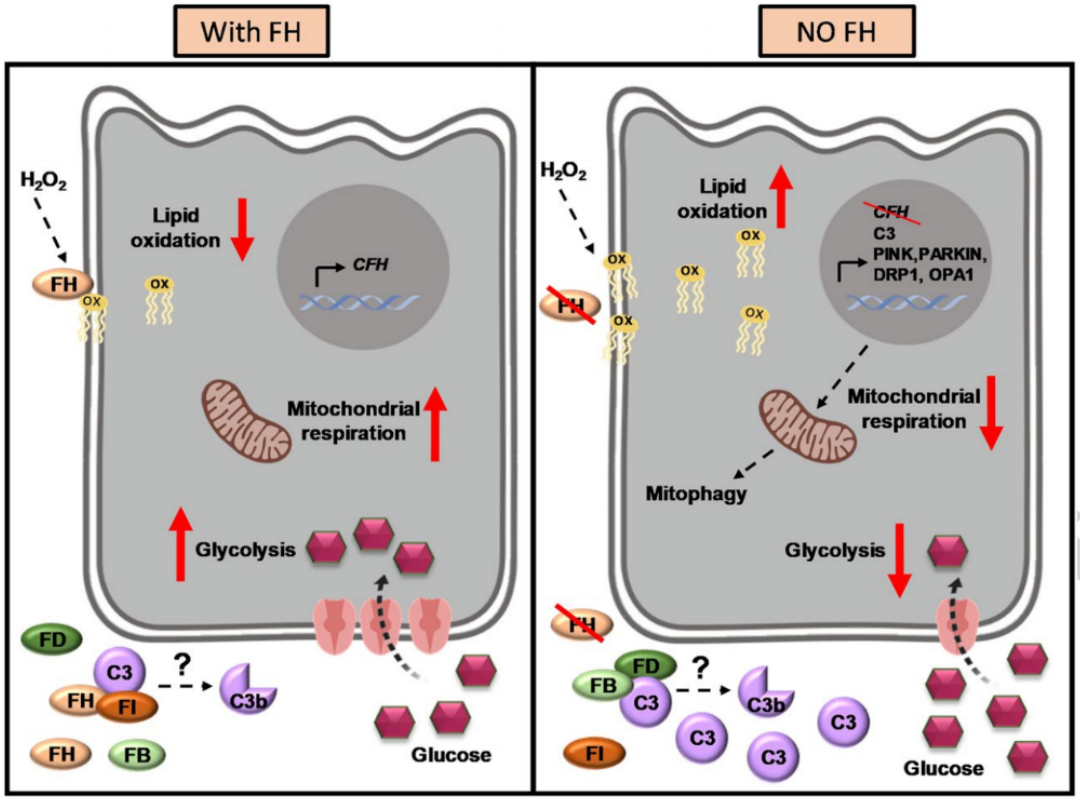

Figure 1.5: Schematic presentation of the effects of FH on the energy metabolism in RPE cells
Reference: Armento, A., Honisch, S., Panagiotakopoulou, V. *et al.* Loss of Complement Factor H impairs antioxidant capacity and energy metabolism of human RPE cells. *Sci Rep* **10,** 10320 (2020).

In the presence of FH peroxide treatment did not result in any of the aforementioned changes (left panel Fig. 1.5). The data suggest that FH has protective properties on RPE cells towards oxidative stress. Further, FH seems to be involved in the transcriptional and metabolic homeostasis of RPE cells, pointing out a novel role of FH (Armento et al. 2020).

1.7 Objective of this study

The aim of this study was to investigate the function of endogenous FH in the regulation of inflammatory processes and the modulation of the complement system in RPE cells. Moreover, an additional objective was to specify the underlying signaling pathways modulated by FH in RPE cells, which may help to understand the contribution of FH dysregulation in AMD pathogenesis.

2 Material and methods

2.1 Chemicals & kits

Deionized water is labelled with dH_2O, ultra-pure water is marked as ddH_2O.

Table 2.1: Chemicals

Chemical	Supplier
2-Propanol p.a.	Honeywell, Germany
Bovine serum albumin (BSA)	Roth, Germany
CAPE	Tocris Bioscience, UK
Chloroform p.a.	Merck, Germany
Complement component C3b	Merck, Germany
Dimethysulfoxid (DMSO)	Roth, Germany
dNTP Mix	Promega, USA
Ethanol p.a.	ITW reagents (AppliChem), Germany
Factor H & Complement component C3	CompTech, USA
Fetal calf serum (FCS)	Sigma-Aldrich, USA
Glycine	Roth, Germany
HCl 25%	Merck, Germany
iTaq Universal SYBR Green Supermix	Bio-Rad, USA
M-MLV Reverse Transcriptase	Promega, USA
M-MLV RT 5x Buffer	Promega, USA
Methanol p.a.	Honeywell, Germany
MG132	Tocris Bioscience, UK
Milk powder	Roth, Germany
Nuclease-free water	Promega, USA
NuPAGE LDS Sample Buffer	Invitrogen, USA
NuPAGE Sample Reducing Agent	Invitrogen, USA
PageRuler Plus Prestained Protein Ladder	ThermoFisher Scientific, USA
PBS	Sigma-Aldrich, USA
Penicillin-Streptomycin	Life Technologies, USA
Pierce ECL Western Blotting Substrate	ThermoFisher Scientific, USA
Pierce IP Lysis Buffer	ThermoFisher Scientific, USA

Protease & Phosphatase Inhibitor Complex 100x	ThermoFisher Scientific, USA
Protein Assay Dye Reagent Concentrate	Bio-Rad, USA
PureZOL	Bio-Rad, USA
RAGE antagonist peptide	Tocris Bioscience, UK
Random Primers	Promega, USA
Roti-Free Stripping buffer	Roth, Germany
Sodium Chloride p.a.	Merck, Germany
Sodium dodecyl sulfate (SDS)	Sigma-Aldrich, USA
Sodium pyruvate	Gibco, USA
Thiazolyl blue (MTT)	Roth, Germany
TriFast	PeqLab Biotechnology, Germany
Tris ultrapure	ITW reagents, Germany
Trypsin-EDTA	Gibco, USA
Tween20	Sigma-Aldrich, USA
Viromer Blue transfection reagent	Lipocalyx, Germany

Table 2.2: Kits

Kits	Supplier
Proteome Profiler Antibody Arrays Human Cytokine Array	R&D Systems, USA Catalog No. ARY005B

2.2 Buffers & media

Table 2.3: Buffers

Name	Ingredients
Blocking solution	5% BSA or non-fat milk in TBST (1x)
Running buffer (10x)	Rotiphorese 10x SDS-PAGE; Roth, Germany
Running buffer (1x)	10% Running buffer (10x) in dH_2O
TBS (10x)	300 mM Tris 1.5 M NaCl in ddH_2O (adjust pH to 7.4 using HCl)

TBST (1x)	10% TBS (10x) 0.1% Tween20 in dH_2O
Transfer buffer (10x)	1.92 M Glycine 250 mM Tris in ddH_2O
Transfer buffer (1x)	10% Transfer buffer (10x) 20% Methanol in dH_2O

Table 2.4: Media

Medium	Supplemented by	Supplier
DMEM with phenol red (cell maintenance)	- Sodium pyruvate 100mM (1%) - Penicillin/Streptomycin (1%) - FCS inactivated (10%)	Sigma, UK
DMEM without phenol red (experiments)	- Sodium pyruvate 100mM (1%) - Penicillin/Streptomycin (1%) - FCS inactivated (10%) - without FCS → **serum-free** (**SFM)**	Gibco, USA

2.3 Equipment & software

Table 2.5: Equipment

Equipment	Name	Supplier
Centrifuge	Heraeus Fresco 21	ThermoFisher Scientific, USA
Centrifuge	Heraeus MultifugeX3R	ThermoFisher Scientific, USA
CO_2 incubator	HeraCell 150i	Heraeus, Germany
Electrophoresis system	XCell *Sure*Lock	Invitrogen, USA
Imaging camera	Fusion FX	Vilber, France
Microplate reader	Spark 10M	Tecan, Switzerland
Microscope	PrimoVert	Zeiss, Germany
Microscope	AXIO	Zeiss, Germany
PCR machine	CFX96 Real-Time System C1000TouchThermal Cycler	Bio-Rad, USA
Platform shaker	Duomax 1030	Heidolph, Germany
Spectrophotometer	Nanodrop ND-1000	ThermoFisher Scientific, USA

Thermo-Shaker	Thermomixer Univortemp	UniversalLabortechnik,Germany
Vortex Mixer	Vortex Genie 2	Scientific industries, USA
Water bath		Memmert, Germany
Western blotting system	Mini-Protean Tetra system	Bio-Rad, USA

Table 2.6: Software

Software	Developer
Excel	Microsoft Corporation, USA
GraphPad Prism 9	GraphPad Software Inc., USA
ImageJ	National Institute of Health, USA (public domain license)
ZEN Imaging Software	Carl Zeiss microcopy GmbH, Germany

Methods

2.4 Cell culture

For all experiments hTERT-RPE1 cells, purchased from the American Type Culture Collection (ATCC), were used and cultured in flasks containing Dulbecco's modified Eagle's medium (DMEM; Sigma, UK), supplemented with 10% inactivated fetal calf serum (FCS), penicillin (100 U/ml) and streptomycin (100 μg/ml). The cells were continuously incubated at 37°C in a humidified atmosphere containing 5% CO_2 and were split two times a week (every 3-4 days). During each passage, the cells were carefully washed with PBS and detached with 0.05% Trypsin-EDTA (Gibco, USA). For the experiments, the cells were used from passage 18-22.

2.5 Experimental setting

Unless stated otherwise the cells were seeded in 12-well plates at a density of 120,000 cells per well and cultivated overnight in DMEM + FCS (Gibco, Germany). Upon reaching a confluency of 60-80% the cells were transfected for 24 h with silencing RNA (siRNA), specific for the complement factor H (*CFH)* gene, the *RELA* (p65 NF-κB subunit) gene or a negative control (siNeg). After silencing, a time period of 48 h followed, with either an incubation time in serum-free medium (SFM) or a treatment with different inhibitors (RAP, MG132, CAPE)

or complement sources (FH, C3, C3b) in either SFM or DMEM + FCS. Since many different setups and timespans were employed, the respective details can be found at the corresponding point in the results section. All experiments were stopped after a total of 48 h and cell pellets as well as cell culture supernatants were collected for further processing.

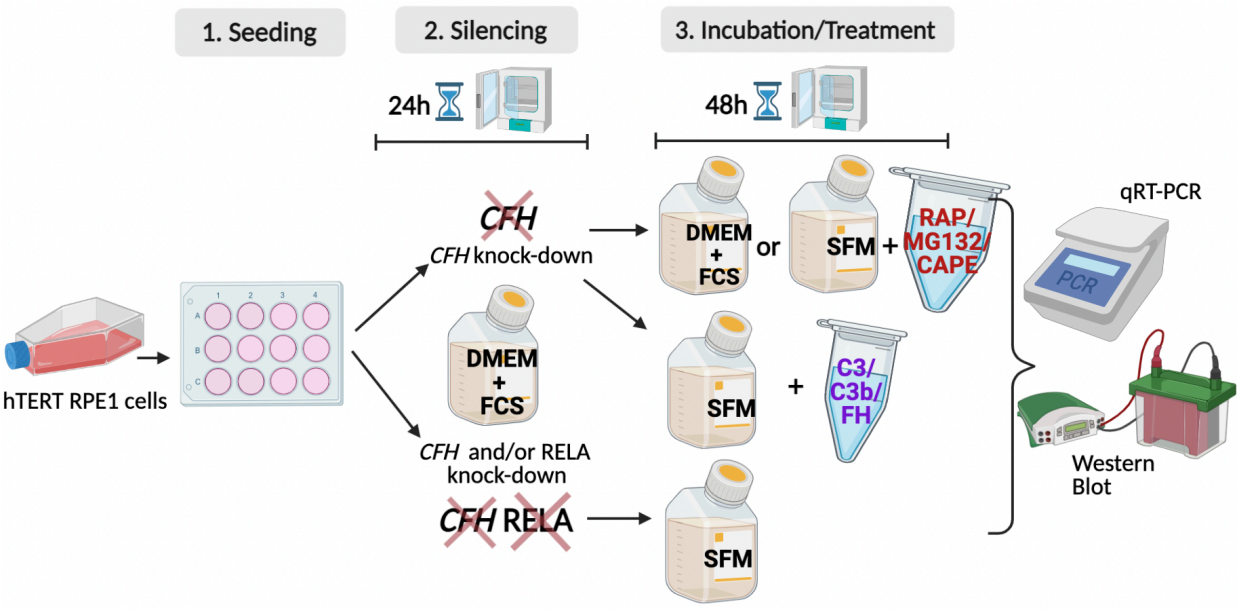

Figure 2.1: Schematic illustration of the different experimental setups
Cells (hTERT-RPE1) were seeded in 12-well plates, cultured overnight and silenced for 24 h with either a negative control (siNeg) or siRNA specific for *CFH* (siCFH) and/or the NF-κB p65 subunit (siRELA). Subsequently, the cells were maintained in the respective medium (DMEM+FCS or SFM) for 48 h. Depending on the setup, the cells were treated with different inhibitors (RAP, MG132, CAPE) or external complement sources (FH, C3, C3b) for different timespans (for exact treatment times, see the respective results section).
For all setups, the experiments were stopped after 48 h and cell pellets and cell supernatants were collected for further processing (Western Blotting, qRT-PCR).Image was acquired with biorender.com

2.6 Cell treatments

2.6.1 siRNA treatment

As mentioned above the cells were transfected one day after seeding upon reaching a confluency of 60-80%. For silencing experiments, the transfection reagent Viromer Blue (Lipocalyx, Germany) was used and mixed with either 3 different double stranded siRNAs, that are specific for *CFH*, 3 specific sequences for *RELA* or a negative control (siNeg), according to the provider's recommendations. For siRNA treatment the medium was changed to fresh

DMEM + FCS, the siRNA mixture was added drop by drop and incubated for 24 h. Concerning the double silenced experiments (siCFH + siRELA) an extra amount of siNeg was added to the single silenced approaches (siNeg, siCFH and siRELA) in order to avoid artifacts and to create comparable conditions. All siRNAs were double stranded and obtained from Integrated DNA technologies (IDT technologies, USA) as listed in table 2.7.

Table 2.7: List of silencing RNAs (siRNA)

siRNA	Supplier	Sequences
Negative control	Integrated DNA technologies (IDT), USA	according to provider's recommendation
CFH	IDT, USA	5´AUCAUGUGAUAAUCCUUAUAUUCCA 3´ 5´AAGUUCUUUCCUGCACUAAUCACAA 3´ 5´AUGGAAAAAUUGUCAGUAGUGCAA 3´
RELA	IDT, USA	5´AUAUGAGACCUUCAAGAGCAUCATG 3´ 5´CUUUCUACUCUGAACUAAUAAAUCT 3´ 5´GCCCAUGGAAUUCCAGUACCUGCCA 3´

2.6.2 Chemical treatment

After transfection, in some experiments a treatment with different substances followed. Therefore, on the one hand, the cells were treated with one of three different chemical inhibitors: RAGE receptor antagonist peptide (RAP), MG132 or caffeic phenylethyl ester (CAPE). All of them were obtained from Tocris Bioscience (UK). RAP was solved in deionized water (dH_2O), whether MG132 and CAPE were solved in dimethyl sulfoxide (DMSO). Experiments were performed using the following concentrations: 2 & 10 μM for RAP, 2 μM for MG132 and 5, 10, 20, 40 μM for CAPE. Control cells (Ctrl) were cultured in the respective medium (DMEM + FCS or SFM), containing an equal concentration of DMSO compared to the corresponding treatment. As part of the optimization process several setups with different incubation times, concentrations and different incubation media have been employed. An overview of the different

setups is provided by figure 2.2. Regardless of whether the treatment time was short or long, all experiments were stopped after 48 h.

On the other hand, the cells were treated for 48 h in SFM with exogenous factor H (FH) or the complement component C3, as well as its cleaved variant C3b. FH was added in a final concentration of 1 μg/ml, C3 and C3b of 100 ng/ml. Complement C3b was purchased from Merck, Germany (No. 204860-250UG), C3 and FH were obtained from CompTech, USA.

Figure 2.2: Overview of different experimental setups (inhibitor treatment with RAP, MG132 or CAPE) Cells (hTERT-RPE1) were seeded, cultured overnight and silenced for 24 h with either a negative control (siNeg) or siRNA specific for *CFH* (siCFH). Subsequently, the cells were incubated in either DMEM + FCS or serum-free medium (SFM) and treated for the indicated timespans with the inhibitors (RAP, MG132, CAPE). All experiments were stopped after 48 h.

2.7 Cell viability

For viability experiments the cells were seeded in 24-well plates at a density of 60,000 cells per well. In order to check cytotoxic effects mediated by the inhibitors MG132 and CAPE a 3-(4,5-dimethylthiazol-2-yl)-2,5-diphenyl-2H-tetrazolium bromide (MTT) assay was performed, determining viability by measuring the metabolic activity. Cells were treated in the same way as already described: after knocking down *CFH* for 24 h, the cells were treated with different concentrations of MG132 and CAPE following the different setups. Viability was assessed after 48 h: the medium was removed, 500 μl of MTT solution (1:10 diluted with SFM) (see table 2.8) was added per well and the plates were placed back in the incubator for 1-2 h. Then the medium was removed again, and the plates were

fully dried. Subsequently, 300 µl of lysis solution (composition see table 2.8) was given to each well. The absorption was directly measured at Spark multimode microplate reader (Tecan, Switzerland) at 590 nm.

Table 2.8: MTT assay solutions

Solution name	Ingredients
MTT stock solution	100 mg Thiazolyl blue (MTT) + 20 ml PBS (pH 7.4)
MTT lysis solution	49.7 ml DMSO + 0.3 ml HCl + 5g SDS

2.8 Protein extraction, SDS-PAGE, Western Blotting

2.8.1 Protein extraction

In order to collect the cell culture supernatants, the cell culture medium was kept in an Eppendorf tube. After centrifugation, the supernatants were precipitated with ice-cold aceton and prepared for Western Blot loading (see below for more details). To collect the cell pellets and proteins, the cells were lysed by addition of 100 µl of lysis buffer (Pierce IP Lysis Buffer; ThermoFisher Scientific, USA) mixed 1:100 with protease and phosphatase inhibitor (Halt Protease & Phosphatase Inhibitor Complex 100x; ThermoFisher Scientific, USA) per well. This was followed by a 20 minute (min) incubation time on the shaker in the cold room (4°C). The lysed cells were scratched off the well and centrifuged at 4°C for 15 min at 13,000 xG. To determine the protein content of each sample, the cell pellet was removed, and the cell lysate supernatants were used subsequently for a Bradford quantification assay. For this 1 µl of sample was diluted in 50 µl of water (dH_2O). After addition of 150 µl 1:5 diluted Bradford reagent (Protein Assay Dye Reagent Concentrate; Bio-Rad, USA) the absorption was measured at 595 nm at the Spark multimode microplate reader (Tecan, Switzerland). The protein content of the samples was set in relation to a calibration line from pipetted BSA samples with different protein content from 0.5 to 10 mg/ml. In order to load 20 µg in a final volume of 25 µl per pocket the calculated amount of sample was dissolved in lysis buffer (1:100 mixed with protease & phosphatase inhibitor) and filled up with NuPAGE LDS Sample Buffer (Invitrogen, USA), mixed 1:10 with

NuPAGE Sample Reducing Agent (Invitrogen, USA). The aceton precipitated cell culture supernatants were solved and resuspended in an equal volume of lysis buffer and NuPAGE LDS Sample Buffer, containing reducing agent (all Invitrogen, USA). All samples were heated to 95°C for 5 min, continuing with the SDS-PAGE.

2.8.2 SDS-PAGE, Western Blotting

All samples were run on 8-16% gels (Invitrogen, USA). Per pocket an amount of 25 µl of sample and 6 µl of marker (PageRuler Plus Prestained Protein Ladder; ThermoFisher Scientific, USA) was loaded. After loading, the gel was run at 120 V for 90 min in 1x running buffer (Rotiphorese SDS PAGE; Roth, Germany) and then immediately transferred onto a polyvinylidene difluoride (PVDF) membrane in 1x transfer buffer for 1 h at 100 V. Once transferred, the membrane was shortly washed in tris-buffered saline with Tween20 (TBST 1x) for 5 min, following 1 h of blocking on a platform shaker at room temperature in either 5% non-fat milk or 5% bovine serum albumin (BSA), both diluted in 1x TBST. Finally, the membrane was incubated in the primary antibody at 4°C overnight. The next day, the membrane was washed three times for 10 min in TBST, followed by a 1 h incubation time at room temperature in the specific secondary HRP-conjugated antibody (Cell Signaling Technologies, USA). This was followed again by a 3 x 10 min wash in TBST. As detection reagent the Pierce ECL-Western Blotting Substrate (ThermoFisher Scientific, USA) was prepared in a 1:1 ratio. Images were acquired with the FusionFX (Vilber Lourmat, France) detection machine, using the automatic modus. Since several antibodies were detected on a membrane, the membrane was incubated in stripping buffer (Roth, Germany) in the water bath for 20 min at 60°C after detection. This was followed by a short wash cycle in water and 2 x 15 min washes in TBST (1x). After blocking at room temperature in 5% non-fat milk or BSA for at least 30 min, the membrane was placed in the new primary antibody to incubate at 4°C overnight. After the last detection the membrane was shortly washed in TBST (1x) and was then frozen at -20°C.

Table 2.9: List of primary antibodies

1° Antibody	Molecular weight (kDa)	Source	Dilution	Buffer	Supplier	Catalog No.
β-actin	45	Mouse	1:2000	5% milk	Cell Signaling	#3700
Complement C3	185	Rabbit	1:1000	5% milk	Invitrogen, ThermoFisher	#PA5-21349
Factor H (FH)	150	Mouse	1:500	5% milk	SantaCruz Biotechnology	sc-166608
p-Akt (Ser473)	60	Rabbit	1:2000	5% BSA	Cell Signaling	#4060
Total Akt	60	Rabbit	1:1000	5% BSA	Cell Signaling	#9272
p-ERK1/2	44, 42	Rabbit	1:2000	5% BSA	Cell Signaling	#4370
Total ERK1/2	44, 42	Rabbit	1:1000	5% BSA	Cell Signaling	#9102
p-NF-κB p65	65	Rabbit	1:1000	5% BSA	Cell Signaling	#3033
Total NF-κB p65	65	Rabbit	1:2000	5% BSA/	Cell Signaling	#8242

Table 2.10: List of secondary antibodies

2° Antibody	Source	Dilution	Supplier	Catalog No.
HRP-conjugated anti-mouse	goat	1:2000	Cell Signaling	#7076
HRP-conjugated anti-rabbit	goat	1:2000	Cell Signaling	#7074

2.9 RNA extraction, cDNA synthesis, quantitative RT-PCR

2.9.1 RNA extraction, cDNA synthesis

Cell culture medium was removed from the wells, kept in an Eppendorf tube and centrifuged. The cell debris was discarded whether supernatants were frozen at -80°C until further processing (e.g. for cytokines array). For RNA extraction 500 μl of either TriFast (PeqLab Biotechnology, Germany) or PureZOL (Bio-Rad Laboratories, USA) were added onto the cells per well. RNA was extracted following the steps recommended in the manufacture's manual. The precipitated, rinsed and dried RNA pellet was resuspended and solved in 20 μl nuclease-free water, before it was boiled at 56°C for 5 min. Subsequently the RNA purity and

concentration were measured by Nanodrop ND-1000 Spectrophotometer (ThermoFisher Scientific, USA). For cDNA synthesis an amount of 1-5 μg of RNA was transcribed into cDNA using M-MLV Reverse Transcriptase (200 U/μl), Random Primers (10 ng/μl), dNTPs (0.5 mM) and M-MLV RT 5x Buffer, all purchased from Promega (USA). The reaction was incubated for 10 min at 25°C, following 60 min at 42°C and 10 min at 72°C. Afterwards the synthesized cDNA was diluted with nuclease-free water in a ratio of 1:100.

2.9.2 Quantitative RT-PCR

According to the manufacturer's instructions (Integrated DNA technologies, USA) the polymerase chain reaction (PCR) primers were diluted to a 100 μM stock solution. 20 μl of both, forward and reverse primer of the respective target gene, were diluted in 160 μl of RNAse free water in order to get a primer mix with a final concentration of 10 μM, that was further used for the PCR. For each well a master-mix out of 7.5 μl iTaq Universal SYBR Green Supermix (Bio-Rad, USA), 1.5 μl from the respective primer-mix and 1 μl of Nuclease-free water was prepared. When performing the PCR 10 μl of the respective master-mix and 5 μl of the diluted cDNA were pipetted into each well. Each sample was pipetted in duplicates. The amplification was run by CFX96^{TM} Real-Time System (Bio-Rad, USA), providing a PCR protocol for a total of 40 cycles. More precisely a cycle comprised: 5 seconds at 95°C (denaturation) and 30 seconds at 57°C (annealing/extension). The gene expression was quantified by first determining the ΔCT ($\Delta CT=CT_{(gene)}-CT_{(housekeeping)}$) value. Then the ΔΔCT ($\Delta\Delta CT=\Delta CT_{(sample)}-\Delta CT_{(control)}$) and foldchange (n-fold= $2^{-\Delta\Delta CT\,(gene)}$) values were calculated. All primer sequences are listed in table 2.11. As housekeeping gene, the ribosomal protein lateral stalk subunit P0 (PRLP0) was used.

Table 2.11: List of qRT-PCR primers

Target gene	Forward primer	Reverse primer
CFH	5´ CTG ATC GCA AGA AAG ACC AGT A 3´	5´ TGG TAG CAC TGA ACG GAA TTA G 3´
CFB	5´ GCT GTG AGA GAG ATG CTC AAT A 3´	5´ GAC TCA CTC CAG TAC AAA G 3´
CFI	5`- TAC TCA CCT CTC CTG CGA TAA- 3´	5`- GGG CAC TGA TAC GGT AGT TTA C -3`
C3	5´ ACG GCC TTT GTT CTC ATC TC 3´	5´ CAA GGA AGT CTC CTG CTT TAG T 3´
C5	5´ CGA TGG AGC CTG CGT TAA TA 3´	5´ CTT GCG ACG ACA CAA CAT TC 3´
CCL2	5´ GGC TGA GAC TAA CCC AGA AAC 3`	5´ GAA TGA AGG TGG CTG CTA TGA 3`
IL6	5´ CCA GGA GAA GAT TCC AAA GAT GTA 3´	5´ CGT CGA GGA TGT ACC GAA TTT 3´
CXCL8	5´ AAA TCT GGC AAC CCT AGT CTG 3´	5´ GTG AGG TAA GAT GGT GGC TAA T 3´
RELA	5´ CTG TCC TTT CTC ATC CCA TCT T 3´	5´ TCC TCT TTC TGC ACC TTG TC 3´
GPX1	5´ CAT CAG GAG AAC GCC AAG AA 3´	5´ GCA CTT CTC GAA GAG CAT GA 3´
PRARGC1A	5´ AGA GCG CCG TGT GAT TTA T 3`	5´ CTC CAT CAT CCC GCA GAT TTA 3´
PARKIN	5´ CCA CAC TAC GCA GAA GAG AAA 3´	5´ GAG ACT CAT GCC CTC AGT TAT G 3´
PRLP0	5´ GGA GAA ACT GCT GCC TCA TAT C 3´	5´ CAG CAG CTG GCA CCT TAT T 3´

2.10 Cytokine array

To better investigate the different expression levels of different cytokines and chemokines in cell culture supernatants, a human cytokine array was performed (Proteome Profiler Human Cytokine Array; R&D Systems, USA). With this it was possible to analyze the relative expression of 36 cytokines and chemokines. The cell culture supernatants were collected from the well-plates when the experiments were stopped (as described above) and after purification from cell debris *via* centrifugation they were frozen at -80°C until further processing. According to the manufacturer's instructions, the membranes were first incubated in blocking buffer (Array buffer 4) for 1 h on an end-to-end shaker. 400 µl of sample was mixed with 500 µl of Array buffer 4, 600 µl of Array buffer 5 and 15 µl of Detection Antibody Cocktail and incubated for 1h at room temperature (RT). After this time, the blocking buffer fluid was fully removed from the membranes and the prepared sample mix was added in the different chambers and incubated at 4°C overnight. The next day, the membranes were washed 3 x 10 min in 1x

washing buffer, and then incubated in diluted Streptavidin-HRP (1:2000 in Array buffer 5) for 30 min shaking at RT. After the incubation, the membranes were washed 3 x 10 min again and then prepared for detection, using the Chemi Reagent Mix (1:1 ratio). The membranes were placed on a plastic sheet protector, the Chemi was added and incubated for 1 min covered with the plastic sheet protector. After drying the membrane carefully with an absorbent wipe, the signals were acquired at the FusionFX detection machine (Vilber Lourmat, France) in the automatic mode and in an individual programmed mode (images with an increasing detection time of 30 s, 1 min, 1.5 min, 2 min, 4 min, 6 min, 10 min). The images were analyzed with the Fusion software and ImageJ measuring the intensity density. For further analysis, the negative control values were subtracted from all samples, before each samples value was divided by the mean value of the positive controls for the respective membrane.

2.11 Statistical Analysis

Data are shown as mean with the standard error of the mean (SEM). The graphs were generated and tested for their significancy with GraphPad Prism 9. The Shapiro-Wilk test was deployed to test normal distribution of the data sets. Provided that a normal distribution was confirmed, an unpaired student's t-test was applied to compare two conditions. Without the data sets normally distributed, the Mann-Whitney test was applied. Values were considered significant with *$p<0.05$, **$p<0.01$, *** $p<0.001$, ****$p<0.0001$

3 Results

Parts of the data presented in this thesis have been published in *The International Journal of Molecular Sciences* under the title *'CFH Loss in Human RPE Cells Leads to Inflammation and Complement System Dysregulation via the NF-κB Pathway'* (Armento, Schmidt et al. 2021). This mainly concerns data of chapter 3.3 and 3.4: a reference can be found at the respective passages.

3.1 Effects of FH loss on inflammation in RPE cells

3.1.1 Effects of FH loss on complement system and cytokines gene expression

In previous studies Armento et al. investigated the effects of FH loss on the cell energy metabolism and antioxidant capacity in RPE cells and established a *CFH* knock-down model in hTERT-RPE1 cells (Armento et al. 2020). For the current experiments the same hTERT-RPE1 cell model was used. Thereby, the levels of endogenous FH in hTERT-RPE1 cells were reduced *via* silencing of the *CFH* gene (siCFH). This condition (siCFH) was compared with hTERT-RPE1 cells transfected with a negative control (siNeg).

The focus of this work was to investigate the inflammatory changes, that arise in the absence of FH, as inflammation is known to play a decisive role in the pathogenesis of AMD (see chapter 1.4). First, we confirmed the efficiency of silencing *CFH* after 48 h, as previously shown (Armento et al. 2020): we detected significantly reduced levels of *CFH* mRNA in siCFH condition by qRT-PCR, reaching a knock-down efficiency of up to 90% (Fig. 3.1 a). Further, we could confirm a significant increase in the gene expression levels of the complement component 3 (*C3*) (Armento et al. 2020) and the complement factor B (*CFB*), both coding for proteins of the alternative pathway of the complement system. Hereby, we observed a 20-fold increase in *C3* levels (Fig. 3.1 b), and a nearly 2-fold increase in *CFB* (Fig. 3.1 c) after 48 h.

In the next step, we investigated the gene expression levels of the inflammatory cytokines, interleukin 6 (IL6) and interleukin 8 (CXCL8), as well as the C-C motif chemokine ligand 2 (CCL2). Here we observed a significant upregulation of both IL6 mRNA (5-fold) (Fig. 3.1 c), as well as CCL2 mRNA levels (2-fold) (Fig. 3.1 d) under FH loss. CXCL8 mRNA levels were tendentially upregulated under *CFH* knock-down.

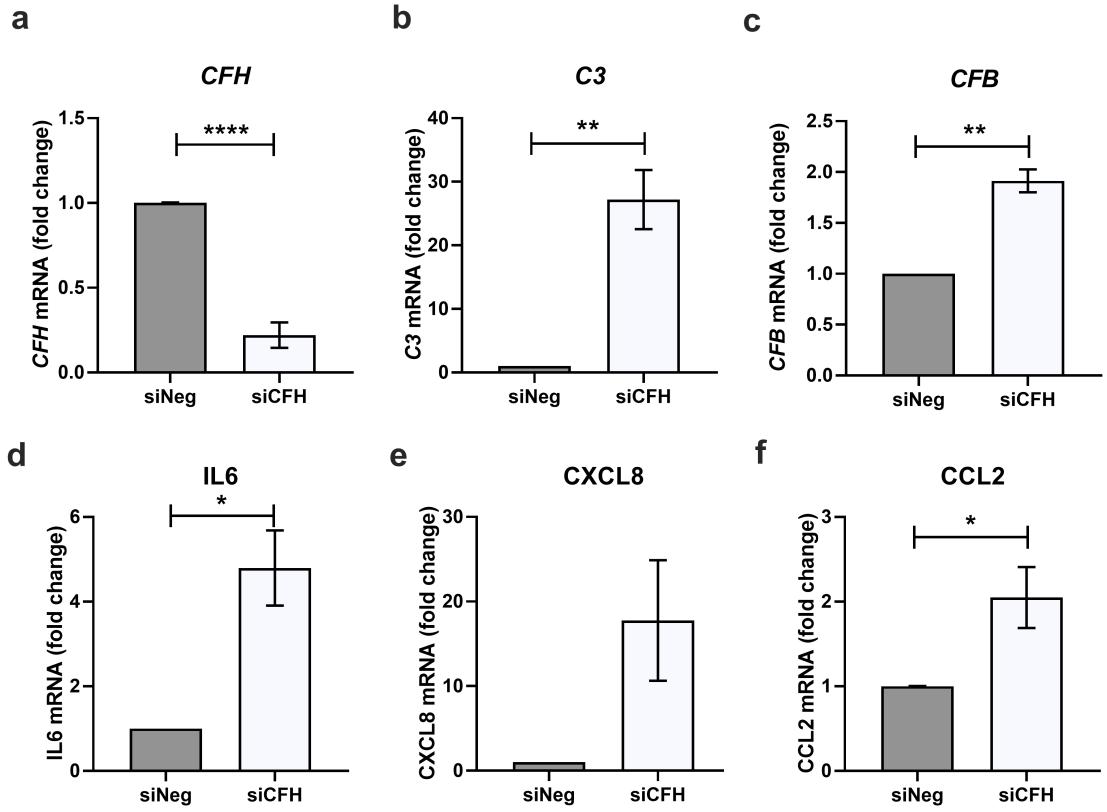

Figure 3.1: Effects of FH loss on the expression levels of complement and inflammatory factors
Cells (hTERT-RPE1) were seeded, cultured overnight and silenced for 24 h with either a negative control (siNeg) or siRNA specific for *CFH* (siCFH). Subsequently, the cells were maintained in serum-free medium (SFM) for 48 h, before collecting cell pellets for further processing.
a-f mRNA analysis on different complement components and cytokines measured by qRT-PCR. Data were normalized to the housekeeping gene PRLP0 and analyzed using the ΔΔCt method. Results are presented as mean ± SEM, n=3-4:
a complement factor H (*CFH*), **b** complement component 3 (*C3*), **c** complement factor B (*CFB*), **d** interleukin-6 (IL6), **e** interleukin-8 (CXCL8), **f** C-C motif chemokine ligand 2 (CCL2).
Significance levels assessed by student's t-test: *p<0.05, **p<0.01, *** p<0.001, ****p<0.0001.

3.1.2 Effects of FH loss on the NF-κB signaling pathway

The NF-κB pathway is considered to be one of the main pathways involved in the inflammatory response in several different cell types (Mitchell, Vargas, and Hoffmann 2016). As we detected a significant increase in inflammatory mediators under FH loss, we checked this pathway by performing a Western Blot (WB) analysis on the NF-κB p65 subunit of cell lysates. Protein levels of phosphorylated p65 (p-p65) - considered the active form that translocates into the nucleus (Christian, Smith, and Carmody 2016) - and levels of total p65 (total-p65) were measured with β-actin used for loading control. Performed WBs showed a strong increase of phosphorylated p65, whereas no major changes were observed in the amount of total p65 in the absence of FH (Fig. 3.2 a). The ratio of phosphorylated to total p65 NF-κB, considered an indicator of NF-κB pathway activation, is graphically shown in figure 3.2 b. Hereby, we found a significant increase in NF-κB activation, as the ratio of the p-p65 to the total-p65 form is consistently around 2-fold elevated in siCFH cells (Fig. 3.2 b).

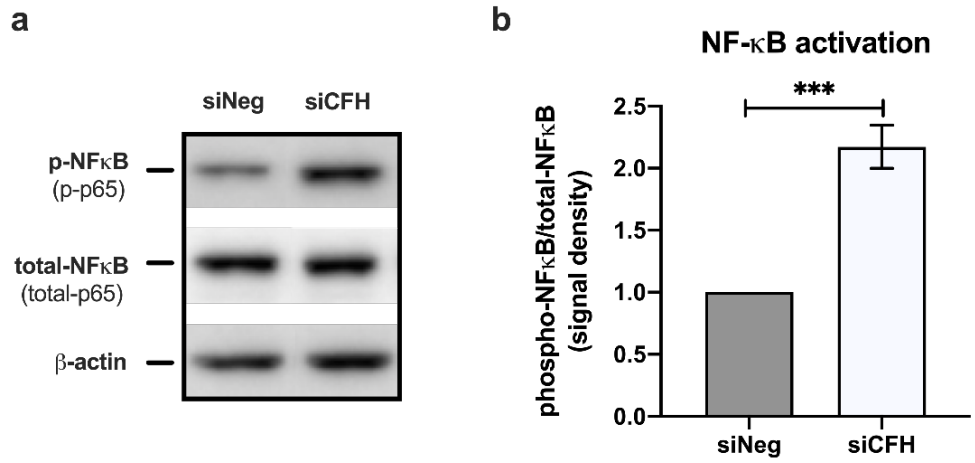

Figure 3.2: Effects of FH loss in RPE cells on NF-κB activation levels
Cells (hTERT-RPE1) were seeded, cultured overnight and silenced for 24 h with either a negative control (siNeg) or siRNA specific for *CFH* (siCFH). Subsequently, the cells were maintained in serum-free medium (SFM) for 48 h, before collecting cell pellets for further processing.
a Western Blot (WB) image on phosphorylated (p-p65) and total levels of the NF-κB p65 subunit in cell lysates after 48 h. Actin as loading control (n=4).
b WB analysis on phosphorylated and total levels of the NF-κB p65 subunit in cell lysates after 48 h. After measuring the signal density, the ratio of p-p65 to total-p65 was calculated. Data show mean ± SEM and are generated from 4 independent experiments (n=4).
Significance levels assessed by student's t-test: **p<0.05, **p<0.01, *** p<0.001, ****p<0.0001.*

3.2 Chemical blockade of NF-κB signaling pathway

Our findings indicate that the NF-κB pathway is activated and therefore may play a role in mediating inflammatory processes in the absence of FH. To further investigate the interactions between the NF-κB pathway, inflammation and complement dysregulation, we designed a series of experiments with the aim to inhibit the NF-κB pathway in either control cells (siNeg) or in the absence of FH (siCFH). In this way, we can examine if the effects mediated by FH loss are directly dependent on this pathway and can conceivably be counteracted by NF-κB blockade. To do so, three different inhibitory chemicals were tested, that are known to interfere at three different levels of the NF-κB pathway. Figure 3.3 shows a simplified schema on the main steps of the canonical NF-κB pathway and visualizes at which points the inhibitors interact.

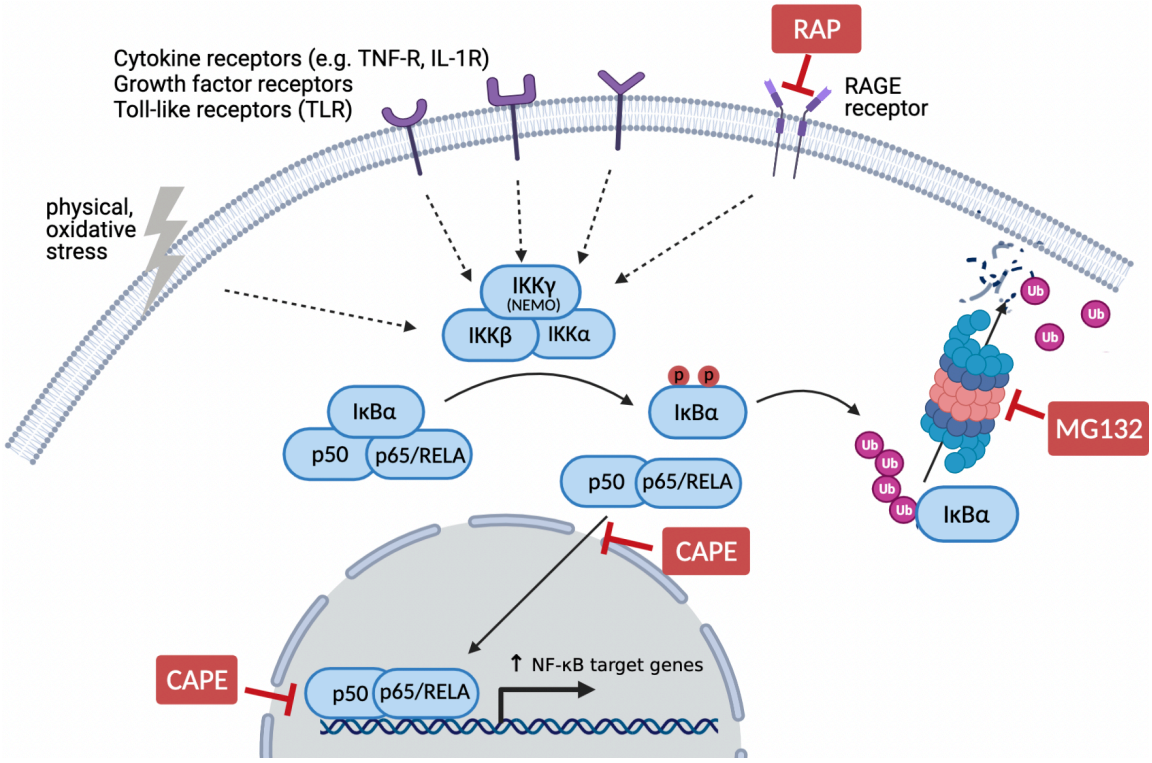

Figure 3.3: Canonical NF-κB pathway (simplified) with interaction points of different inhibitors
The canonical NF-κB signaling pathway can be activated by a wide range of stimuli (only a selection shown). Once activated the IκB kinase (IKK) phosphorylates the IκBα protein, that normally binds and inhibits the p50/p65 heterodimer (= transcription factor). Phosphorylation of IκBα leads to its degradation in the proteasome. As a consequence, the dimer of p50/p65 is released, can translocate into the nucleus and initiate the transcription of NF-κB target genes. Inhibitors that were used: (1) RAP (RAGE antagonist peptide) = prevents interaction of RAGE receptor and its ligands; (2) MG132 = inhibits the proteasome and prevents degradation of IκBα; (3) caffeic phenylethylester (CAPE) = prevents the translocation of p65 into the nucleus and its DNA binding.

3.2.1 RAGE antagonist peptide (RAP)

The first inhibitor that was tested, is the RAGE (receptor for advanced glycation end products) antagonist peptide (RAP). RAP acts as a competitive antagonist to the RAGE receptor and can prevent the interaction between the receptor and its ligands (Arumugam et al. 2012). The RAGE receptor is present in RPE cells and found to be elevated near basal drusen deposits in RPE cells of AMD patients (Yamada et al. 2006), underlining the potential role in AMD pathogenesis and disease progression (Howes et al. 2004). Supportively, the RAGE receptor is known to promote inflammation *via* several pathways, including activation of the NF-κB pathway (Tóbon-Velasco, Cuevas, and Torres-Ramos 2014). It was found that a stable signaling of the receptor requires the formation of RAGE-Heparan sulfate (HS) complexes (Xu et al. 2013). Interestingly, FH is a known interactor of HS and this interaction is impaired in the high-risk FH variant H402 associated with a reduced binding affinity to HS (see chapter 1.3.3). We therefore hypothesized that *CFH* might modulate the NF-κB pathway *via* RAGE receptor - HS interfering and we wanted to investigate this linkage by using RAP (hypothesis see Fig. 3.4 a).

Preliminary experiments with the addition of RAP revealed no cytotoxic effect or any impact on cell growth, as shown in figure 3.4 b. According to literature, two different concentrations of RAP were chosen, 2 μM and 10 μM. As part of the optimization process, we used these two concentrations in two different setups: 1) an inhibition time of 48 h in SFM (48 h SFM) or 2) a short inhibition time of 4 h in DMEM + FCS followed by an incubation for 44 h in SFM (4 h DMEM/FCS + 44 h SFM). Investigations on NF-κB activation on these setups and concentrations revealed no inhibitory effect, as WB analyses measuring levels of p-p65 and total-p65 showed no differences.

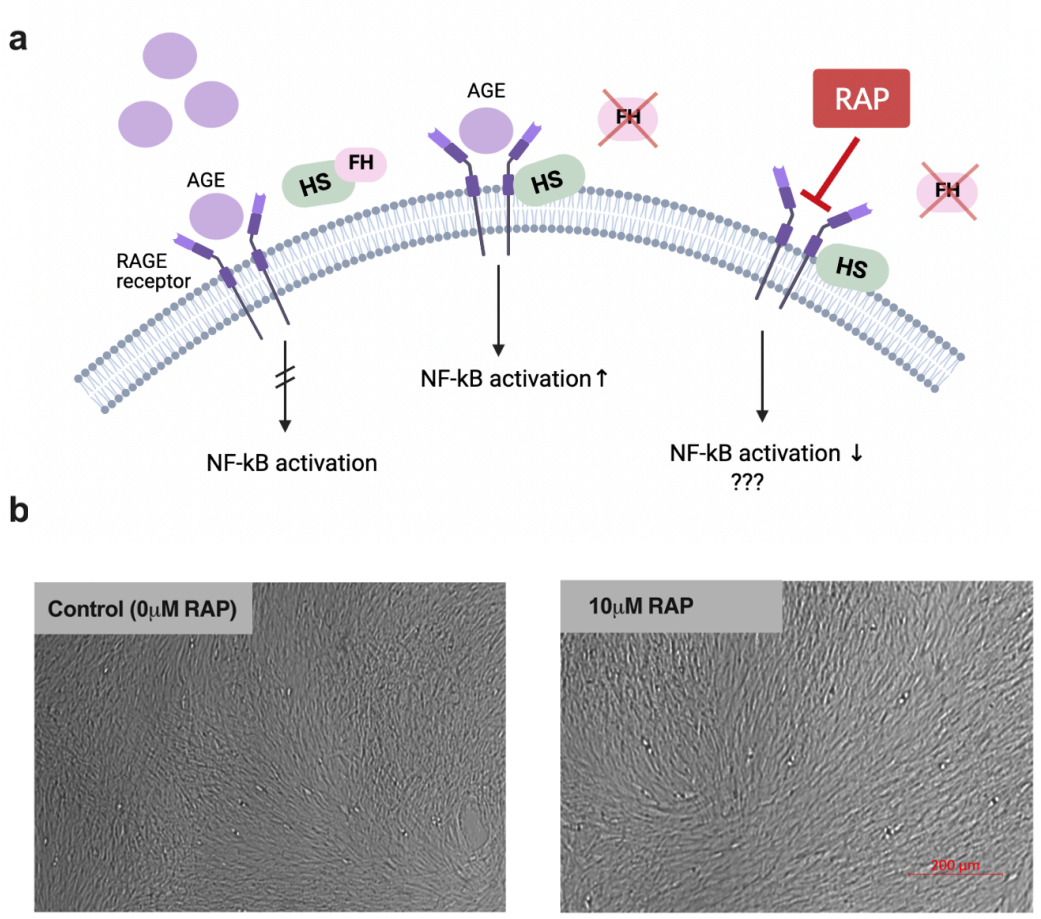

Figure 3.4: Effect of RAGE antagonist peptide (RAP)
a Hypothesis of how impaired function of FH might lead to NF-κB activation *via* RAGE receptor mediated signaling. RAGE receptor = receptor for advanced glycation endproducts; AGE = advanced glycosylation end products; HS = heparan sulfate; FH = complement factor H protein; RAP = RAGE antagonist peptide (Note: strongly simplified facts).
b Images of RPE cells were acquired with ZEISS AXIO microscope (4x magnification). Cells were seeded, left to attach overnight and then treated with the indicated concentration of RAP for 48 h in serum free medium (SFM).

We therefore modified the experimental setups to 1) a 48 h inhibition in DMEM + FCS (48 h DMEM/FCS) and 2) a 4 h inhibition following a 44 h incubation in SFM (44 h + 4 h SFM) with a concentration of 10 μM RAP. Here, too, the addition of RAP did not cause any changes in the levels of NF-κB activation measured *via* WB either in siNeg nor in siCFH condition (Fig. 3.5 a-b).

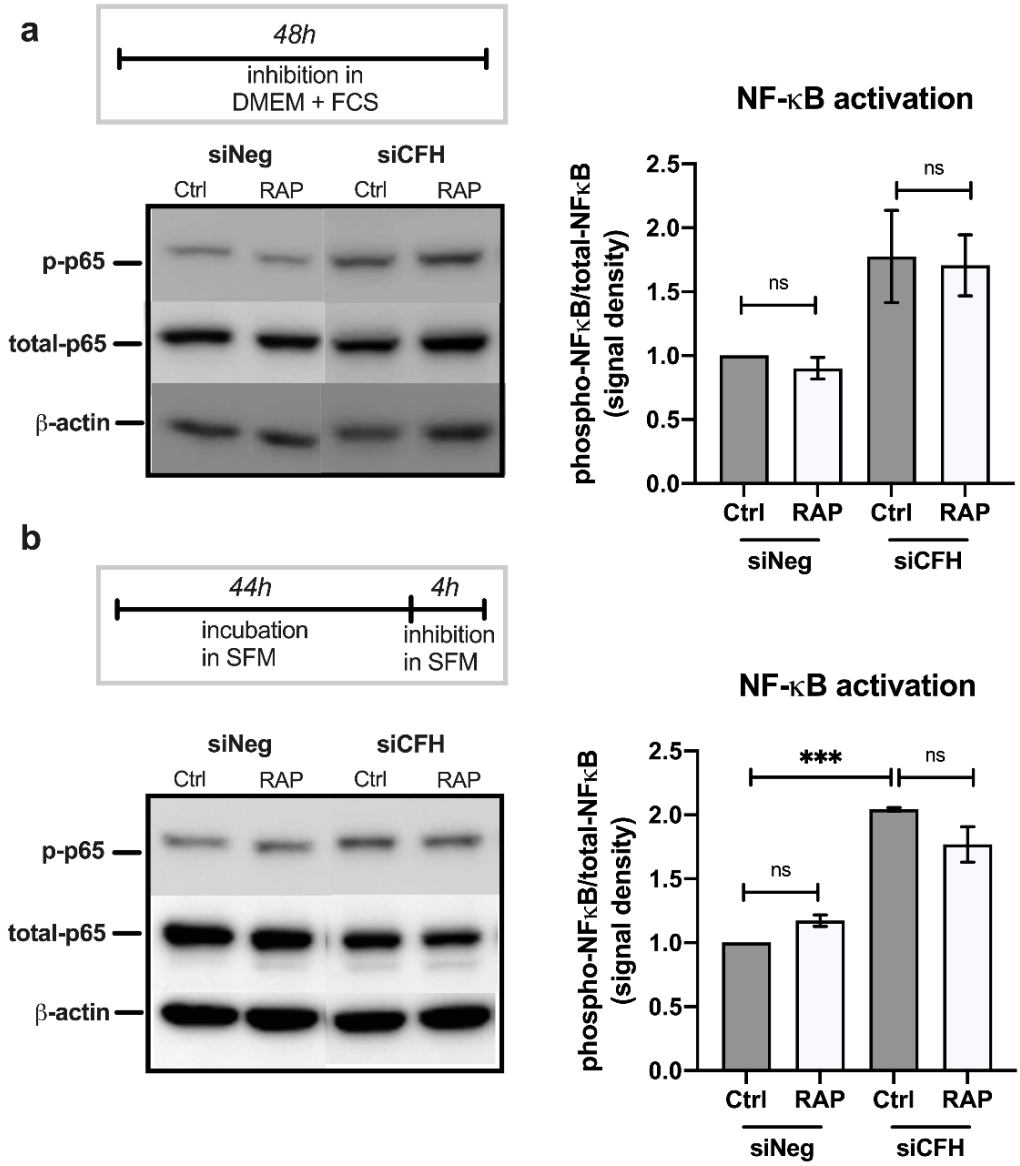

Figure 3.5: Effects of RAP on NF-κB activation levels in RPE cells
Cells (hTERT-RPE1) were seeded, cultured overnight and silenced for 24 h with either a negative control (siNeg) or siRNA specific for *CFH* (siCFH). Subsequently, the cells were maintained in the respective medium (DMEM+FCS or SFM) and treated with 10 μM of RAP for the indicated time, before collecting cell pellets for further processing after 48 h.
a-b Western Blot (WB) images and quantification shown on phosphorylated and total levels of the NF-κB p65 subunit in cell lysates treated with 10 μM of RAP for 48 h (**a**) and 4 h (**b**). After measuring the signal density, the ratio between phospho-p65 and total-p65 was taken. Actin was used as loading control.
Data show mean ± SEM: a: n=3; b: n=2. Significance levels assessed by student's t-test: **p<0.05, **p<0.01, *** p<0.001, ****p<0.0001.*

In a next step, we investigated whether the RAGE receptor signaling axis is involved in the observed upregulation of cytokines and complement factors under the absence of FH, but not *via* the NF-κB pathway. Therefore, we performed qRT-

PCR on inflammatory markers (IL6, CXCL8, CCL2) and complement genes (*C3, CFB*) after *CFH* silencing and RAGE inhibition. However, the results were inconsistent within the replicates and did not give any indication that RAP reduces the effects mediated by FH loss (data not shown).

3.2.2 MG132

The next inhibitor that was employed, is MG132, known to be a potent proteasome inhibitor and to inhibit NF-κB activation by preventing the degradation of IκBα (Kisselev and Goldberg 2001). As in preliminary experiments, strong cytotoxic effects were observed. Cytotoxicity was assessed *via* a MTT assay with a range of increasing concentrations of MG132 according to literature recommendations. The cell viability was measured in siNeg and siCFH RPE cells exposed to different concentrations of MG132 (0.1 – 10 μM) in two different experimental setups: 1) a treatment time of 48 h (48 h in SFM) and 2) a short treatment time of 4 h followed by 44 h of incubation (4 h DMEM/FCS + 44 h SFM) (Fig. 3.6). The viability was strongly reduced when the inhibitor was added over the entire duration of 48 h (Fig. 3.6 a). Already low concentrations of MG132 did highly decrease cell viability and especially in siCFH condition, the percentage of viable cells was decreased e.g. down to 10% with 0.5 μM MG132 (Fig. 3.6 a). The toxic effect was also seen by microscopy observation (Fig. 3.6 b). Similar effects were detectable when shortening the treatment period to 4 h (Fig. 3.6 c): with low concentrations of MG132 the viability was higher than in the long treatment (48 h), but when a shorter exposure time is employed usually higher inhibitor's concentrations are required to reach an inhibitory effect. At a concentration of 10 μM MG132, less than 50% of viable cells remained in siNeg and siCFH condition (Fig. 3.6 c), also confirmed by microscopy observation (Fig. 3.6 d).

To avoid toxic effects, the setup of a long treatment time over the entire 48 h was not pursued any further. Instead, the following experiments were performed with 2 μM of MG132 with either a 1) 4 h inhibition time at the beginning or 2) at the end of a 48 h time duration. Under these conditions, there were reduced, but still

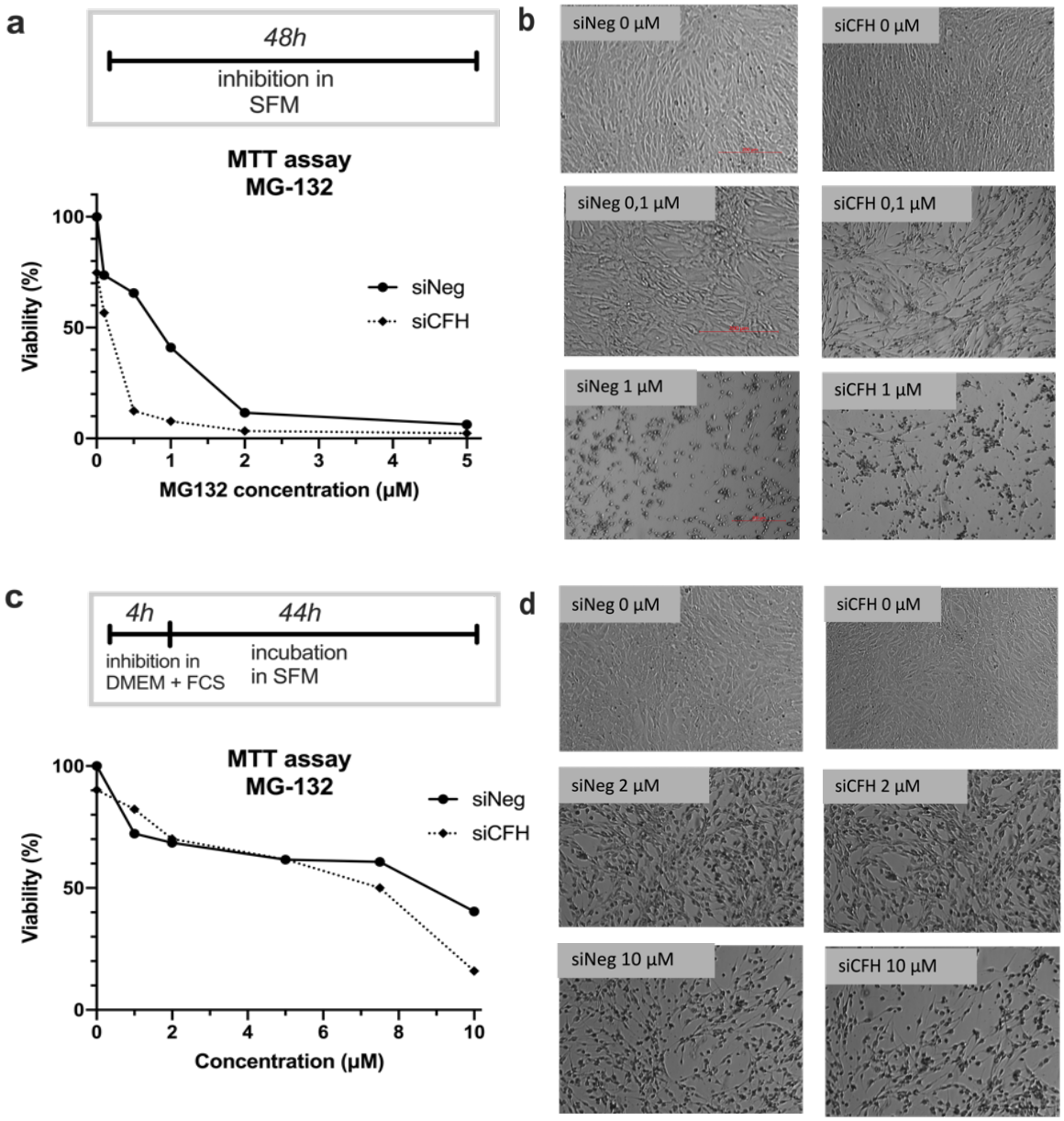

Figure 3.6: MTT viability assay on *CFH* silenced RPE cells treated with MG132
Cells (hTERT-RPE1) were seeded, cultured overnight and silenced for 24 h with either a negative control (siNeg) or siRNA specific for *CFH* (siCFH). Subsequently, the cells were maintained in the respective medium (DMEM+FCS or SFM) and treated with different concentrations of MG132 for the indicated time.
a Viability assessed by MTT assay with a treatment time of MG132 (0.1, 0.5, 1, 2, 5 µM) for 48 h. n=1
b Microscopy pictures (ZEISS AXIO with 4x magnification) on cells treated with indicated MG132 concentrations
c Viability assessed by MTT assay: 4 h treatment with MG132 (1, 2, 5, 7.5, 10 µM), followed by 44 h incubation. n=1
d Microscopy pictures (ZEISS AXIO with 4x magnification) on cells treated with indicated MG132 concentrations

cytotoxic effects observable. Further analyses of NF-κB activation *via* WB on the collected cell lysates, did show a strong increase in the proportion of phosphorylated p65 under addition of MG132 in siNeg and siCFH compared to the untreated controls (Fig. 3.7 a). Contrarily, the amount of total-p65 was strongly reduced by the addition of MG132 (Fig. 3.7 a). When the ratio of phosphorylated to total p65 was calculated, a significant increase of NF-κB activation was detected under addition of MG132 in both siNeg and siCFH condition (Fig. 3.7 b). Considering that the NF-κB pathway is also activated as pro-survival pathway in response to stress, MG132 and the associated proteasome inhibition possibly caused stress in RPE cells, so that the RPE cells in a compensatory fashion enhanced NF-κB activation to survive. While the data in Fig. 3.7 show the results for the setup 44 h + 4 h treatment in SFM, comparable results were obtained from the setup 4 h treatment + 44 h incubation SFM (data not shown). Since the addition of MG132 did not lead to a reduction, but to a strong increase in NF-κB activation levels, no further experiments were carried using MG132.

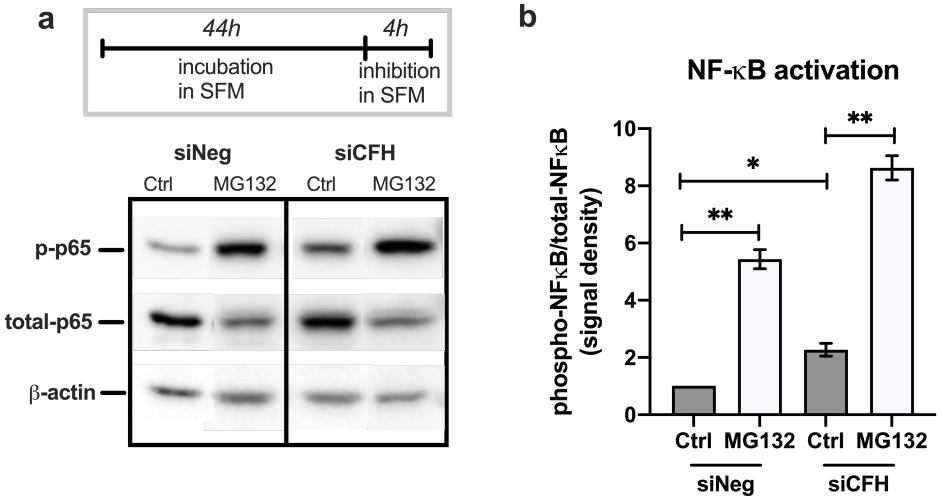

Figure 3.7: Effects of MG132 on NF-κB activation in RPE cells
Cells (hTERT-RPE1) were seeded, cultured overnight and silenced for 24 h with either a negative control (siNeg) or siRNA specific for *CFH* (siCFH). Subsequently, the cells were maintained in the SFM medium for 44 h and treated with 2 μM of MG132 for 4 h, before collecting cell pellets for further processing after a total of 48 h.
(**a**) Western Blot (WB) image and (**b**) quantification on phosphorylated and total levels of the NF-κB p65 subunit in cell lysates treated with 2 μM of MG132 for 4 h. After measuring the signal density, the ratio between phospho-p65 and total-p65 was calculated. Actin was used as loading control. Data show mean ± SEM: n=2.
Significance levels assessed by student's t-test: **p<0.05, **p<0.01, *** p<0.001, ****p<0.0001.*

3.2.3 Caffeic phenylethyl ester (CAPE)

Caffeic phenylethyl ester (CAPE), the third chemical inhibitor, is considered to be a potent and specific inhibitor of the NF-κB pathway: it is described to inhibit the translocation of the p65 subunit into the nucleus and to further prevent its DNA binding (Natarajan et al. 1996). Besides its anti-inflammatory effect CAPE is known to have antioxidant effects (Tolba et al. 2016).

To assess cytotoxicity of CAPE, cell viability was determined by performing a MTT assay. As part of the optimization process, initially two experimental setups were employed: 1) a 48 h treatment in SFM and 2) a 4 h treatment in DMEM/FCS + 44 h incubation in SFM. Under these conditions we observed a partial decrease in viability (see Fig. 3.8 a-d) and, moreover, no inhibition of NF-κB activation in WB analyses (data not shown, n=1) in both the setups. To avoid cytotoxicity, in further experiments, the 48 h long term treatment was performed in the presence of FCS (DMEM+FCS), in order to prevent cell cytotoxicity and to improve cell viability in a medium containing more nutrients. Additionally, a second setup was employed: the cells were incubated for 44 h in SFM followed by a 4 h inhibition time (44 h+4 h in SFM).

A MTT assay was performed to assess viability for both these setups (Fig. 3.9): it was observed that the viability with increasing CAPE concentration was quite stable. Fig. 3.9 a shows the results after a treatment over the entire experiment duration (48 h), with the corresponding microscopy pictures: no changes in viability with increasing CAPE concentrations (Fig. 3.9 b) were found. Also, within the setup 44 h+4 h in SFM the viability was not affected (Fig. 3.9 c) and a fully grown cell carpet was seen *via* microscopy observation (Fig. 3.9 d).

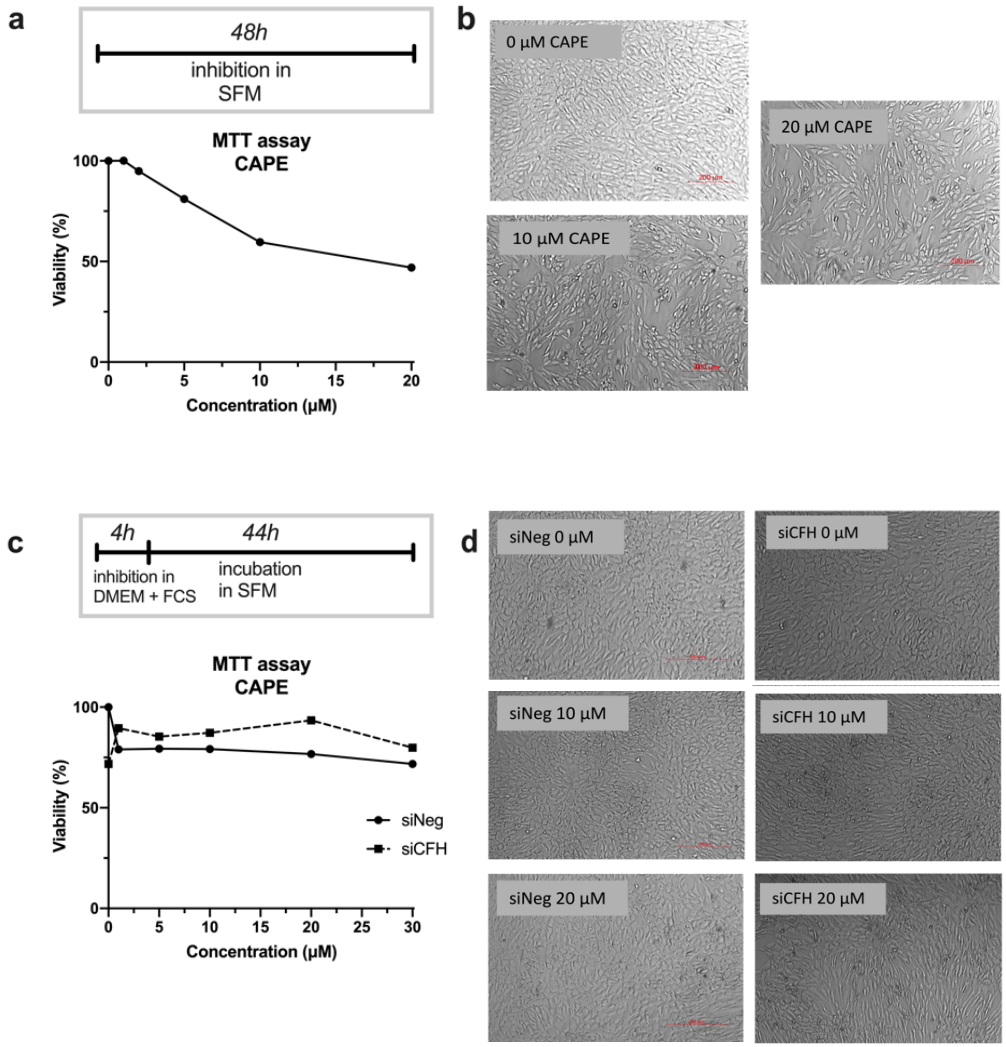

Figure 3.8: Preliminary viability assays on treatment with CAPE
Cells (hTERT-RPE1) were seeded, cultured overnight and silenced for 24 h with either a negative control (siNeg) or siRNA specific for *CFH* (siCFH). Subsequently, the cells were maintained in the respective medium (DMEM+FCS or SFM) and treated with different concentrations of CAPE for the indicated time.
a Viability assessed by MTT assay with a treatment time of CAPE (0.1, 1, 2, 5, 10 µM) for 48 h. n=1
b Microscopy pictures (ZEISS AXIO with 4x magnification) on cells treated with indicated CAPE concentrations
c Viability assessed by MTT assay: 4 h treatment with CAPE (1, 5, 10, 20, 30 µM) followed by 44 h incubation in SFM. n=1
d Microscopy pictures (ZEISS AXIO with 4x magnification) on cells treated with indicated CAPE concentrations

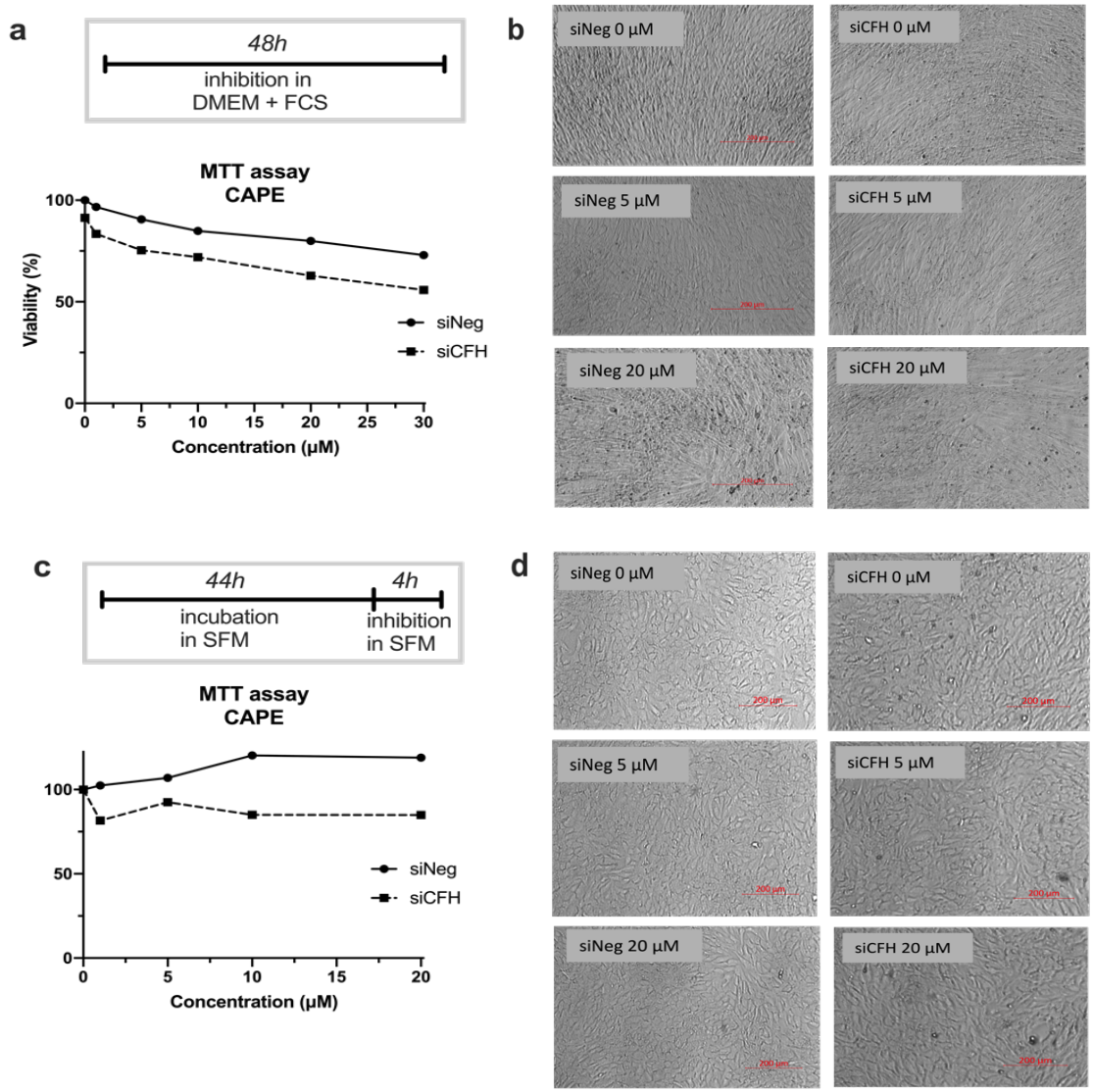

Figure 3.9: MTT viability assay on *CFH* silenced RPE cells treated with CAPE
Cells (hTERT-RPE1) were seeded, cultured overnight and silenced for 24 h with either a negative control (siNeg) or siRNA specific for *CFH* (siCFH). Subsequently, the cells were maintained in the respective medium (DMEM+FCS or SFM) and treated with different concentrations of CAPE for the indicated time.
a Viability assessed by MTT assay with a treatment time of CAPE (1, 5, 10, 20, 30 µM) for 48 h. n=1
b Microscopy pictures (ZEISS AXIO with 4x magnification) on cells treated with indicated CAPE concentrations
c Viability assessed by MTT assay: 44 h incubation followed by a 4 h treatment with CAPE (1, 5, 10, 20 µM). n=1
d Microscopy pictures (ZEISS AXIO with 4x magnification) on cells treated with indicated CAPE concentrations

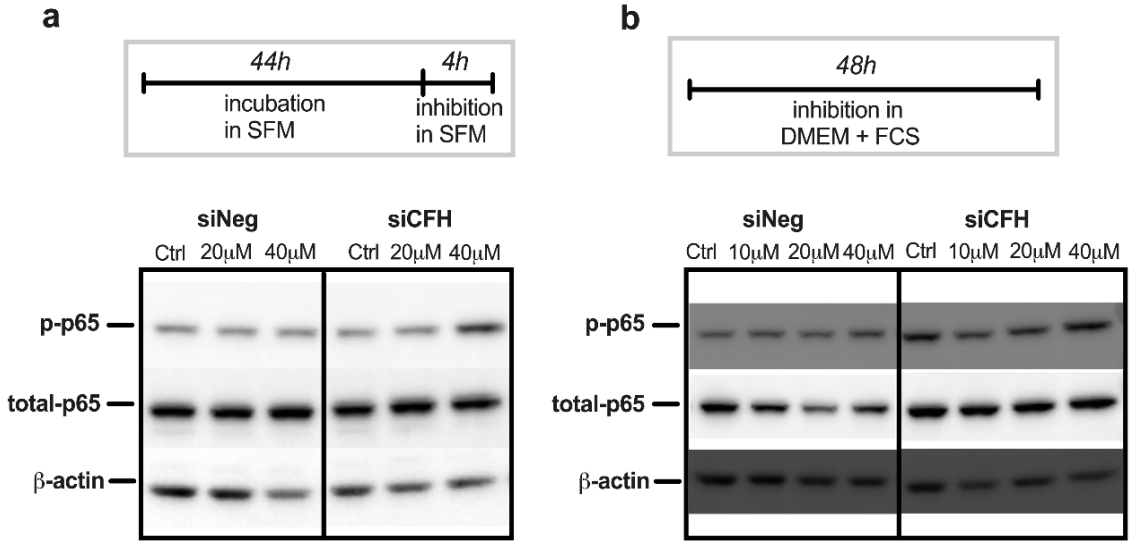

Figure 3.10: Effects of CAPE treatment on NF-κB activation levels in FH deprived RPE cells
Cells (hTERT-RPE1) were seeded, cultured overnight and silenced for 24 h with either a negative control (siNeg) or siRNA specific for *CFH* (siCFH). Subsequently, the cells were maintained in the respective medium (DMEM+FCS or SFM) and treated with CAPE for the indicated time, before collecting cell pellets for further processing after a total of 48 h.
a Western blot (WB) image on phosphorylated (p-p65) and total (total-p65) levels of the NF-κB p65 subunit on cell lysates treated with 20, 40 μM of CAPE for 4 h in SFM, with prior incubation of 44 h. Actin as loading control.
b WB image on phospho- and total p65 subunit on cell lysates treated with 10, 20, 40 μM of CAPE for 48 h in DMEM + FCS. Actin as loading control.
Significance levels assessed by student's t-test: **p<0.05, **p<0.01, *** p<0.001, ****p<0.0001*

Interestingly, an increase in p-p65 NF-κB was observed when high CAPE concentrations of 20 μM - 40 μM were used (see Fig. 3.10). Based on this observation, the following experiments were performed using a concentration of 5 μM and 10 μM CAPE and the effects of CAPE on NF-κB activation and gene expression were monitored. WB analyses did not reveal any significant changes in the activation levels of NF-κB in either siNeg or siCFH RPE cells in the two different experimental setups: 1) 48 h treatment in DMEM/FCS (Fig. 3.11 a-b) and 2) 44 h SFM + 4 h treatment SFM (Fig. 3.11 c-d).

In the same way, gene expression levels of genes altered by FH loss were not significantly changed by CAPE treatment. First, we analyzed the effects of CAPE on genes of the complement system in the 44 h + 4 h setup: we confirmed *CFH* silencing efficiency (Fig. 3.12 a), and checked *C3* (Fig. 3.12 b), and *CFB* (Fig. 3.12 c) expression, where no changes by the addition of CAPE in siNeg or siCFH

were noticed. Then, we analyzed the expression of inflammatory cytokines: CAPE could not revert the effects of *CFH* knock-down on inflammatory cytokines IL6, CXCL8 and CCL2 in siCFH cells (Fig. 3.12 d-f). Interestingly, we observed a significant increase by the addition of CAPE in IL6 (Fig. 3.12 d) and CXCL8 (Fig. 3.12 e), but not in CCL2 (Fig. 3.12 f) in negative control conditions (siNeg).

As CAPE is considered to have antioxidant capacities, we further investigated the expression of genes involved in antioxidant capacity, like the glutathione peroxidase 1 (GPX1), and mitochondrial stability, like the peroxisome proliferator-activated receptor gamma coactivator 1-alpha (PGC1α) & the E3 ubiquitin-protein ligase parkin (PARKIN), that were found to be changed under FH loss in previous studies (Armento et al. 2020). Hereby we could confirm a significant upregulation of GPX1 (Fig. 3.12 h) and PARKIN (Fig. 3.12 i) expression levels in siCFH compared to siNeg. Also, PGC1α levels were tendentially elevated in siCFH (Fig. 3.12 g). CAPE did not affect mRNA levels in all of those three genes, neither in the negative nor under silenced *CFH* conditions.

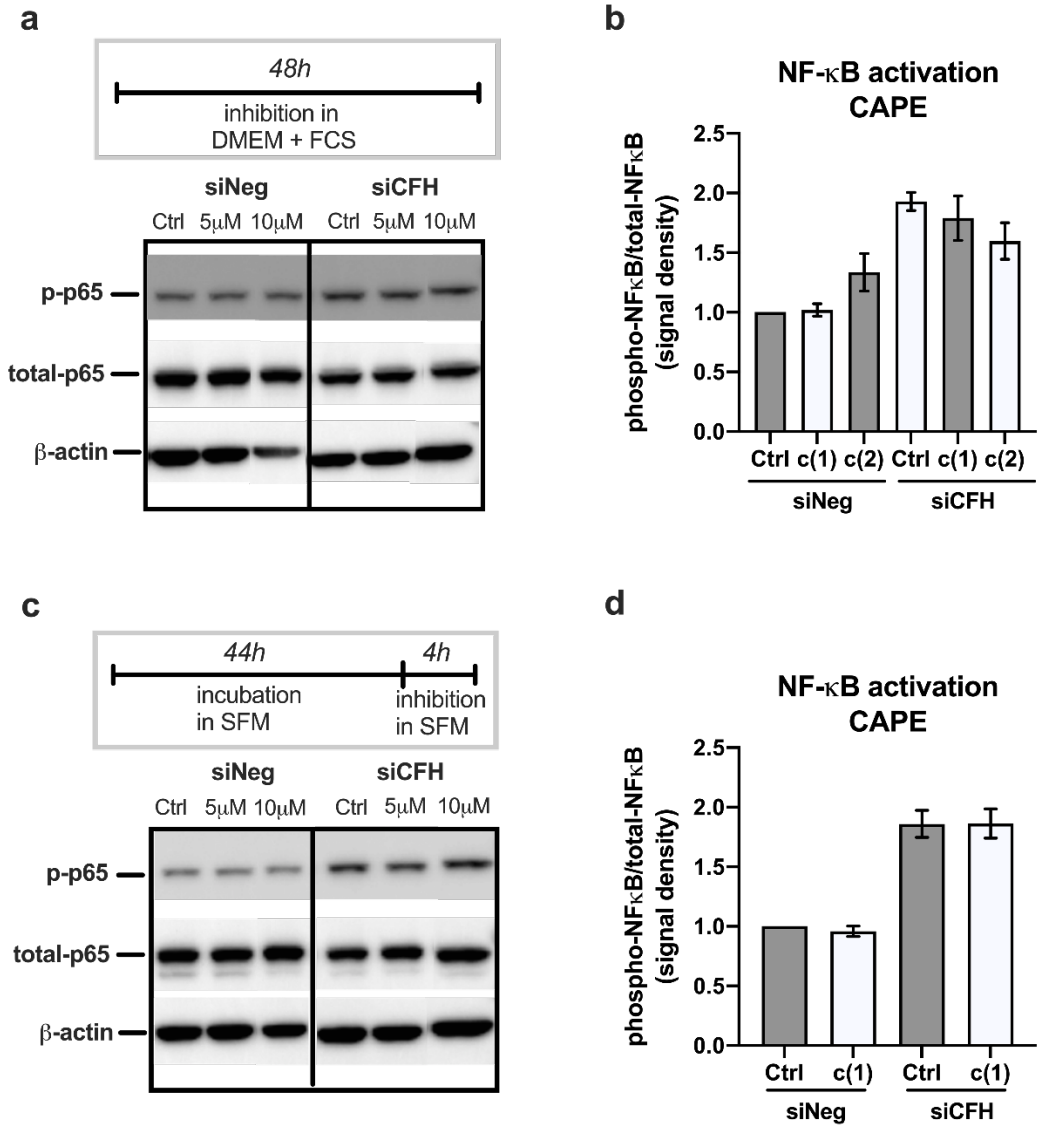

Figure 3.11: Effects of CAPE on NF-κB activation in RPE cells
Cells (hTERT-RPE1) were seeded, cultured overnight and silenced for 24 h with either a negative control (siNeg) or siRNA specific for *CFH* (siCFH). Subsequently, the cells were maintained in the respective medium (DMEM+FCS or SFM) and treated with CAPE for the indicated time, before collecting cell pellets for further processing after a total of 48 h.
a Western blot (WB) image on phosphorylated (p-p65) and total (total-p65) levels of the NF-κB p65 subunit on cell lysates treated with 5, 10 μM of CAPE for 48 h in DMEM supplemented with FCS. Actin as loading control.
b WB quantification (referring to a): c(1) = 5 μM, c(2) = 10 μM CAPE. After measuring the signal density, the ratio of p-p65 to total-p65 was calculated. Data show mean ± SEM: n=2
c WB image on phospho- and total p65 subunit on cell lysates treated with 5, 10 μM of CAPE for 4 h in SFM after 44 h incubation in SFM. Actin as loading control.
d WB quantification (referring to c): c(1) = 5 μM CAPE. Ratio of p-p65 to total-p65 shown. Data presented as mean ± SEM: n=4
Significance levels assessed by student's t-test: **p<0.05, **p<0.01, *** p<0.001, ****p<0.0001*

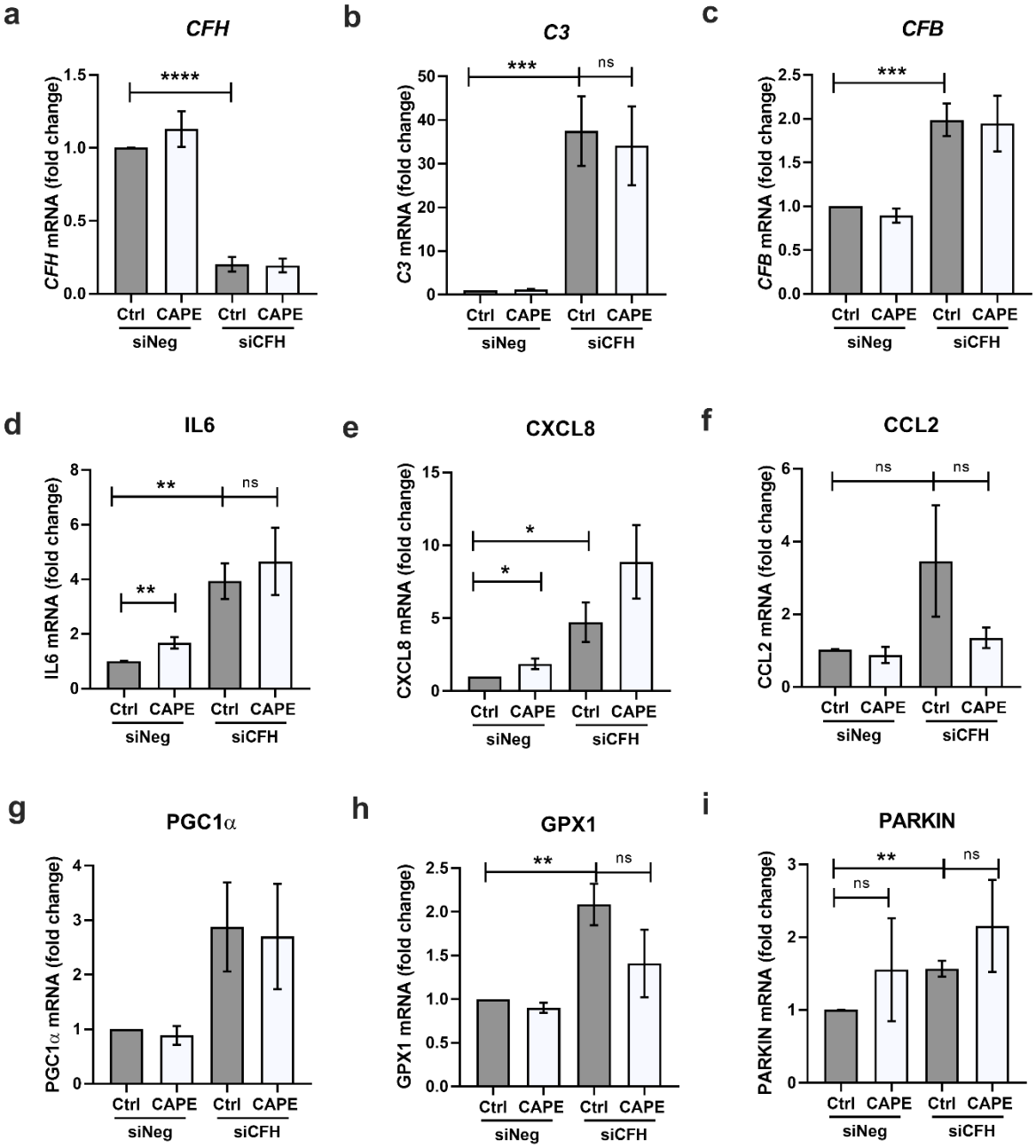

Figure 3.12: Effects of CAPE on gene expression levels in RPE cells
Cells (hTERT-RPE1) were seeded, cultured overnight and silenced for 24 h with either a negative control (siNeg) or siRNA specific for *CFH* (siCFH). Subsequently, the cells were maintained in serum-free medium (SFM) for 44 h, followed by a treatment time of 4 h with CAPE 5 μM, before cell pellets were collected for further processing.
a-i mRNA analysis of different cytokines, complement and antioxidant/metabolic genes measured by qRT-PCR. Data were normalized to the housekeeping gene PRLP0 and analyzed using the ΔΔCt method. Results are presented as mean ± SEM, n=4: **a** complement factor H (*CFH*), **b** complement component 3 (*C3*), **c** complement factor B (*CFB*), **d** interleukin-6 (IL6), **e** interleukin-8 (CXCL8), **f** C-C motif chemokine ligand 2 (CCL2), **g** peroxisome proliferator-activated receptor gamma coactivator 1-alpha (PGC1α), **h** glutathione peroxidase1 (GPX1), **i** E3 ubiquitin-protein ligase parkin (PARKIN)
Significance levels assessed by student's t-test: *p<0.05, **p<0.01, *** p<0.001, ****p<0.0001.

3.3 Blockade of NF-κB signaling pathway on gene level

Since all approaches aiming to inhibit the NF-κB signaling pathway chemically at its protein level (see chapter 3.2) were not effective, further experiments to inhibit NF-κB on gene level were designed. Therefore, the p65 subunit (also known as *RELA*) was silenced. Cell viability was not affected with siCFH, siRELA or under double silenced conditions (siCFH + siRELA) as shown by microscopy observation (Fig. 3.13 a-d).

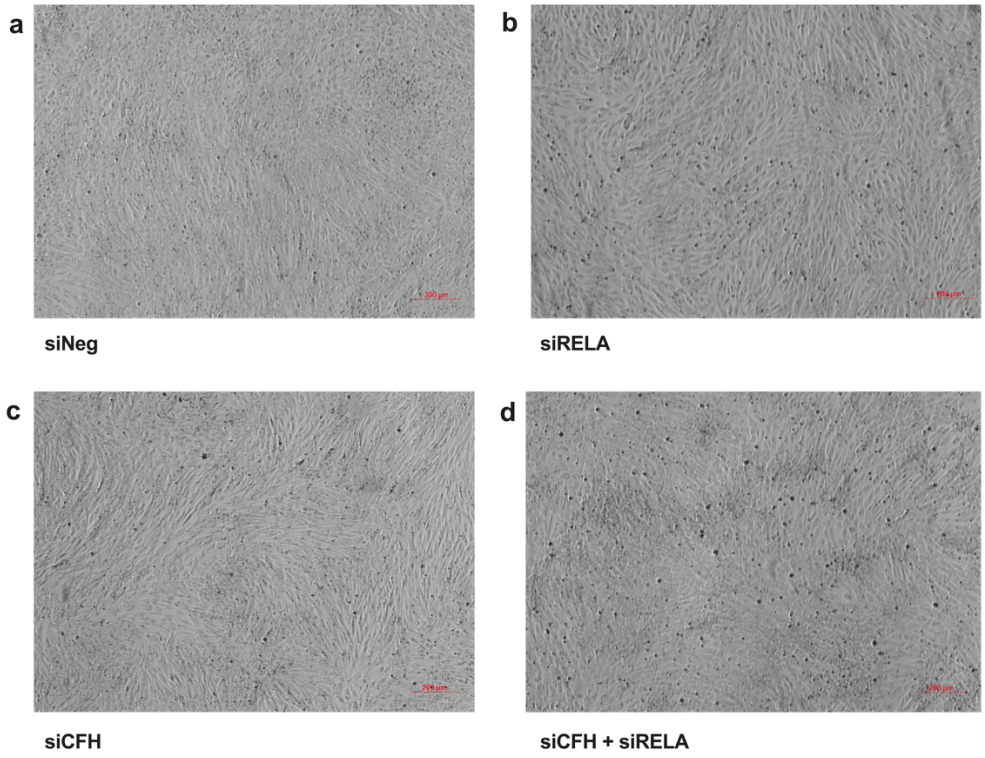

Figure 3.13: Effects of CFH and/or RELA knock-down on RPE cells
Cells (hTERT-RPE1) were seeded, cultured overnight and silenced for 24 h with either a negative control (siNeg) or siRNA specific for *CFH* (siCFH) and/or *RELA* (siRELA). Subsequently, the cells were maintained in serum-free medium (SFM) for 48 h, before cell pellets and cell supernatants were collected for further processing. Pictures were acquired directly before the collection with the ZEISS AXIO microscope (4x magnification).

The efficiency of silencing on the *RELA* gene was proved *via* qRT-PCR, as shown in Fig. 3.14 c: mRNA levels of *RELA* were significantly reduced (down to 10%), in both siRELA and siCFH+siRELA conditions. Also, NF-κB p65 protein levels were strongly reduced, in both phospho-p65 and total-p65 when *RELA* or *CFH*+*RELA* were knocked-down, as shown by WB (Fig. 3.14a) and in the

corresponding quantification, where the ratio to actin was calculated (Fig. 3.14b). This indicates that the observed NF-κB activation under FH loss can be abolished by silencing the *RELA* gene.

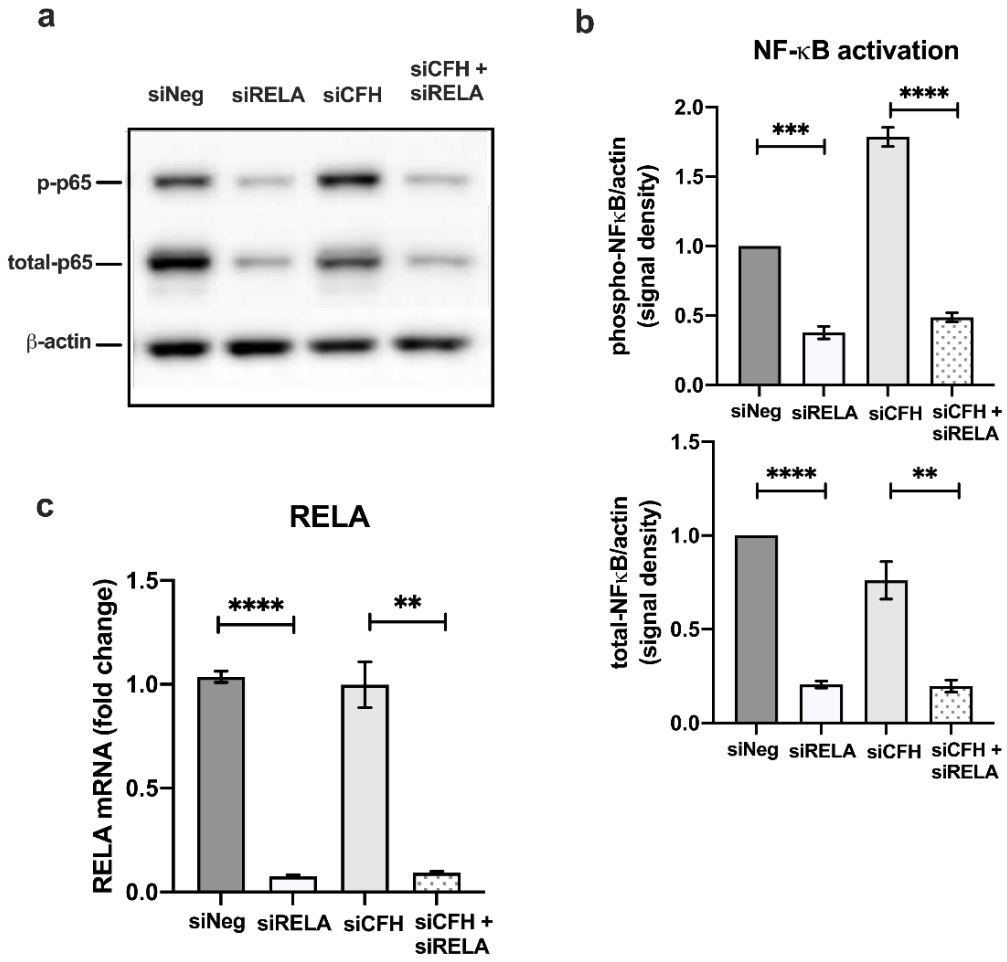

Figure 3.14: Effects of NF-κB blockade *via* silencing RELA gene
Cells (hTERT-RPE1) were seeded, cultured overnight and silenced for 24 h with either a negative control (siNeg) or siRNA specific for *CFH* (siCFH) and/or *RELA*/p65 (siRELA). Subsequently, the cells were maintained in serum-free medium (SFM) for 48 h, before cell pellets and cell supernatants were collected for further processing.
a Western Blot (WB) image of cell lysates on the phosphorylated and total p65 subunit with beta-actin for loading control. **b** WB quantification on phospho- and total-p65 of 3 independently performed experiments. Signal density was measured and the ratio to actin was calculated. Data show mean ± SEM, n=3. **c** mRNA analysis on RELA gene expression by qRT-PCR on cell lysate samples. Data were normalized to the housekeeping gene PRLP0 and analyzed using the ΔΔCt method: mean ± SEM, n=3.
Significance levels assessed by student's t-test: *p<0.05, **p<0.01, *** p<0.001, ****p<0.0001.
Parts of this data were published in (Armento, Schmidt et al. 2021)

In a next step, the effects of RELA knock-down on cytokines expression levels were investigated. Interestingly, silencing RELA alone (siRELA) led to a significant reduction of CXCL8 (Fig. 3.15 b) and CCL2 (Fig. 3.15 c) gene levels, but not of IL6 (Fig. 3.15 a) levels. Moreover, the effects mediated by FH loss on cytokines expression were abolished, when NF-κB activation was reduced *via* double silencing *CFH* & *RELA*: a clear trend of a reduction in IL6 (Fig. 3.15 a) and CXCL8 (Fig. 3.15 b) gene levels was seen. This reduction was significantly also observed in CCL2 expression (Fig. 3.15 c).

In further analyses the impact of NF-κB blockade on complement components was investigated. It was observed that *CFH* gene expression levels were significantly downregulated under *RELA* silenced conditions (Fig. 3.16a). The same trend was found on protein level: FH levels in cell supernatants detected *via* WB were significantly reduced under NF-κB blockade (siRELA) (Fig. 3.16 b), hinting that the NF-κB pathway modulates *CFH* expression. As the complement component 3 (*C3*) and complement factor B (*CFB*) were detected to be elevated under FH loss (Fig. 3.1) we checked if NF-κB knock-down abolishes these effects: indeed, *C3* levels were found to be significantly reduced in siCFH + siRELA (Fig. 3.16 c), and, moreover, also decreased in siRELA cells without the impact of *CFH* (Fig. 3.16 c). *CFB* levels also were observed to be reduced by NF-κB blockade, as it could be seen in siCFH + siRELA (Fig. 3.16 e), but not in siRELA alone.

Due to these findings, additional complement factors were evaluated. Contrary to *C3*, expression levels of *C5*, another main component of the complement cascade, were significantly reduced under the absence of FH, as well as under NF-κB blockade in siRELA cells (Fig. 3.16 d).

RNA levels of complement factor I (*CFI)* were elevated under FH loss and tendentially downregulated *via* NF-κB blockade (Fig. 3.16 f). Besides, blocking NF-κB alone (siRELA) had a reducing effect on *CFI* levels (Fig. 3.16 f).

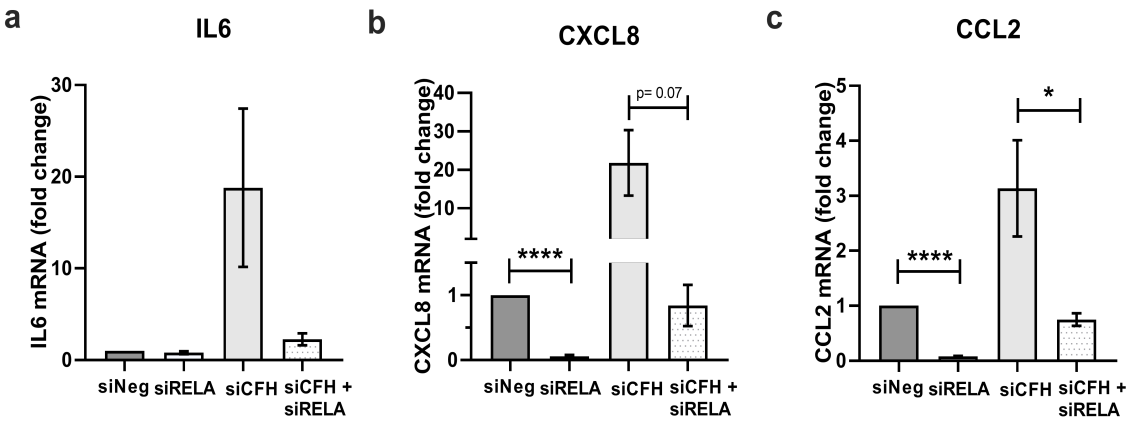

Figure 3.15: Effects of NF-κB blockade on proinflammatory cytokines
Cells (hTERT-RPE1) were seeded, cultured overnight and silenced for 24 h with either a negative control (siNeg) or siRNA specific for CFH (siCFH) and/or RELA/p65 (siRELA). Subsequently, the cells were maintained in serum-free medium (SFM) for 48 h, before cell pellets and cell supernatants were collected for further processing.
a-c mRNA analysis of **a** interleukin-6 (IL6), **b** interleukin-8 (CXCL8), and **c** C-C motif chemokine ligand 2 (CCL2) gene levels by qRT-PCR. Data were normalized to the housekeeping gene PRLP0 and analyzed using the ΔΔCt method: shown as mean ± SEM, n=3-4.
Significance levels assessed by student's t-test: *p<0.05, **p<0.01, *** p<0.001, ****p<0.0001.
Parts of this data were published in (Armento, Schmidt et al. 2021)

In addition to cytokines and complement components, we checked the expression of genes involved in oxidative stress response that were affected by FH loss (see Fig. 3.12) to further investigate whether the NF-κB pathway modulates also this aspect of RPE homeostasis. Out of the selected genes, only PGC1α levels were affected by NF-κB inhibition as they were significantly reduced in siCFH + siRELA cells (Fig. 3.17 a). Glutathione peroxidase1 (GPX1) was (tendentially) upregulated under FH loss (also see Fig. 3.12b) but blocking NF-κB did not lead to significant changes (Fig. 3.17 b). The levels of E3 ubiquitin-protein ligase parkin (PARKIN) were found to be significantly elevated under NF-κB blockade in siCFH + siRELA cells (Fig. 3.17 c).

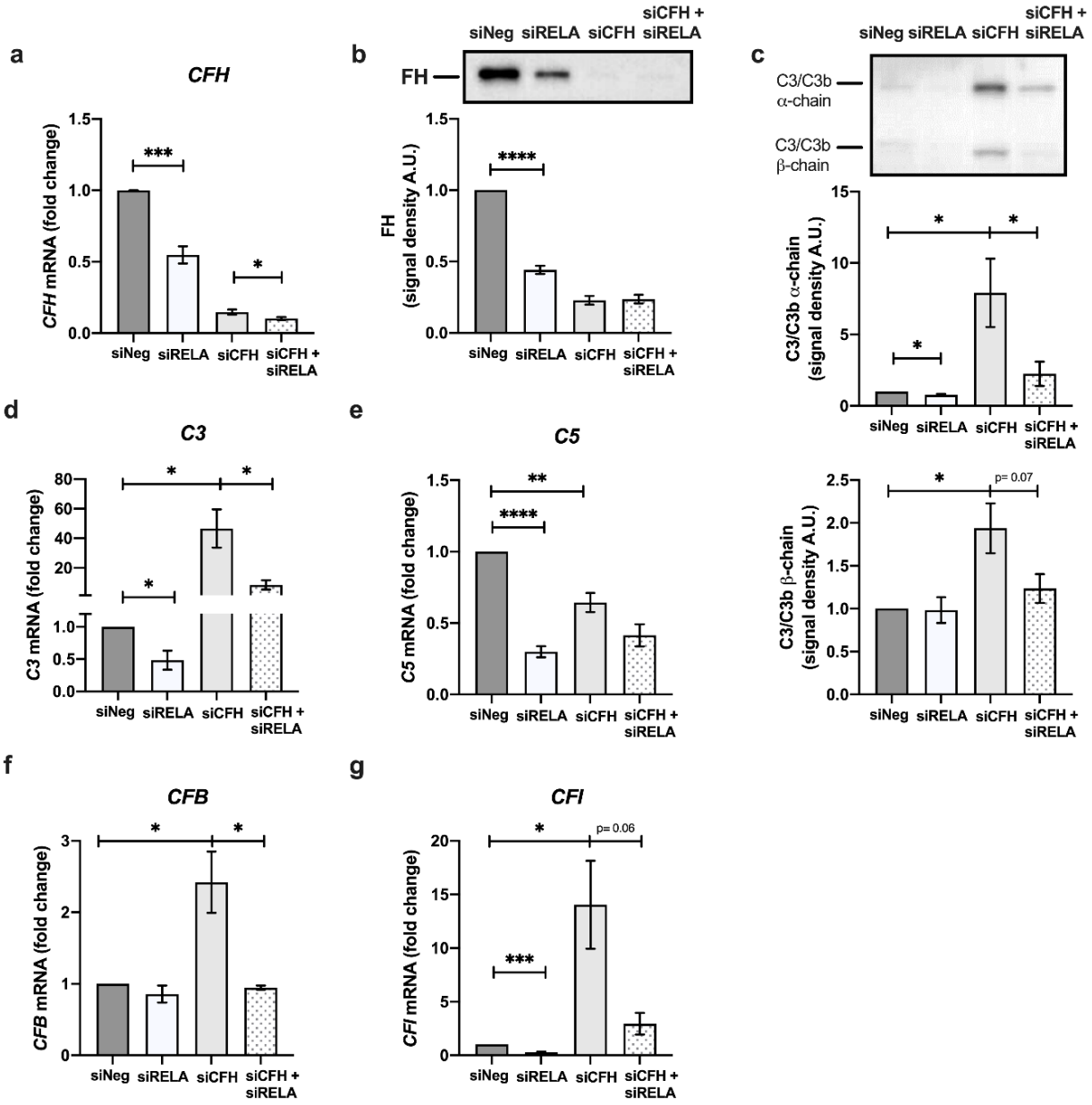

Figure 3.16: Effects of NF-κB blockade on complement system genes
Cells (hTERT-RPE1) were seeded, cultured overnight and silenced for 24 h with either a negative control (siNeg) or siRNA specific for *CFH* (siCFH) and/or *RELA*/p65 (siRELA). Subsequently, the cells were maintained in serum-free medium (SFM) for 48 h, before cell pellets and cell supernatants were collected for further processing.
a mRNA analysis of complement factor H (CFH) expression levels by qRT-PCR on cell supernatants. Data were normalized to the housekeeping gene PRLP0 and analyzed using the ΔΔCt method: shown as mean ± SEM, n=4.
b Western blot (WB) quantification of Factor H (FH) protein levels on cell supernatants. n=3.
c WB quantification of C3 alpha- and beta-chain protein levels in cell supernatants. n=4
d-g mRNA analysis by qRT-PCR on cell lysates: **d** complement component 3 (C3), **e** complement component 5 (C5), **f** complement factor B (CFB), **g** complement factor I (CFI)
Data normalized to the housekeeping gene PRLP0 and analyzed using the ΔΔCt method: shown as mean ± SEM, n=3-4. Significance levels assessed by student's t-test: *p<0.05, **p<0.01, *** p<0.001, ****p<0.0001. Parts of this data were published in (Armento, Schmidt et al. 2021)

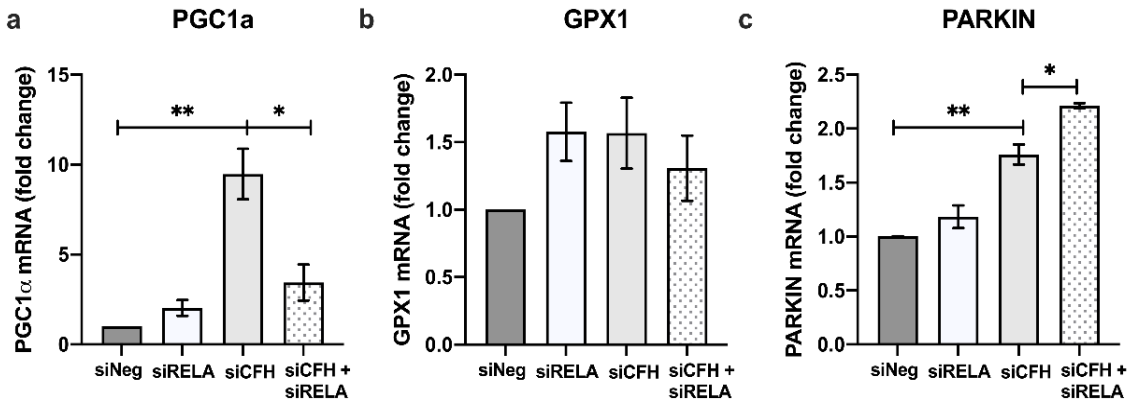

Figure 3.17: Effects of NF-κB blockade on a selection of oxidative stress response genes
Cells (hTERT-RPE1) were seeded, cultured overnight and silenced for 24 h with either a negative control (siNeg) or siRNA specific for *CFH* (siCFH) and/or RELA/p65 (siRELA). Subsequently, the cells were maintained in serum-free medium (SFM) for 48 h, before cell pellets and cell supernatants were collected for further processing. mRNA analysis on cell lysates by qRT-PCR. Data were normalized to the housekeeping gene PRLP0 and analyzed using the ΔΔCt method: shown as mean ± SEM, n=3:
a peroxisome proliferator-activated receptor gamma coactivator 1-alpha (PGC1a), **b** glutathione peroxidase1 (GPX1), **c** E3 ubiquitin-protein ligase parkin (PARKIN)
Significance levels assessed by student's t-test: *p<0.05, **p<0.01, *** p<0.001, ****p<0.0001.

So far, we have been able to investigate several changes on different complement components and inflammatory cytokines that arise under the absence of FH and can be rescued by blockade of the NF-κB signaling pathway. To focus and to find out more about inflammatory changes and a possible involvement of the NF-κB pathway, we performed a cytokines array, to investigate the secreted levels of 36 cytokines and chemokines (Fig. 3.18). With this, several different cytokines could be identified to be expressed by RPE cells and secreted in cell culture supernatants of hTERT-RPE1 cells. First of all, the upregulation of IL-6 and IL-8 could be confirmed: secreted levels were significantly elevated under the absence of FH, and for both this effect was abolished under NF-κB blockade (Fig. 3.19 a,b). MCP-1 (gene name: CCL2) levels were lower, compared to IL-6 & IL-8, but tendentially elevated in siCFH and rescued *via* silencing *RELA* (Fig. 3.19 c). Further, inflammatory mediators were found to follow the same kinetics: the granulocyte-macrophage colony-stimulating-factor (GM-CSF) (Fig. 3.19 d), the plasminogen activator inhibitor-1 (SerpinE1) (Fig. 3.19 e) and the C-X-C motif chemokine ligand 1 (GROα) (Fig. 3.19 f) were all upregulated under

the absence of FH and brought back to basal levels blocking the NF-κB p65 subunit (siCFH + siRELA). Additionally, another set of cytokines was influenced and found to be elevated by FH loss, but not affected by NF-κB blockade. Indeed, increased levels of C-C motif chemokine ligands 3 & 4 (MIP-1α/MIP-1β) (Fig.3.19 g) and the interleukin 1 receptor antagonist (IL1-ra) (Fig. 3.19 h) were detected under *CFH* knock-down, but no significant reduction could be observed by inhibition of NF-κB p65 (siCFH + siRELA).

In addition to these two groups, other cytokines could be identified that were secreted in RPE cell supernatants but not influenced by *CFH* nor NF-κB blockade. This includes the macrophage migration inhibitor factor (MIF) (Fig. 3.20 a), as well as the cytokines interleukin 1a (IL-1a), interleukin 18 (IL-18) and interleukin 21 (IL-21) (Fig. 3.20 b-d). Only for IL-21 a reduction was noticed when *CFH* and *RELA* were simultaneously silenced (Fig. 3.20 d).

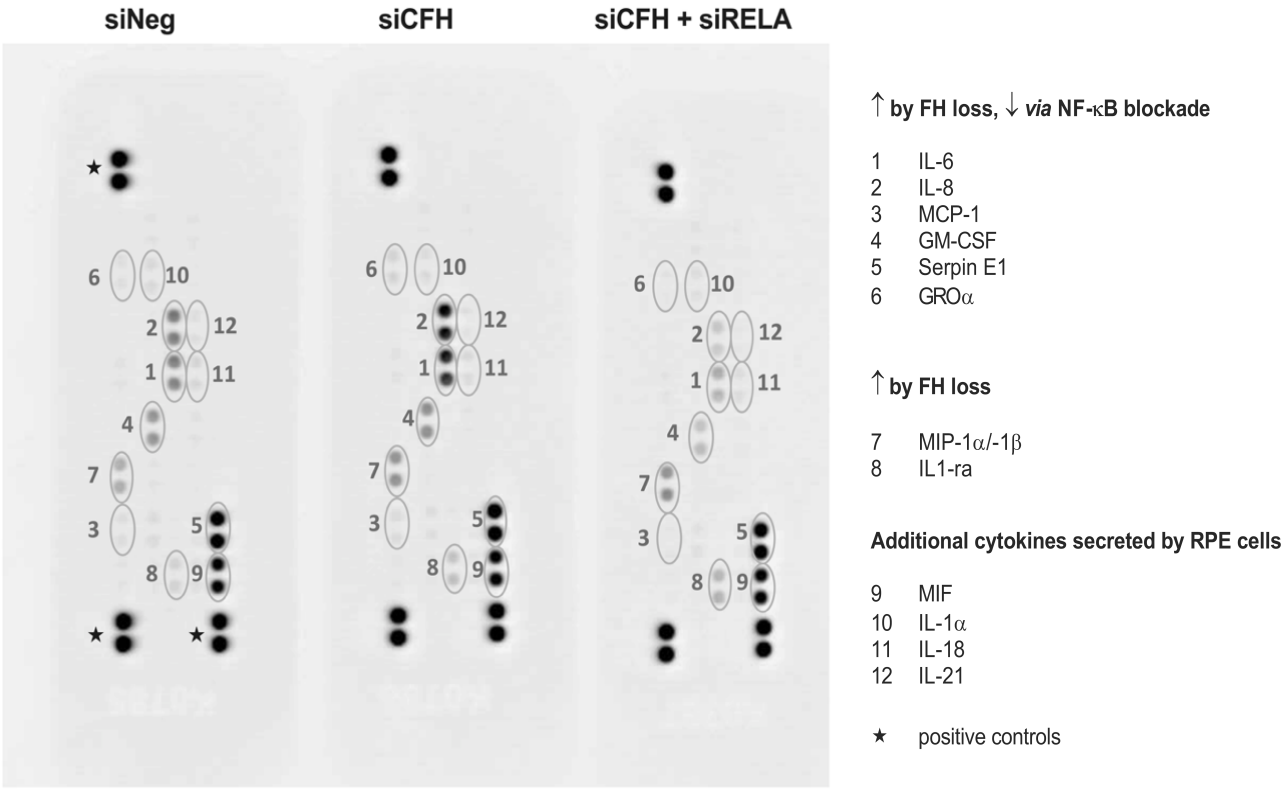

Figure 3.18: Image of Proteome Profiler Cytokine Array on cell culture supernatants
Cells were seeded, silenced and kept for 48 h in SFM, before cell supernatants were collected (more details see Fig. 3.19). Images were acquired with Fusion FX detection machine.

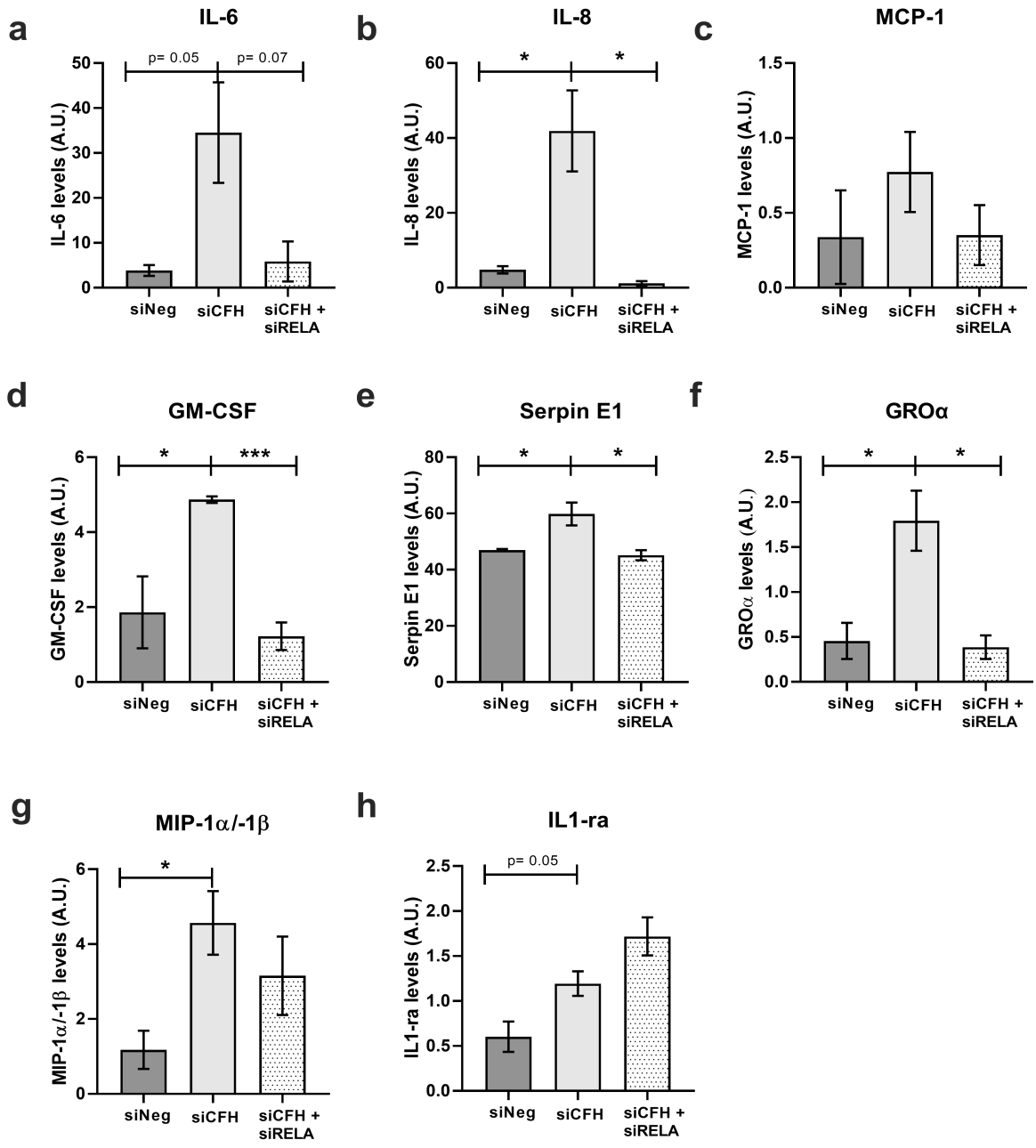

Figure 3.19: Expression levels of secreted cytokines influenced by FH and NF-κB
Cells (hTERT-RPE1) were seeded, cultured overnight and silenced for 24 h with either a negative control (siNeg) or siRNA specific for *CFH* (siCFH) and/or *RELA*/p65 (siRELA). Subsequently, the cells were maintained in serum-free medium (SFM) for 48 h, before cell culture supernatants were collected for further processing.
The proteome profiler cytokine array was performed according to the manufacturer's instructions. Signal density was measured of 3 independent performed experiments. Data are shown as mean ± SEM, n=3:
a interleukin 6 (IL-6), **b** interleukin 8 (IL-8), **c** C-C motif chemokine ligand 2 (MCP-1), **d** granulocyte-macrophage colony stimulating factor (GM-CSF), e plasminogen activator inhibitor-1 (SerpinE1), f C-X-C motif chemokine ligand 1 (GROα), **g** C-C motif chemokine ligands 3 & 4 (MIP-1a/MIP-1b), **h** interleukin 1 receptor antagonist (IL1-ra).
Significance levels assessed by student's t-test: *p<0.05, **p<0.01, *** p<0.001, ****p<0.0001.
Parts of this data were published in (Armento, Schmidt et al. 2021)

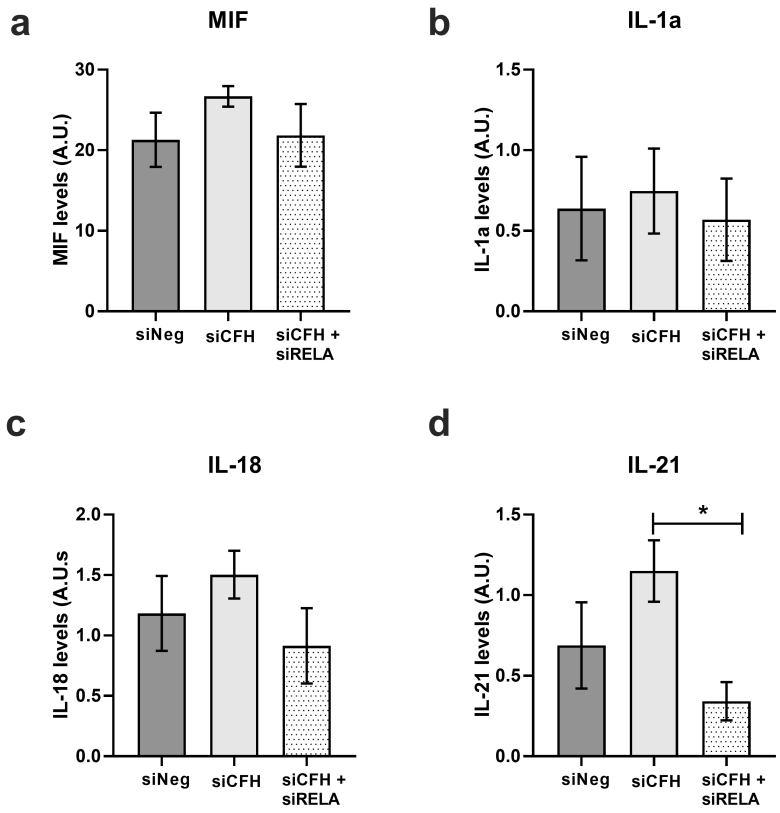

Figure 3.20: Expression levels of secreted cytokines in RPE cells
Cells culture supernatants were collected after 48 h (same conditions as described in Fig. 15).
The proteome profiler cytokine array was performed according to the manufacturer's instructions. Signal density was measured of 3 independent performed experiments. Data are shown as mean ± SEM, n=3:
a macrophage migration inhibitor factor (MIF), **b** interleukin 1a (IL-1a), **c** interleukin 18 (IL-18), **d** interleukin 21 (IL-21).
Significance levels assessed by student's t-test: *p<0.05, **p<0.01, *** p<0.001, ****p<0.0001.
Parts of this data were published in (Armento, Schmidt et al. 2021).

3.4 Effects of the addition of exogenous complement sources

In the following section we further studied the role of endogenous factor H (FH) in RPE cells and investigated whether the addition of exogenous factor H or complement component 3 (C3) had an effect on NF-κB activation levels and gene expression in FH deprived RPE cells. In addition to C3, also its cleaved and active component C3b was employed in a separate approach. Considering that C3 and C3b levels are increased after FH deprivation, with the addition of either C3 or C3b we wanted to explore whether the effects caused by FH loss are dependent on the increased levels of C3/C3b and whether the effects under *CFH* knock-down conditions (siCFH) can be additionally intensified. By addition of exogenous FH, we wanted to check whether it abolishes the effects mediated through an endogenous/intracellular FH loss (siCFH) and protects *CFH* knocked down cells from the induction of proinflammatory processes.

First, analyses on NF-κB activation levels were assessed *via* WB, measuring p-p65 to total-p65 protein levels in cell lysates. Thus, no significant effects could be shown: neither the addition of exogenous FH, nor C3 or C3b did change NF-κB activation levels in control conditions (siNeg) or under the absence of endogenous FH (siCFH) in comparison to the respective, untreated control cells (siNeg Ctrl; siCFH Ctrl). The WB image and corresponding quantification are shown in Fig. 3.21.

Further, qRT-PCR analyses were performed to explore the impact of exogenous FH, C3 and C3b on gene expression. mRNA levels of *C3*, *CFB*, IL6 and CCL2 were examined: it was found that neither in siNeg nor in siCFH conditions levels of these genes were significantly altered by addition of FH, C3 or C3b compared to the respective knocked-down control cells (Ctrl) (Fig. 3.22 a-d).

The findings so far suggest that an application of exogenous FH doesn't affect and can't abolish the effects that are mediated by a loss of endogenous FH. Further, the addition of exogenous C3 and C3b doesn't influence the cell's complement system in the balanced (siNeg) or dysregulated (siCFH) state. Both findings highlight the possible role of endogenous FH and intracellularly regulation mechanisms of the complement system.

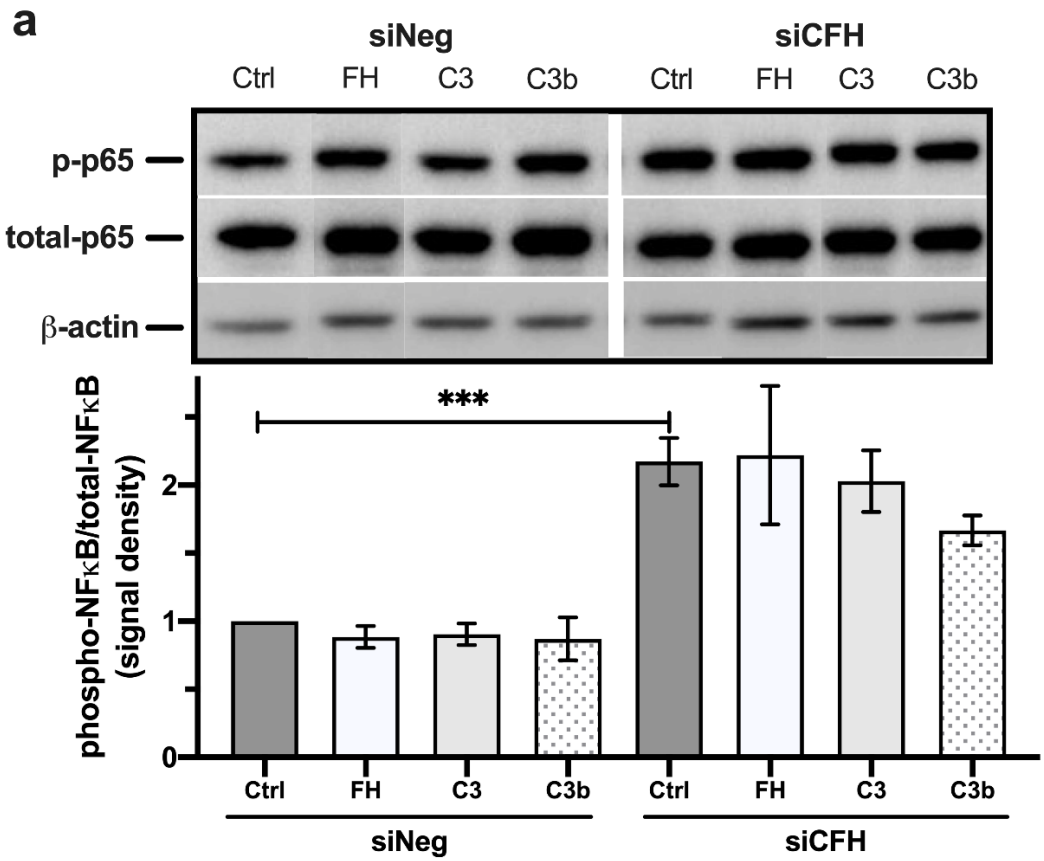

Figure 3.21: NF-κB activation levels altered by the addition of exogenous FH, C3, C3b
Cells (hTERT-RPE1) were seeded, cultured overnight and silenced for 24 h with either a negative control (siNeg) or siRNA specific for *CFH* (siCFH). Subsequently, the cells were treated with Factor H (FH) (1 μg/ml), complement component C3 (100 ng/ml) or C3b (100 ng/ml) in serum-free medium (SFM) for 48 h, before cell pellets were collected for further processing.
a Western Blot (WB) image of cell lysates on the phosphorylated (p-p65) and total p65 subunit with beta-actin for loading control. Corresponding WB quantification: Signal density was measured and the ratio of p-p65 to total-p65 was calculated. Data show mean ± SEM, n=3.
Significance levels assessed by student's t-test: *p<0.05, **p<0.01, *** p<0.001, ****p<0.0001.
Parts of this data were published in (Armento, Schmidt et al. 2021)

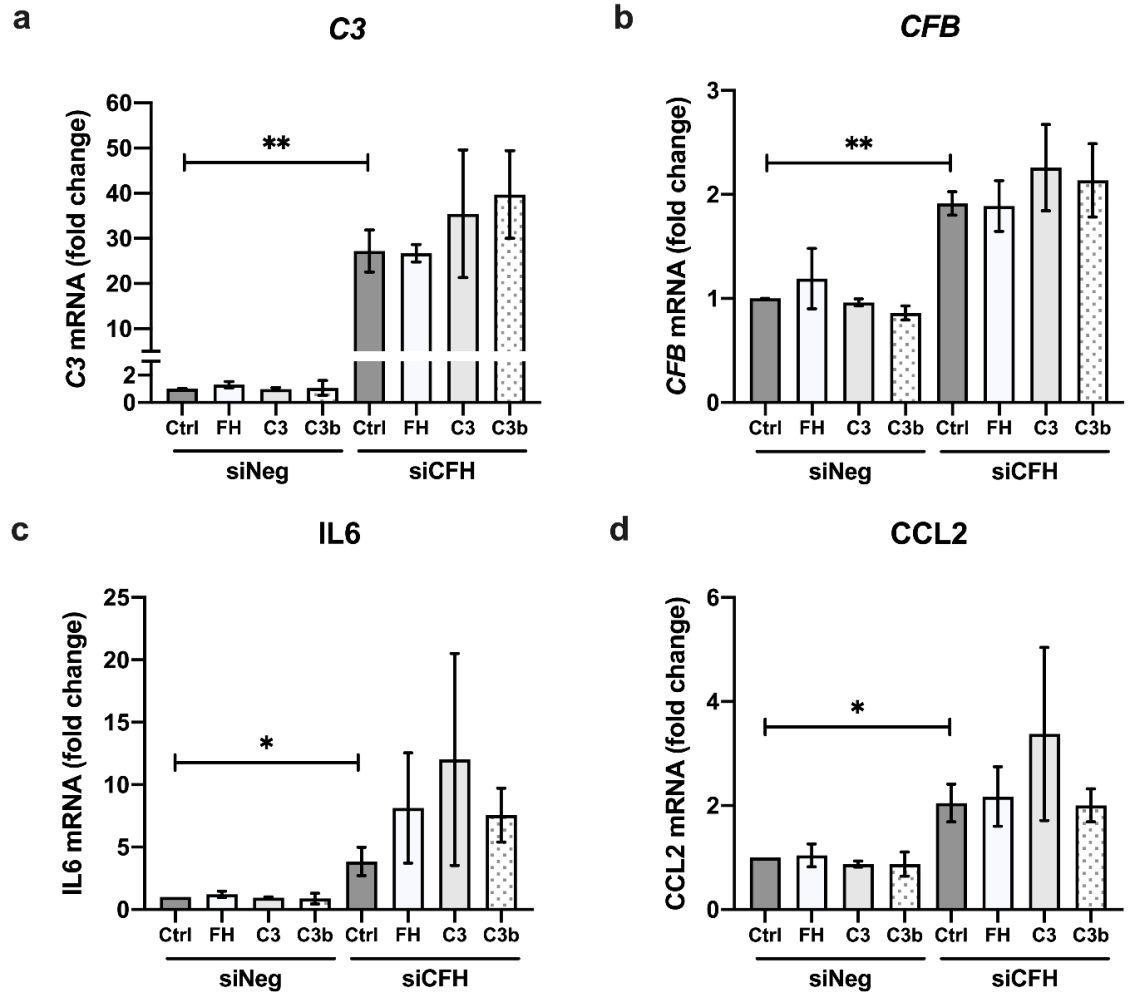

Figure 3.22: Expression levels of complement and cytokine genes altered by addition of FH, C3, C3b
Cells (hTERT-RPE1) were seeded, cultured overnight and silenced for 24 h with either a negative control (siNeg) or siRNA specific for *CFH* (siCFH). Subsequently, the cells were treated with Factor H (FH) (1 μg/ml), complement component C3 (100 ng/ml) or C3b (100 ng/ml) in serum-free medium (SFM) for 48 h, before cell pellets were collected for further processing.
mRNA analysis on gene expression levels by qRT-PCR on cell lysates. Data were normalized to the housekeeping gene PRLP0 and analyzed using the ΔΔCt method: shown as mean ± SEM, n=3:
a complement component 3 (C3), **b** complement factor B (CFB), **c** interleukin 6 (IL6), **d** C-C motif chemokine ligand 2 (CCL2).
Significance levels were assessed by student's t-test: *p<0.05, **p<0.01, *** p<0.001, ****p<0.0001.
Parts of this data were published in (Armento, Schmidt et al. 2021)

3.5 Investigation of additional signaling pathways modulated by FH

As stated in the introduction, the NF-κB signaling pathway is a major pathway involved in inflammation, survival and cell proliferation. It is a pathway, that can be activated quickly through a wide range of different stimuli and further is known to be tightly regulated and in interaction with several other pathways (Oeckinghaus, Hayden, and Ghosh 2011). In addition to the NF-κB pathway, we also wanted to investigate whether other pathways that are known to promote pro-survival processes, oxidative stress response or inflammation are altered in FH deprived RPE cells. Therefore, we monitored the PI3K/Akt signaling pathway as well as parts of the MAPK pathway (ERK subfamily). Both of these pathways are also stated to interfere with the NF-κB pathway (Oeckinghaus, Hayden, and Ghosh 2011).

The PI3K/Akt signaling pathway mediates many cellular functions, as it is involved in cell metabolism and growth, survival, proliferation, protein synthesis, transcription and apoptosis and simplified consists out of a cascade of PI3K-PDK1-Akt (Hemmings and Restuccia 2012). To observe the PI3K/Akt pathway levels of the phosphorylated Akt protein (Ser473) and total Akt were measured *via* WB. The results are shown in Fig. 3.23 a: we detected a strong reduction in phosphorylated Akt (p-Akt) levels under *CFH* knock-down conditions, while the amount of total Akt was found to be stable (Fig. 3.23 a). After measuring the intensity density of the WB bands, the ratio of p-Akt to total-Akt was calculated, confirming a significant decrease in Akt activation in siCFH condition compared to the negative control (siNeg) (Fig. 3.23 a).

Concerning the MAPK (Mitogen-activated protein kinase) signaling pathway, we investigated the extracellular signal-regulated kinases (Erk1/2) protein levels. This molecule is part of the Ras-Raf-MEK-ERK signaling cascade and known to be involved in cell survival, proliferation, migration and differentiation (Roskoski 2012). Here as well, activation levels were assessed *via* WB detecting the phosphorylated Erk1/2 and total Erk1/2 levels. For this component no significant changes were noticed in siCFH conditions compared to the respective control (siNeg) (Fig. 3.23 b). The MAPK signaling pathway can be divided into three main

MAP kinase cascades, the Erk1/2, c-jun N terminal kinase (JNK) and p38 signaling pathways. As JNK and p38 are considered to play a role in cell death and protection against cytokines and environmental stress and discussed to be involved activation of NF-κB (Schulze-Osthoff et al. 1997), it might be worth to investigate also these components in future studies.

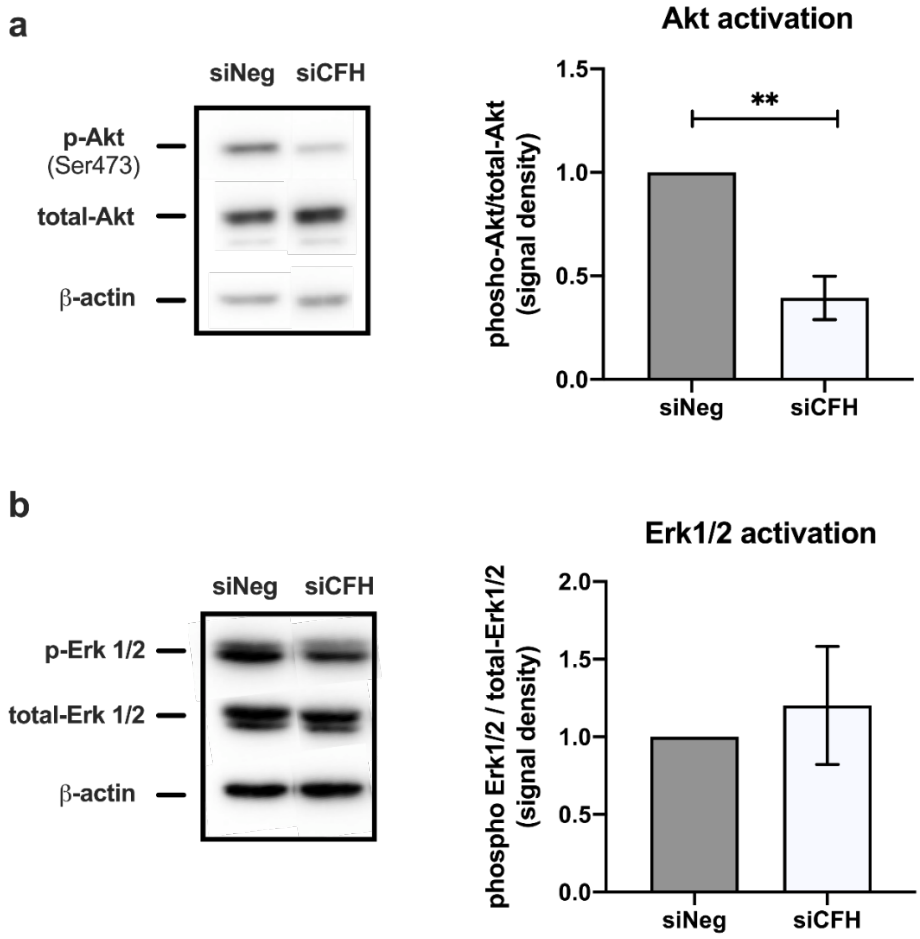

Figure 3.23: Activation levels of Akt and Erk1/2 proteins in cell lysates of FH deprived RPE cells
Cells (hTERT-RPE1) were seeded, cultured overnight and silenced for 24 h with either a negative control (siNeg) or siRNA specific for *CFH* (siCFH). Subsequently, the cells were maintained in serum-free medium (SFM) for 48 h, before collecting cell pellets for further processing.
a Western Blot (WB) image and quantification of phosphorylated (Ser473) and total levels of the Akt protein (60kDa) in cell lysates after 48 h. Actin as loading control (45kDa). After measuring the signal density, the ratio of phospho-Akt to total-Akt was calculated. Data show mean ± SEM and are generated from 3 independent experiments (n=3).
b Western Blot (WB) image and quantification of phosphorylated and total levels of the extracellular signal-regulated kinase (Erk1/2) protein (44, 42 kDa) in cell lysates after 48 h. Actin as loading control (45kDa). After measuring the signal density, the ratio of phospho-Erk1/2 to total-Erk1/2 was calculated. Data show mean ± SEM, n=3.
Significance levels assessed by student's t-test: **p<0.05, **p<0.01, *** p<0.001, ****p<0.0001.*

4 Discussion

Although AMD's pathogenesis is not yet fully understood and multiple factors contribute to its manifestation, there is solid evidence for the involvement of inflammation and complement system dysregulation. In line with this, one of the most important risk factors for AMD development and progression is a common single nucleotide polymorphism (SNP) in the complement factor H (*CFH*) gene ("Y402H polymorphism") (see 1.3.3). This polymorphism is known to go along with an impaired function of factor H (FH), which under normal conditions tightly regulates and acts as a major regulator of the alternative pathway of the complement system. However, the exact mechanism how FH impairment contributes to the progression of AMD has not been clarified yet.

In our studies we investigated whether there is a possible connection between a dysregulated function of FH, complement system activation and inflammation in RPE cells. In addition, we investigated the underlying signaling pathways. To do so, we employed a *CFH* knock-down model, that has previously been established by Armento et al. (2020), mimicking an almost complete loss of FH in hTERT-RPE1 cells.

4.1 Regulation of cytokines by FH

Our initial data showed a significant increase in the gene expression levels of the proinflammatory cytokines, interleukin 6 (IL6), interleukin 8 (CXCL8) and the c-c motif chemokine 2 (CCL2/MCP-1) in RPE cells under *CFH* knock-down. Additionally, we also found these cytokines to be elevated at protein level in cell culture supernatants. These findings indicate that FH loss led to the induction of a proinflammatory gene expression profile in RPE cells in our model, underlining the involvement of inflammation in the absence of FH. Indeed, RPE cells are known to be cytokine producers (e.g. IL-6, IL-8) and thus may contribute to ocular inflammation (Elner et al. 1992) (Holtkamp et al. 1998). While our study focused on RPE cells, elevated levels of IL-6 have also been found in the blood of AMD patients carrying the Y402H polymorphism (Mooijaart et al. 2007), which points towards an involvement of systematic inflammation in AMD pathogenesis (Cao

et al. 2013). Alterations in the *CFH* gene thus appear to be associated locally and/or systemically with increased inflammatory activity and highlight the involvement of FH in the connection between complement system and inflammation.

So far, the *CFH* Y402H polymorphism among others has been identified to affect the binding site to heparan sulfate (HS), going along with a decreased binding affinity (Clark and Bishop 2015) (see chapter 1.3.3). It has been speculated that the impaired binding of FH to HS, especially within Bruch's membrane, could result in an increased complement turnover and local inflammation (Clark and Bishop 2015). At present, however, the mechanism by which FH dysregulation contributes to inflammation has not yet been fully elucidated: it remains to be investigated whether this occurs *via* an over-activation of the complement system or in a yet unknown and non-canonical way.

Our observations of an increased cytokine production in the absence of FH led us to investigate the underlying signaling pathway mediating these effects. As the NF-κB signaling pathway is known to be one of the main pathways involved in inflammation and cell survival in many different cell types (Mitchell, 2016), we measured its activation levels by determining the ratio of phosphorylated to total p65. Indeed, we found the NF-κB signaling pathway to be consistently activated in FH deprived RPE cells.

To further prove whether FH modulates cytokine gene expression *via* the NF-κB pathway in RPE cells, we employed different strategies to inhibit this pathway by using chemical inhibitors, which turned out to be not successful (see chapter 1.4), and *via* silencing. The silencing was achieved *via* knock-down of the NF-κB p65 subunit (RELA gene) in control conditions (siRELA) and simultaneously with *CFH* (siCFH + siRELA). In our experiments, we observed that the effects mediated by *CFH* knock-down could be abolished by NF-κB knock-down, as cytokines expression levels of IL6, CXCL8 and CCL2 returned back to basal levels in double silenced conditions (siCFH + siRELA). This strongly supports our hypothesis that FH regulates the expression of inflammatory cytokines *via* the NF-κB signaling pathway.

Besides these effects, we also found gene expression levels of CXCL8 and CCL2 to be significantly downregulated by silencing RELA alone (siRELA). This indicates that NF-κB participates independently from FH in the regulation of these cytokines.

Interestingly, the NF-κB signaling pathway was also seen to be overactivated in ARPE19 cells in response to oxidative stress (H_2O_2 treatment) with concomitant increase in cytokines production and inflammasome activation (Macchioni et al. 2020), illustrating that the NF-κB pathway can be activated by various stimuli. Moreover, increased levels of IL-6, IL-8 and MCP-1 as well as NF-κB activation were observed in ARPE19 cells treated with serum containing human complement factors (Lueck et al. 2015). In line with our results, this group hypothesized that complement factors activated the NF-κB pathway in ARPE19 cells leading to an increased release of proinflammatory cytokines (Lueck et al. 2015). However, the role of FH was not elaborated.

Besides the observed proinflammatory cytokines (IL6, CXCL8, CCL2), we identified several other cytokines and chemokines to be expressed by RPE cells. These could be divided into three different groups: cytokines that (1) are dependent on FH and NF-κB, that (2) are dependent only on FH, and that (3) are expressed independently of FH and NF-κB. The following paragraphs are intended to briefly illustrate the function of the respective cytokines/chemokines and to provide a short overview with respect to already discussed knowledge about a possible involvement in retinal diseases like AMD.

In addition to IL-6, IL-8 and MCP-1, we found the granulocyte-macrophage stimulating factor (GM-CSF), the plasminogen activator inhibitor-1 (Serpin E1) and the C-X-C motif chemokine ligand 1 (CXCL1/GROα) to be elevated under the absence of FH, an effect that was abolished by NF-κB blockade.

GM-CSF is considered to be involved in the regulation of differentiation and activation of macrophages, granulocytes and dendritic cells and has been found to be produced by RPE cells in response to stimulation with IL-1β, TNFα and TGFβ (Crane et al. 1999). Elevated levels of GM-CSF in the vitreous of

postmortem human Y402H-carrying eyes point towards a link between GM-CSF and the Y402H polymorphism (Wang et al. 2015). This underlines our results, that FH dysregulation leads to a local production of GM-CSF in RPE cells. Moreover, we could identify the NF-κB pathway to be the underlying pathway in this context.

Serpin E1, also known as plasminogen activator inhibitor-1 (PAI-1), functions as an important regulator of the fibrinolytic system. Further, it has been reported to be involved in angiogenesis and to have a proangiogenic effect on choroidal neovascularization in diseases like diabetic retinopathy and neovascular AMD (Lambert et al. 2001). In addition, PAI-1 has been discussed as a marker and mediator of senescence, that is associated with age-related pathologies (Vaughan et al. 2017).

Moreover, the cytokine **CXCL1/GROα** follows the same trend. GROα is considered to be involved in angiogenesis and inflammation due to its chemoattracting function of neutrophils and interestingly, levels of GROα were observed to be elevated in the aqueous humor of AMD patients compared to controls (Agrawal et al. 2019).

In addition, we identified further cytokines, **MIP-1α/MIP-1β** (gene names: CCL3/CCL4) and the IL-1 receptor antagonist (**IL-1ra**), that were regulated by FH in RPE cells, but independent of NF-κB. RPE cells were described to produce both of these cytokines. CCL3 & CCL4 gene expression levels were shown to be increased after light damage (Rutar et al. 2015). Furthermore, IL-1ra was expressed much higher in mice RPE cells after stimulation with IL-1β and TNFα (Sugita et al. 2013). The fact, that NF-κB does not seem to be involved here, leads to the speculation, that other pathways or mechanisms are responsible for the observed changes (see also chapter 4.6).

Additionally, we found that RPE cells expressed macrophage migration inhibitor factor (MIF), interleukin 1a (IL-1a), interleukin 18 (IL-18) and interleukin 21 (IL-21), but expression levels were not impacted by *CFH* and/or RELA knock-down.

Taken together, dysregulation of FH in RPE cells led to an increased production of a variety of different cytokines, that all might contribute to the creation of a local pro-inflammatory microenvironment. Furthermore, the NF-κB signaling pathway has been identified to be a major driver. Possibly FH contributes to the regulation of the respective cytokines - directly or indirectly - *via* this signaling pathway.

4.2 Regulation of complement genes by FH

Besides the effects of FH dysregulation on cytokine expression levels, we investigated the role of FH on complement gene expression in RPE cells and evaluated the influence of the NF-κB signaling pathway in this context.

First, we could confirm results already obtained by Armento et al. (2020) as we found C3 mRNA and protein levels to be elevated under *CFH* knock-down. Moreover, subtotal FH loss led to a significant upregulation of *CFB* and *CFI* gene expression levels, while *C5* mRNA levels were downregulated.

The observed effects suggest that FH fulfills an important function in RPE cells by directly or indirectly regulating complement genes and contributing to complement system homeostasis. Disturbances of this system (e.g. mediated through FH loss) could lead to an imbalance of the whole system.

Interestingly, we identified the NF-κB pathway to be involved in the regulation of almost all the investigated complement factors. In line with this, the measured changes induced by *CFH* knock-down could be reversed by NF-κB blockade (siCFH + siRELA) for *C3*, *CFB* and *CFI*. It appears that FH plays a significant and critical role in the regulation of complement factors in RPE cells and mediates these effects *via* the NF-κB signaling pathway.

Evidence that NF-κB interferes with the regulation of the complement system has already been suggested in other cell types, e.g. in human intestinal epithelial cells, as it could be shown that IL1β increases the production of C3 *via* the NF-κB signaling pathway (Moon et al. 1999). Moreover, C3 has been identified to be a target of NF-κB in astroglia cells, as an upregulation of NF-κB and C3 levels in astroglia cells was observed after exposure to amyloid beta (Aβ) (Lian et al. 2015).

Evidence of complement gene regulation has also been discussed in RPE cells: Luo et al. identified RPE cells and microglia as an important source of complement gene expression and further suggested, that complement gene expression in primary RPE cells is regulated by inflammatory cytokines (e.g. INFγ, TNFα) (Luo, Chen, and Xu 2011). Furthermore, it was observed, that complement factors (like CFB, C3) were upregulated by INFγ, TNFα stimulation in RPE cells (Chen et al. 2008). While these works show a link between cytokine stimulation and the complement system, our work focuses on the role of FH in regard to the transcriptional balance of the complement system. Disturbances, e.g. mediated by FH dysregulation, might contribute to a dysbalance in the regulation of other complement factors. Further investigations are necessary to understand whether the increased inflammatory mediators in our model have an additional, possibly reinforcing influence on the effects already caused by FH loss.

In addition to the studies mentioned above, which mainly show a link between NF-κB/inflammation-induced changes in complement gene regulation, there is also considerable evidence for NF-κB activation in response to complement-mediated damage, mostly highlighting the pro-survival role of NF-κB. Gancz et al. (2012) found mouse embryonic fibroblasts (MEF) and HeLa cells lacking the NF-κB p65 subunit to be more susceptible to complement dependent cytotoxicity than wildtype controls. In this context they hypothesized the underlying mechanism to be located in a crosstalk between NF-κB and JNK, more specifically in the suppression of JNK-mediated cell death by NF-κB. Doing so, they emphasized the protective and antiapoptotic properties of NF-κB, rather than NF-κB being involved in inflammation or complement system regulation (Gancz, Lusthaus, and Fishelson 2012). Further, it was shown, that complement system activation, in form of MAC formation in HUVEC cells, led to proinflammatory effects by activation of NF-κB in a non-canonical way (Jane-wit et al. 2015). As can be noted, a number of possible connections between inflammation, complement regulation, complement injury and the involvement of NF-κB have

been drawn in previous studies. Nevertheless, none of these built up a connection with FH and FH dysregulation as a major regulator of the homeostasis of cytokines and complement components in RPE cells and identifies the NF-κB pathway as an important link in this context.

Moreover, we discovered that under NF-κB knock-down alone (siRELA condition), gene expression levels of *C3*, *C5* and *CFI* were significantly downregulated. This indicates that the NF-κB signaling pathway might participate in the regulation of these complement factors independently of FH.

CFH itself seems to be regulated by NF-κB. Upon NF-κB knock-down, we noticed a significant reduction of both, *CFH* gene expression as well as FH protein levels. Interestingly, RPE cells were found to constitutively produce FH and reduced mRNA levels of *CFH* in response to IL-6 and TNFα stimulation have been observed (Chen, Forrester, and Xu 2007). Whether NF-κB could also be the underlying signaling pathway in this case was not examined. In any case, future investigation could aim to clarify whether IL-6 or other cytokines are able to create a negative feedback loop for the expression of FH.

To summarize, we found FH to have the intrinsic ability to modulate the regulation of several complement system genes in RPE cells. Moreover, we could identify the NF-κB signaling pathway to be involved in the transcriptional regulation of these complement genes.

4.3 Regulation of antioxidant response & mitochondrial stability by FH

Since previous results of our group showed alterations in the antioxidant capacity and the energy metabolism of RPE cells under *CFH* knock-down (Armento et al., 2020), we additionally investigated whether the observed effects mediated by FH loss were dependent on the NF-κB signaling pathway. Therefore, we explored expression levels of the peroxisome proliferator-activated receptor gamma coactivator 1-alpha (PGC1α), an important marker for mitochondrial biogenesis, the glutathione peroxidase1 (GPX1), an important antioxidant enzyme, and the E3 ubiquitin-protein ligase parkin (PARKIN), a well-studied marker for mitophagy. We confirmed all these genes to be upregulated on gene expression level under

CFH knock-down (Armento et al. 2020), which highlights the role of endogenous FH in regard to antioxidant response and mitochondrial stability. However, NF-κB seems to be involved in the regulation of PGC1α, as only for this gene the effects mediated by FH loss could be abolished by NF-κB blockade. In contrast, the effects of FH loss on GPX1 and PARKIN levels were not counteracted by NF-κB blockade. PGC1α in RPE cells is described to possess protective properties against oxidative stress as it is known to induce a wide range of antioxidant enzymes, like GPX1 (Khadka, Iacovelli, and Saint-Geniez 2015). Further, PGC1α in RPE cells has been identified to have the ability to improve mitochondrial biogenesis and negatively regulate senescence, that normally is associated with mitochondrial dysfunction and related to the ageing processes (Kaarniranta et al. 2018).

There has been evidence of a connection between NF-κB and PGC1α in other cell types. In cardiac cells, the p65 subunit of NF-κB was shown to bind to PGC1α and thus to repress the activity of PGC1α (Alvarez-Guardia et al. 2010). In skeletal muscle cells PGC1α was observed to negatively affect the transcriptional activity of NF-κB (Eisele et al. 2013). In RPE cells, on the other hand, the NF-κB pathway has not been described in a regulatory context of PGC1α yet, especially not in regard to FH dysregulation and the complement system.

4.4 Chemical inhibition of NF-κB

Since we could identify the NF-κB pathway as a main driver in our model, we employed different strategies to inhibit this pathway on a chemical level (*via* addition of MG132, RAP, CAPE), also in order to examine the NF-κB pathway as a possible therapeutic target. When MG132 was applied, we observed a significant and strong increase in NF-κB activation levels. Through its function as a proteasome inhibitor, MG132 exerts its role as an NF-κB inhibitor rather nonspecifically, since the degradation of several other (metabolic) products is inhibited in addition to this process, which can disturb the cell's equilibrium and can cause cellular stress. Indeed, in our model MG132 seems to cause cellular stress. We observed strongly reduced cell viability and increased NF-κB

activation levels upon addition, possibly suggesting an additional activation of this pathway in its pro-survival role to protect the cells.

RAP was applied to test whether *CFH* modulates the NF-κB pathway by interfering with the RAGE receptor - HS axis (see chapter 3.2.1). With RAP treatment we did not detect any consistent changes in the gene expression levels or NF-κB activation. However, further examination of the proposed hypothesis would certainly be interesting in future studies. In this context a higher concentration of RAP or a possible modulation of the RAGE-HS interaction, possibly *via* enzymatic cleavage of the binding sites, may be considered.

Among the selected NF-κB inhibitors, CAPE is described to be the most specific. It is described to directly prevent the translocation of p65 into the nucleus and, thus, to prevent it from DNA binding (see chapter 3.2.3). However, also this inhibitor did not consistently block NF-κB activation in our model, neither in control conditions nor in siCFH condition. One possible explanation could be that the NF-κB signaling pathway, once activated, is rather difficult to influence by the addition of a chemical inhibitor, since we know that this pathway acts quickly and rapidly and is responsive to a wide range of stimuli. Furthermore, in comparable cell lines such as ARPE19 cells, CAPE was mostly applied for preincubation *prior* to a specific stimulus for NF-κB activation (Dinc, Ayaz, and Kurt 2017) (Paeng et al. 2015), whereas we added CAPE *after* the stimulus (in our case stimulus = silencing of *CFH*).

In summary, we couldn't achieve successful inhibition of NF-κB in our model by addition of different chemical inhibitors despite the use of different inhibitor concentrations and a range of different incubation times. In contrast, knock-down of NF-κB p65 proved to be more effective.

4.5 Effects of the addition of exogenous complement sources

In other studies, the exogenous addition of human complement serum was reported to influence complement activation and inflammation (Lueck et al. 2015). Therefore, we tested whether the addition of C3 or C3b could additionally influence inflammation and the complement system in our model. Besides, we

also investigated whether FH added exogenously has the ability to rescue the effects mediated by an internal loss of *CFH* (knock-down).

To do so, we measured the gene expression levels of *C3*, *CFB*, IL6 and CCL2, as well as NF-κB activation levels in RPE cells under control conditions (siNeg) and *CFH* knock-down (siCFH) after the addition of FH, C3, or its activated form C3b. Addition of either FH, C3 or C3b did not lead to significant changes in the expression levels of *C3*, *CFB* or IL6, CCL2 neither in control cells, nor in cells lacking *CFH* (siCFH condition). This strongly indicates that exogenous application of complement sources did not affect RPE cell physiology and the observed changes under *CFH* knock-down in our model: exogenously applied FH can't compensate the effects of an endogenous FH loss and isn't able to exert protective properties on RPE cells lacking the *CFH* gene. This finding points towards a novel role for endogenous FH as an important regulator of complement homeostasis/balance and cytokines gene expression in RPE cells. This observation could also give hints towards a potential intracellular complement system involvement, which has recently been the subject of increasing discussion by several authors. It has been speculated, that the complement system beside its external influence *via* the secreted complement factors, also intracellularly can be activated and impact functions regarding cell differentiation, metabolism, e.g. in T-cells (Reichhardt and Meri 2018), and can be involved in other host cell functions (Liszewski et al. 2017).

Further, no effects on gene expression levels were observed by addition of exogenous C3 or C3b. This indicates that exogenous addition can't additionally increase and trigger complement system activation and the inflammatory response neither in control nor in *CFH* knock-down conditions in our model. This finding is consistent with previous reports that RPE cells have a certain tolerance level to complement induced damage with respect to their location and function. RPE cells have been reported to possess specific membrane complement regulatory proteins (mCRPs), like CD46, CD55, and CD59, in order to protect themselves from complement mediated attack (Yang et al. 2009).

Moreover, we didn't detect any changes in activation levels of NF-κB by addition of FH, C3 or C3b compared with the respective controls (siNeg, siCFH). This goes along with our findings that the addition of external complement sources (FH, C3, C3b) neither influences complement system genes or cytokine expression levels under control conditions nor has an effect on them - stimulating or rescuing - once the system is dysbalanced (siCFH).

Put together, all of our results highlight the important role of endogenous FH in RPE cells, as we could show that the regulation of complement and cytokine gene expression, as well as NF-κB activation levels, in RPE cells in our model was independent of external complement stimulation.

4.6 Additional pathways altered by FH loss

In our model we could identify several cytokines/chemokines to be dependent on FH and NF-κB. Other cytokines altered by *CFH* knock-down, in contrast, were found to be independent of NF-κB. For a disease as complex as AMD, it seems unlikely that only one signaling pathway underlies the whole process. In the literature there are several pathways discussed to be affected in AMD, including the PI3K/Akt and MAPK pathway (see chapter 1.5). Both of them play a role in cell survival, proliferation and growth, and are implicated in processes like oxidative stress and inflammation. Hence, we investigated whether FH loss affected activation levels of Akt and the MAP-Kinase, Erk1/2. A possible connection between complement system activation and these pathways has been shown in previous studies, as the anaphylatoxins C3a and C5a were described to strongly increase activation levels of Erk1/2 in HUVEC cells (MONSINJON et al. 2003). Further, C3a was identified to mediate chemokine production in human mast cells by Erk1/2 and Akt phosphorylation (Venkatesha et al. 2005). C3a and C5a mediated induction of Erk1/2 as well as Akt phosphorylation was also observed in human mesenchymal stem cells (Schraufstatter et al. 2009). As can be seen, a link between the two signaling pathways (Akt, Erk1/2) and specific complement components (C3a, C5a) has

been demonstrated in different cell lines. Nevertheless, the effects of FH in this context have not been clarified.

In our experiments we observed a significant reduction in Akt phosphorylation (Ser473) upon *CFH* knock-down, indicating that this pathway might be downregulated in the absence of FH.

Interestingly, FH was identified to exert protective properties in the kidney by activation of the PI3K/Akt signaling pathway (Hu et al. 2018). This group noticed complement activation to play a role in the pathogenesis of renal ischemia reperfusion injury (IRI) and observed that the addition of the complement inhibitor FH (conjugated with the complement receptor CRIg) mitigated renal IRI by activation of the PI3K/Akt pathway in their mouse model. Activation of PI3K/Akt thereby led to an inhibition of glomerular/renal apoptosis and improved the dysregulated production of cytokines, that they observed in the context of renal IRI. Thus, they found p-Akt (S473) levels to be nearly 2-fold elevated under FH treatment (Hu et al. 2018). Interestingly, we found a similar dependency in our model, but in the opposite manner: under FH loss, we experienced a reduction in Akt phosphorylation levels by about half. Both findings can interlink with each other and may lead to the hypothesis that FH can fulfill a protective role in cells by activation of pro-survival pathways like the Akt signaling axis, a process that is disturbed under FH loss. In addition, Yang et al. (2006) suggested an activation of Akt as a pro-survival mechanism to protect RPE cells from oxidant-induced injury. Thereby, they reported Akt activation in response to oxidative stress (H_2O_2 treatment) (Yang et al. 2006) and did not connect Akt to complement system dysregulation.

Since it is known that Akt and the mechanistic target of rapamycin kinase (mTOR) are closely connected and abnormal mTOR activation has been reported to be involved in RPE degeneration (Huang et al. 2019) as well as mTOR has been speculated to be involved in the context of intracellular complement system activation (Ebeling et al. 2021), it might be worth to additionally investigate the mTOR pathway in regard to FH dysregulation in our model in future experiments.

Concerning the MAPK signaling pathway, we investigated levels of the extracellular signal-regulated kinase, Erk1/2, a component of the MAPK signaling cascade. Thereby we couldn't observe any significant changes in the activation levels of Erk1/2. As previously mentioned, the Erk1/2 component was found to be activated in response to complement anaphylatoxins, like C3a and C5a. Further, Busch et al. (2018) investigated the effects of human complement serum (HCS) addition on the activation of the Erk1/2 pathway in ARPE19 cells. In addition to treatment with HCS, the cells were pretreated with UV-irradiated photoreceptor outer segments (UV-POS). Thereby, they observed an increase in Erk1/2 activation levels under UV-POS and HCS treatment, but no changes in Erk1/2 activation under HCS treatment alone (Busch et al. 2018). Moreover, they observed that HCS treatment led to an increase in cytokines like IL-6, IL-8 and MCP-1, but that this process was independent of UV-POS addition. Their findings led them to the conclusion that Erk1/2 does not seem to be the pathway that mediates the effects in response to complement stimulation in ARPE19 cells. The Erk1/2 axis instead seems to be more involved in the regulation of oxidative and cellular stress response (Busch et al. 2018). These findings are consistent with our results, as we found no changes in the Erk1/2 axis due to FH loss as well, which may be accompanied by an increased complement turnover. Furthermore, speculation arises whether the HCS-induced increase in inflammatory mediators that Busch et al. observed could also be mediated by the NF-κB pathway, as we were able to identify this signaling pathway in our model to be responsible for the upregulation of proinflammatory cytokines. As is known, there are two other important MAPK subfamily pathways in addition to the Erk pathway: the c-jun N terminal kinase (JNK) and the p38 pathway (Schulze-Osthoff et al. 1997), which both could be interesting to investigate in further studies - especially since JNK and p38 have been described to participate in the activation of NF-κB and to play a key and protective role in the regulation of inflammatory processes (Schulze-Osthoff et al. 1997).

In summary, we did elaborate on the role of FH on the Akt and MAPK/Erk pathway. Besides the NF-κB pathway, we could identify the Akt pathway to be

affected by FH dysregulation, whereas the Erk1/2 pathway seems to be not altered. For future investigations it might be worth to investigate the impact of FH on other up-/downstream components in the Akt pathway, like for example mTOR, and, regarding the MAPK pathway, to also examine other subfamilies, such as p38 in more detail.

4.7 Conclusion & outlook

In this thesis, the influence of FH on the regulation of cytokines and complement system factors in RPE cells was examined and first mechanistic insights into the underlying pathways could be gained.

We were able to demonstrate that *CFH* knock-down is associated with numerous changes in the expression pattern of various cytokines. Hence, *CFH* knock-down leads to a strong increase in cytokines and chemokines (e.g. IL-6, IL-8, MCP-1, GM-CSF etc.) in RPE cells. In addition, dysregulation of FH leads to a misbalance in the transcription pattern of various complement system genes (C3↑, CFB↑, CFI↑, C5↓), suggesting that FH participates in the regulation of complement system genes in RPE cells. It is important to emphasize that the observed effects are attributed to endogenous FH in RPE cells, considering in particular that the addition of external complement sources (FH, C3, C3b) did not affect RPE cells, neither under control nor under *CFH* knock-down conditions. The reported effects point out FH, especially endogenous FH, as a major player responsible for RPE cell homeostasis and balance. FH seems to have the intrinsic ability to modulate inflammatory processes and complement system balance in RPE cells.

We could further give insights into the underlying signaling pathways altered by FH dysregulation in RPE cells. The NF-κB signaling pathway was thereby identified to mediate the effects of *CFH* knock-down. We could show this pathway to be responsible for the regulation of inflammatory factors and for the balance of complement genes. Thus, FH seems to regulate the levels of inflammatory cytokines/chemokines and several complement system components in RPE cells *via* the NF-κB signaling pathway.

Besides, phosphorylation levels of Akt were significantly reduced under *CFH* knock-down, which might be explained due to a protective role of FH on RPE cells through an activation of Akt in a pro-survival manner, a process that is disturbed when FH is dysregulated.

Of course, the RPE cell model that we employ is limited in its ability to reflect the complex nature of a disease such as AMD, which is strongly dependent on the interplay of the different tissues and layers in the eye. Therefore, it might be worth to perform further experiments in an extended model, e.g. in a coculture model of cultured RPE cells with porcine retinal explant, or in other cell lines, like iPSC-RPE cells. Conclusions regarding potential therapeutics, so far, still remain premature. However, the knowledge acquired on mechanisms altered by FH dysregulation in RPE cells can be an important impetus for further research with the long-term goal of developing therapeutic options through a better understanding of the complex mechanisms involved in this disease.

As an outlook, an important aspect to be clarified is the chain of causality involved. While we know that oxidative stress, inflammation and complement dysregulation, among others, all account for changes and damage in RPE cells, it remains unclear which mechanism is altered first, and how exactly the changes are connected with each other. For future studies, it will certainly be a challenge to identify feedback loops, that reinforce or counteract each other.

Also, the exact mechanisms by which FH assists to maintain cellular balance and by which FH dysregulation leads to the observed alterations still need to be further investigated. It is certainly of interest to clarify whether the alterations of FH dysregulation are due to an over-activation of the complement system (loss of FH = loss of protection against uncontrolled complement activation) or whether FH acts in a non-canonical way, possibly with endogenous FH intervening intracellularly in the regulation of the mentioned components in a yet unknown way.

The main results of this work are graphically illustrated in figure 4.1.

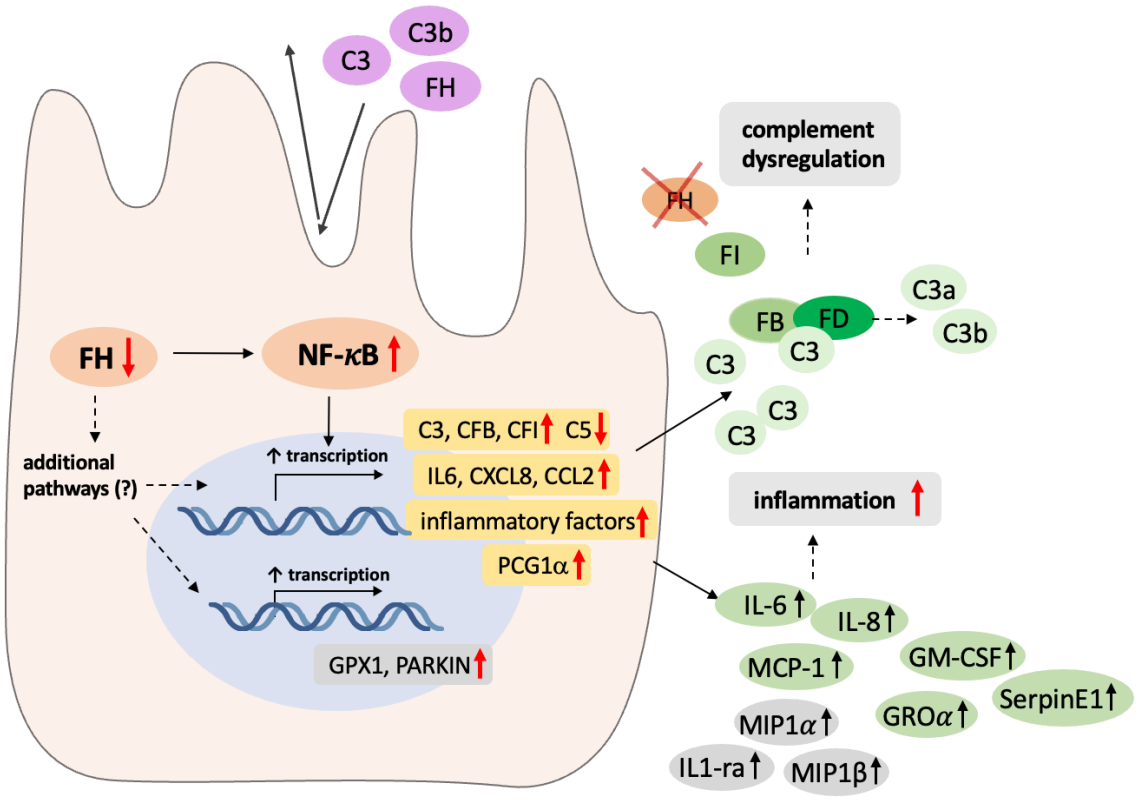

Figure 4.1: Effects of *CFH* knock-down on RPE cells
FH dysregulation, induced by *CFH* knock-down, in RPE cells leads to the activation of the NF-κB pathway (orange). This in turn causes changes in the expression pattern of several inflammatory (e.g. IL6, IL8, CCL2) and complement system factors on mRNA (yellow) and protein level (green & grey). Alterations that were directly dependent on NF-κB are highlighted in yellow and green. Genes and cytokines that were not regulated by NF-κB are labeled in grey, which can be an indication for other signaling pathways being involved. Addition of exogenous complement sources, like C3, C3b or FH (purple), did not affect the processes mediated by endogenous *CFH* knock-down.

5 Summary

Purpose: Age-related macular degeneration (AMD) constitutes the leading cause of blindness among the elderly worldwide. To date, due to the complex nature of the disease, the exact pathogenesis is not yet fully understood. Ageing, lifestyle and genetic components are considered important risk factors. In particular, a number of single nucleotide polymorphisms (SNP) have been identified in complement system genes, particularly in the complement factor H (*CFH*) gene, that are associated with an increased risk for AMD. The purpose of this study was to investigate the function of the *CFH* protein (FH) in the regulation of inflammatory processes and the complement system in retinal pigment epithelium (RPE) cells. Furthermore, we aimed to identify the cellular signaling pathways influenced by endogenous FH dysregulation in RPE cells.

Methods: The *CFH* gene was knocked-down in human RPE cells (hTERT-RPE1) in order to mimic an almost complete loss of the FH protein. We investigated the effects of FH dysregulation on the gene expression levels of several cytokines (IL6, CXCL8, CCL2) and complement system factors (*C3*, *C5*, *CFB*, *CFI*). To examine the effects of exogenous complement sources, FH, C3 or C3b were supplemented to the cell culture media. Phosphorylated and total NF-κB p65 levels were measured *via* Western Blot (WB). To further study the NF-κB pathway under FH deprived conditions, several NF-κB inhibitors were employed (RAP, MG132, CAPE), as well as knock-down of the p65 NF-κB subunit (RELA gene). Besides, activation levels of the Akt and MAPK/Erk signaling pathways under *CFH* knock-down were examined *via* WB.

Results: Under *CFH* knock-down (siCFH) in RPE cells, we detected a significant increase in proinflammatory factors at gene and protein level (IL-6, IL-8, MCP-1, GM-CSF, etc.). In addition, we observed a dysregulation in the transcription pattern of several complement system genes. FH dysregulation in RPE cells led to an increase in levels of *C3, CFB, CFI,* and to a decrease in *C5*. All of these changes were independent of the addition of exogenous complement factors (FH, C3 or C3b). Activation levels of NF-κB were significantly increased under *CFH*

knock-down. Silencing of NF-κB p65 reversed the observed changes under *CFH* knock-down in most cytokines and complement components. In addition, we found the activation levels of Akt decreased by siCFH, whereas we did not observe any effect on Erk activation levels.

Conclusion: In RPE cells, endogenous FH has the intrinsic ability to modulate the expression of several inflammatory and complement system factors. Dysregulation of FH leads to an increase in proinflammatory cytokines and a misbalance of factors of the complement system in a NF-κB dependent manner. Our findings suggest that FH and the NF-κB pathway are involved in maintaining inflammatory and complement system homeostasis in RPE cells. Dysregulation of either one of them, likely causes a loss of balance in the complement system and leads to a shift in RPE cells towards a pro-inflammatory AMD-like phenotype.

6 Zusammenfassung (German)

Hintergrund: Die altersbedingte Makuladegeneration (AMD) ist weltweit die häufigste Ursache für Erblindung bei älteren Menschen. Aufgrund der komplexen Natur der Erkrankung ist die genaue Pathogenese bis heute nicht vollständig geklärt. Alter, Lebensstil und genetische Komponenten werden als wichtige Risikofaktoren angesehen. Insbesondere wurde eine Reihe von Einzelnukleotid-Polymorphismen (SNP) in Genen des Komplementsystems, vor allem im Gen des Komplementfaktors H (*CFH*), identifiziert, die mit einem erhöhten Risiko für AMD assoziiert sind. Das Ziel dieser Studie war es, die Funktion des *CFH* Proteins (FH) bei der Regulation von Entzündungsprozessen und des Komplementsystems in retinalen Pigmentepithelzellen (RPE) zu untersuchen. Außerdem war es unser Ziel, die zellulären Signalwege zu identifizieren, die durch eine gestörte Funktion von endogenem FH in RPE Zellen beeinflusst werden.

Methoden: Das *CFH* Gen wurde in humanen RPE Zellen (hTERT-RPE1) herunter-geknockt, um einen nahezu vollständigen Verlust des FH Proteins zu imitieren. Wir untersuchten die Auswirkungen einer Dysregulation von FH auf die Genexpressionslevel verschiedener Zytokine (IL6, CXCL8, CCL2 etc.) und Komponenten des Komplementsystems (C3, C5, CFB, CFI). Um die Auswirkungen exogener Komplementfaktoren zu untersuchen, wurde FH, C3 oder C3b zu den Zellkulturmedien hinzugefügt. Der Gehalt an phosphoryliertem und totalem NF-κB p65 wurde mittels Western Blot (WB) bestimmt. Um den NF-κB Signalweg unter FH deprivierten Bedingungen weiter zu erforschen, wurden verschiedene NF-κB Inhibitoren (RAP, MG132, CAPE) verwendet, sowie ein Knock-down der p65 NF-κB Untereinheit (RELA Gen) durchgeführt. Außerdem wurden die Aktivitätsniveaus des Akt und des MAPK/Erk Signalwegs unter *CFH* Knock-down mittels WB untersucht.

Ergebnisse: Unter *CFH* Knock-down (siCFH) detektierten wir einen signifikanten Anstieg von proinflammatorischen Faktoren auf Gen- und Proteinebene (IL-6, IL-8, MCP-1, GM-CSF, etc.) in RPE Zellen. Darüber hinaus beobachteten wir eine

Dysregulation im Transkriptionsmuster mehrerer Komplementsystem Gene. FH Dysregulation in RPE Zellen führte zu einem Anstieg der Level von *C3*, *CFB*, *CFI* und zu einer Abnahme von *C5*. Alle diese Veränderungen waren unabhängig von der Zugabe von exogenen Komplementfaktoren (FH, C3 oder C3b). Das Aktivitätsniveau von NF-κB war unter *CFH* Knock-down signifikant erhöht. Eine Blockade der NF-κB p65 Einheit machte die beobachteten Veränderungen unter *CFH* Knock-down bei den meisten Zytokinen und Komplementfaktoren rückgängig. Zudem beobachteten wir, dass das Aktivitätsniveau von Akt unter siCFH Bedingungen verringert war, während wir keinen Effekt auf das Aktivitätsniveau von Erk beobachteten.

Schlussfolgerung: Endogenes FH in RPE Zellen hat die intrinsische Fähigkeit, die Expression verschiedener Entzündungsmediatoren und Faktoren des Komplementsystems zu modulieren. Eine gestörte Funktion von FH führt in einer NF-κB abhängigen Weise zu einem Anstieg von proinflammatorischen Zytokinen und einem Ungleichgewicht von Faktoren des Komplementsystems. Unsere Ergebnisse legen nahe, dass FH und der NF-κB Signalweg an der Aufrechterhaltung der Homöostase des Entzündungs- und Komplementsystem in RPE Zellen beteiligt sind. Eine Dysregulation von einem der beiden führt zu einem Verlust des Gleichgewichts des Komplementsystems und zu einer Verschiebung innerhalb der RPE Zellen in Richtung eines pro-inflammatorischen AMD-ähnlichen Phänotyps.

7 Publications

- Armento, Angela*, Tiziana L. Schmidt*, Inga Sonntag, David A. Merle, Mohamed Ali Jarboui, Ellen Kilger, Simon J. Clark, and Marius Ueffing. 2021. 'CFH Loss in Human RPE Cells Leads to Inflammation and Complement System Dysregulation via the NF-κB Pathway', *International journal of molecular sciences*, 22: 8727. https://doi.org/10.3390/ijms22168727

  *These authors contributed equally to this work.

  (Armento, Schmidt et al. 2021)

8 References

Agrawal, Rupesh, Praveen Kumar Balne, Xin Wei, Veonice Au Bijin, Bernett Lee, Arkasubhra Ghosh, Raja Narayanan, Mukesh Agrawal, and John Connolly. 2019. 'Cytokine Profiling in Patients With Exudative Age-Related Macular Degeneration and Polypoidal Choroidal Vasculopathy', *Investigative Ophthalmology & Visual Science*, 60: 376-82.

Alvarez-Guardia, D., X. Palomer, T. Coll, M. M. Davidson, T. O. Chan, A. M. Feldman, J. C. Laguna, and M. Vázquez-Carrera. 2010. 'The p65 subunit of NF-kappaB binds to PGC-1alpha, linking inflammation and metabolic disturbances in cardiac cells', *Cardiovasc Res*, 87: 449-58.

Armento, A., S. Honisch, V. Panagiotakopoulou, I. Sonntag, A. Jacob, S. Bolz, E. Kilger, M. Deleidi, S. Clark, and M. Ueffing. 2020. 'Loss of Complement Factor H impairs antioxidant capacity and energy metabolism of human RPE cells', *Sci Rep*, 10: 10320.

Armento, A., M. Ueffing, and S. J. Clark. 2021. 'The complement system in age-related macular degeneration', *Cell Mol Life Sci*.

Armento, Angela, Tiziana L. Schmidt, Inga Sonntag, David A. Merle, Mohamed Ali Jarboui, Ellen Kilger, Simon J. Clark, and Marius Ueffing. 2021. 'CFH Loss in Human RPE Cells Leads to Inflammation and Complement System Dysregulation via the NF-κB Pathway', *International journal of molecular sciences*, 22: 8727.

Arumugam, Thiruvengadam, Vijaya Ramachandran, Sobeyda B. Gomez, Ann M. Schmidt, and Craig D. Logsdon. 2012. 'S100P-derived RAGE antagonistic peptide reduces tumor growth and metastasis', *Clinical cancer research : an official journal of the American Association for Cancer Research*, 18: 4356-64.

Beatty, S., H. Koh, M. Phil, D. Henson, and M. Boulton. 2000. 'The role of oxidative stress in the pathogenesis of age-related macular degeneration', *Surv Ophthalmol*, 45: 115-34.

Blackmore, T. K., T. A. Sadlon, H. M. Ward, D. M. Lublin, and D. L. Gordon. 1996. 'Identification of a heparin binding domain in the seventh short consensus repeat of complement factor H', *J Immunol*, 157: 5422-7.

Boulton, M., and P. Dayhaw-Barker. 2001. 'The role of the retinal pigment epithelium: topographical variation and ageing changes', *Eye (Lond)*, 15: 384-9.

Bourne, R. R., J. B. Jonas, S. R. Flaxman, J. Keeffe, J. Leasher, K. Naidoo, M. B. Parodi, K. Pesudovs, H. Price, R. A. White, T. Y. Wong, S. Resnikoff, and H. R. Taylor. 2014. 'Prevalence and causes of vision loss in high-income countries and in Eastern and Central Europe: 1990-2010', *Br J Ophthalmol*, 98: 629-38.

Busch, M., S. Wasmuth, G. Spital, A. Lommatzsch, and D. Pauleikhoff. 2018. 'Activation of the ERK1/2-MAPK Signaling Pathway by Complement Serum in UV-POS-Pretreated ARPE-19 Cells', *Ophthalmologica*, 239: 215-24.

Campochiaro, P. A. 2013. 'Ocular neovascularization', *J Mol Med (Berl)*, 91: 311-21.
Cao, S., J. C. Wang, J. Gao, M. Wong, E. To, V. A. White, J. Z. Cui, and J. A. Matsubara. 2016. 'CFH Y402H polymorphism and the complement activation product C5a: effects on NF-κB activation and inflammasome gene regulation', *Br J Ophthalmol*, 100: 713-8.
Cao, Sijia, Ashley Ko, Marita Partanen, Kaivon Pakzad-Vaezi, Andrew B. Merkur, David A. Albiani, Andrew W. Kirker, Aikun Wang, Jing Z. Cui, Farzin Forooghian, and Joanne A. Matsubara. 2013. 'Relationship between systemic cytokines and complement factor H Y402H polymorphism in patients with dry age-related macular degeneration', *American journal of ophthalmology*, 156: 1176-83.
Chen, M., J. V. Forrester, and H. Xu. 2007. 'Synthesis of complement factor H by retinal pigment epithelial cells is down-regulated by oxidized photoreceptor outer segments', *Exp Eye Res*, 84: 635-45.
Chen, M., E. Muckersie, M. Robertson, J. V. Forrester, and H. Xu. 2008. 'Up-regulation of complement factor B in retinal pigment epithelial cells is accompanied by complement activation in the aged retina', *Exp Eye Res*, 87: 543-50.
Chirco, K. R., E. H. Sohn, E. M. Stone, B. A. Tucker, and R. F. Mullins. 2017. 'Structural and molecular changes in the aging choroid: implications for age-related macular degeneration', *Eye (Lond)*, 31: 10-25.
Christian, F., E. L. Smith, and R. J. Carmody. 2016. 'The Regulation of NF-κB Subunits by Phosphorylation', *Cells*, 5.
Clark, S. J., and P. N. Bishop. 2015. 'Role of Factor H and Related Proteins in Regulating Complement Activation in the Macula, and Relevance to Age-Related Macular Degeneration', *J Clin Med*, 4: 18-31.
Clark, S. J., P. N. Bishop, and A. J. Day. 2010. 'Complement factor H and age-related macular degeneration: the role of glycosaminoglycan recognition in disease pathology', *Biochem Soc Trans*, 38: 1342-8.
Clark, S. J., V. A. Higman, B. Mulloy, S. J. Perkins, S. M. Lea, R. B. Sim, and A. J. Day. 2006. 'His-384 allotypic variant of factor H associated with age-related macular degeneration has different heparin binding properties from the non-disease-associated form', *J Biol Chem*, 281: 24713-20.
Clark, S. J., R. Perveen, S. Hakobyan, B. P. Morgan, R. B. Sim, P. N. Bishop, and A. J. Day. 2010. 'Impaired binding of the age-related macular degeneration-associated complement factor H 402H allotype to Bruch's membrane in human retina', *J Biol Chem*, 285: 30192-202.
Colijn, Johanna M., Gabriëlle H. S. Buitendijk, Elena Prokofyeva, Dalila Alves, Maria L. Cachulo, Anthony P. Khawaja, Audrey Cougnard-Gregoire, Bénédicte M. J. Merle, (…), Christian Wolfram, Jennifer Yip, Jennyfer Zerbib, and Isabella Zwiener. 2017. 'Prevalence of Age-Related Macular Degeneration in Europe: The Past and the Future', *Ophthalmology*, 124: 1753-63.
Crane, I. J., M. C. Kuppner, S. McKillop-Smith, C. A. Wallace, and J. V. Forrester. 1999. 'Cytokine regulation of granulocyte-macrophage colony-

stimulating factor (GM-CSF) production by human retinal pigment epithelial cells', *Clinical and experimental immunology*, 115: 288-93.
Curcio, Christine A., and Mark Johnson. 2013. 'Chapter 20 - Structure, Function, and Pathology of Bruch's Membrane.' in Stephen J. Ryan, SriniVas R. Sadda, David R. Hinton, Andrew P. Schachat, SriniVas R. Sadda, C. P. Wilkinson, Peter Wiedemann and Andrew P. Schachat (eds.), *Retina (Fifth Edition)* (W.B. Saunders: London).
Datta, S., M. Cano, K. Ebrahimi, L. Wang, and J. T. Handa. 2017. 'The impact of oxidative stress and inflammation on RPE degeneration in non-neovascular AMD', *Prog Retin Eye Res*, 60: 201-18.
Detrick, Barbara, and John J. Hooks. 2020. 'The RPE Cell and the Immune System.' in Alexa Karina Klettner and Stefan Dithmar (eds.), *Retinal Pigment Epithelium in Health and Disease* (Springer International Publishing: Cham).
Dinc, Erdem, Lokman Ayaz, and Akif Hakan Kurt. 2017. 'Protective Effect of Combined Caffeic Acid Phenethyl Ester and Bevacizumab Against Hydrogen Peroxide-Induced Oxidative Stress in Human RPE Cells', *Current Eye Research*, 42: 1659-66.
Ebeling, Mara C., Zhaohui Geng, Rebecca J. Kapphahn, Heidi Roehrich, Sandra R. Montezuma, James R. Dutton, and Deborah A. Ferrington. 2021. 'Impaired Mitochondrial Function in iPSC-Retinal Pigment Epithelium with the Complement Factor H Polymorphism for Age-Related Macular Degeneration', *Cells*, 10: 789.
Edwards, A. O., R. Ritter, 3rd, K. J. Abel, A. Manning, C. Panhuysen, and L. A. Farrer. 2005. 'Complement factor H polymorphism and age-related macular degeneration', *Science*, 308: 421-4.
Eisele, Petra S., Silvia Salatino, Jens Sobek, Michael O. Hottiger, and Christoph Handschin. 2013. 'The peroxisome proliferator-activated receptor γ coactivator 1α/β (PGC-1) coactivators repress the transcriptional activity of NF-κB in skeletal muscle cells', *The Journal of biological chemistry*, 288: 2246-60.
Elner, V. M., W. Scales, S. G. Elner, J. Danforth, S. L. Kunkel, and R. M. Strieter. 1992. 'Interleukin-6 (IL-6) gene expression and secretion by cytokine-stimulated human retinal pigment epithelial cells', *Exp Eye Res*, 54: 361-8.
Fletcher, Erica L. 2020. 'Contribution of microglia and monocytes to the development and progression of age related macular degeneration', *Ophthalmic and Physiological Optics*, 40: 128-39.
Fritsche, L. G., W. Igl, J. N. Bailey, F. Grassmann, S. Sengupta, J. L. Bragg-Gresham, K. P. Burdon, S. J. Hebbring, C. Wen, M. Gorski, I. K. Kim, D. Cho, D. Zack, E. Souied, H. P. Scholl, E. Bala, K. E. Lee, D. J. Hunter, R. J. Sardell, P. Mitchell, J. E. Merriam, V. Cipriani, J. D. Hoffman, T. Schick, Y. T. Lechanteur, (…), D. A. Schaumberg, B. E. Klein, S. A. Hagstrom, I. Chowers, A. J. Lotery, T. Leveillard, K. Zhang, M. H. Brilliant, A. W. Hewitt, A. Swaroop, E. Y. Chew, M. A. Pericak-Vance, M. DeAngelis, D. Stambolian, J. L. Haines, S. K. Iyengar, B. H. Weber, G.

R. Abecasis, and I. M. Heid. 2016. 'A large genome-wide association study of age-related macular degeneration highlights contributions of rare and common variants', *Nat Genet*, 48: 134-43.
Gancz, Dana, Michal Lusthaus, and Zvi Fishelson. 2012. 'A Role for the NF-κB Pathway in Cell Protection from Complement-Dependent Cytotoxicity', *The Journal of Immunology*, 189: 860.
Gordon, D. L., R. M. Kaufman, T. K. Blackmore, J. Kwong, and D. M. Lublin. 1995. 'Identification of complement regulatory domains in human factor H', *J Immunol*, 155: 348-56.
Haines, J. L., M. A. Hauser, S. Schmidt, W. K. Scott, L. M. Olson, P. Gallins, K. L. Spencer, S. Y. Kwan, M. Noureddine, J. R. Gilbert, N. Schnetz-Boutaud, A. Agarwal, E. A. Postel, and M. A. Pericak-Vance. 2005. 'Complement factor H variant increases the risk of age-related macular degeneration', *Science*, 308: 419-21.
Hayden, M. S., and S. Ghosh. 2008. 'Shared principles in NF-kappaB signaling', *Cell*, 132: 344-62.
Heesterbeek, T. J., L. Lorés-Motta, C. B. Hoyng, Y. T. E. Lechanteur, and A. I. den Hollander. 2020. 'Risk factors for progression of age-related macular degeneration', *Ophthalmic Physiol Opt*, 40: 140-70.
Hemmings, Brian A., and David F. Restuccia. 2012. 'PI3K-PKB/Akt pathway', *Cold Spring Harbor perspectives in biology*, 4: a011189-a89.
Holtkamp, G. M., A. Kijlstra, R. Peek, and A. F. de Vos. 2001. 'Retinal pigment epithelium-immune system interactions: cytokine production and cytokine-induced changes', *Prog Retin Eye Res*, 20: 29-48.
Holtkamp, G. M., M. Van Rossem, A. F. de Vos, B. Willekens, R. Peek, and A. Kijlstra. 1998. 'Polarized secretion of IL-6 and IL-8 by human retinal pigment epithelial cells', *Clin Exp Immunol*, 112: 34-43.
Howes, Kimberly A., Yang Liu, Joshua L. Dunaief, Ann Milam, Jeanne M. Frederick, Alexander Marks, and Wolfgang Baehr. 2004. 'Receptor for Advanced Glycation End Products and Age-Related Macular Degeneration', *Investigative Ophthalmology & Visual Science*, 45: 3713-20.
Hu, Chao, Long Li, Peipei Ding, Ling Li, Xiaowen Ge, Long Zheng, Xuanchuan Wang, Jina Wang, Weitao Zhang, Na Wang, Hongyu Gu, Fan Zhong, Ming Xu, Ruiming Rong, Tongyu Zhu, and Weiguo Hu. 2018. 'Complement Inhibitor CRIg/FH Ameliorates Renal Ischemia Reperfusion Injury via Activation of PI3K/AKT Signaling', *Journal of immunology (Baltimore, Md. : 1950)*, 201: 3717-30.
Huang, Jiancheng, Shun Gu, Meng Chen, Shu-Jie Zhang, Zhichun Jiang, Xue Chen, Chao Jiang, Guohua Liu, Roxana A. Radu, Xiantao Sun, Douglas Vollrath, Jianhai Du, Biao Yan, and Chen Zhao. 2019. 'Abnormal mTORC1 signaling leads to retinal pigment epithelium degeneration', *Theranostics*, 9: 1170-80.
Hussain, A. A., C. Starita, A. Hodgetts, and J. Marshall. 2010. 'Macromolecular diffusion characteristics of ageing human Bruch's membrane:

implications for age-related macular degeneration (AMD)', *Exp Eye Res*, 90: 703-10.
Jane-wit, D., Y. V. Surovtseva, L. Qin, G. Li, R. Liu, P. Clark, T. D. Manes, C. Wang, M. Kashgarian, N. C. Kirkiles-Smith, G. Tellides, and J. S. Pober. 2015. 'Complement membrane attack complexes activate noncanonical NF-κB by forming an Akt+ NIK+ signalosome on Rab5+ endosomes', *Proc Natl Acad Sci U S A*, 112: 9686-91.
Jarrett, S. G., and M. E. Boulton. 2012. 'Consequences of oxidative stress in age-related macular degeneration', *Mol Aspects Med*, 33: 399-417.
Jonasson, F., D. E. Fisher, G. Eiriksdottir, S. Sigurdsson, R. Klein, L. J. Launer, T. Harris, V. Gudnason, and M. F. Cotch. 2014. 'Five-year incidence, progression, and risk factors for age-related macular degeneration: the age, gene/environment susceptibility study', *Ophthalmology*, 121: 1766-72.
Kaarniranta, Kai, Jakub Kajdanek, Jan Morawiec, Elzbieta Pawlowska, and Janusz Blasiak. 2018. 'PGC-1α Protects RPE Cells of the Aging Retina against Oxidative Stress-Induced Degeneration through the Regulation of Senescence and Mitochondrial Quality Control. The Significance for AMD Pathogenesis', *International journal of molecular sciences*, 19: 2317.
Khadka, Arogya, Jared Iacovelli, and Magali Saint-Geniez. 2015. 'PGC1a rescue retinal pigment epithelial cells from oxidative damage: implication for age-related macular degeneration', *The FASEB Journal*, 29: 148.4.
Kisselev, Alexei F., and Alfred L. Goldberg. 2001. 'Proteasome inhibitors: from research tools to drug candidates', *Chemistry & Biology*, 8: 739-58.
Klaver, C. C., R. C. Wolfs, J. J. Assink, C. M. van Duijn, A. Hofman, and P. T. de Jong. 1998. 'Genetic risk of age-related maculopathy. Population-based familial aggregation study', *Arch Ophthalmol*, 116: 1646-51.
Klein, R. J., C. Zeiss, E. Y. Chew, J. Y. Tsai, R. S. Sackler, C. Haynes, A. K. Henning, J. P. SanGiovanni, S. M. Mane, S. T. Mayne, M. B. Bracken, F. L. Ferris, J. Ott, C. Barnstable, and J. Hoh. 2005. 'Complement factor H polymorphism in age-related macular degeneration', *Science*, 308: 385-9.
Klein, R., M. D. Knudtson, K. J. Cruickshanks, and B. E. Klein. 2008. 'Further observations on the association between smoking and the long-term incidence and progression of age-related macular degeneration: the Beaver Dam Eye Study', *Arch Ophthalmol*, 126: 115-21.
Klos, Andreas, Andrea J. Tenner, Kay-Ole Johswich, Rahasson R. Ager, Edimara S. Reis, and Jörg Köhl. 2009. 'The role of the anaphylatoxins in health and disease', *Molecular immunology*, 46: 2753-66.
Kocur, I., and S. Resnikoff. 2002. 'Visual impairment and blindness in Europe and their prevention', *Br J Ophthalmol*, 86: 716-22.
Kolb, H., R. F. Nelson, P. K. Ahnelt, I. Ortuño-Lizarán, and N. Cuenca. 1995. 'The Architecture of the Human Fovea.' in H. Kolb, E. Fernandez and R. Nelson (eds.), *Webvision: The Organization of the Retina and Visual System* (University of Utah Health Sciences Center

Laine, M., H. Jarva, S. Seitsonen, K. Haapasalo, M. J. Lehtinen, N. Lindeman, D. H. Anderson, P. T. Johnson, I. Järvelä, T. S. Jokiranta, G. S. Hageman, I. Immonen, and S. Meri. 2007. 'Y402H polymorphism of complement factor H affects binding affinity to C-reactive protein', *J Immunol*, 178: 3831-6.

Lambert, V., C. Munaut, A. Noël, F. Frankenne, K. Bajou, R. Gerard, P. Carmeliet, M. P. Defresne, J. M. Foidart, and J. M. Rakic. 2001. 'Influence of plasminogen activator inhibitor type 1 on choroidal neovascularization', *Faseb j*, 15: 1021-7.

Li, Ke, Henrieta Fazekasova, Naiyin Wang, Qi Peng, Steven H. Sacks, Giovanna Lombardi, and Wuding Zhou. 2012. 'Functional modulation of human monocytes derived DCs by anaphylatoxins C3a and C5a', *Immunobiology*, 217: 65-73.

Lian, H., L. Yang, A. Cole, L. Sun, A. C. Chiang, S. W. Fowler, D. J. Shim, J. Rodriguez-Rivera, G. Taglialatela, J. L. Jankowsky, H. C. Lu, and H. Zheng. 2015. 'NFκB-activated astroglial release of complement C3 compromises neuronal morphology and function associated with Alzheimer's disease', *Neuron*, 85: 101-15.

Liszewski, M. K., M. Elvington, H. S. Kulkarni, and J. P. Atkinson. 2017. 'Complement's hidden arsenal: New insights and novel functions inside the cell', *Molecular immunology*, 84: 2-9.

Lueck, K., M. Busch, S. E. Moss, J. Greenwood, M. Kasper, A. Lommatzsch, D. Pauleikhoff, and S. Wasmuth. 2015. 'Complement Stimulates Retinal Pigment Epithelial Cells to Undergo Pro-Inflammatory Changes', *Ophthalmic Res*, 54: 195-203.

Luo, Chang, Mei Chen, and Heping Xu. 2011. 'Complement gene expression and regulation in mouse retina and retinal pigment epithelium/choroid', *Molecular vision*, 17: 1588-97.

Macchioni, L., D. Chiasserini, L. Mezzasoma, M. Davidescu, P. L. Orvietani, K. Fettucciari, L. Salviati, B. Cellini, and I. Bellezza. 2020. 'Crosstalk between Long-Term Sublethal Oxidative Stress and Detrimental Inflammation as Potential Drivers for Age-Related Retinal Degeneration', *Antioxidants (Basel)*, 10.

Makarev, Evgeny, Charles Cantor, Alex Zhavoronkov, Anton Buzdin, Alexander Aliper, and Anotonei Benjamin Csoka. 2014. 'Pathway activation profiling reveals new insights into age-related macular degeneration and provides avenues for therapeutic interventions', *Aging*, 6: 1064-75.

Meri, S., and M. K. Pangburn. 1990. 'Discrimination between activators and nonactivators of the alternative pathway of complement: regulation via a sialic acid/polyanion binding site on factor H', *Proc Natl Acad Sci U S A*, 87: 3982-6.

Merle, B. M. J., J. M. Colijn, A. Cougnard-Grégoire, A. P. M. de Koning-Backus, M. N. Delyfer, J. C. Kiefte-de Jong, M. Meester-Smoor, C. Féart, T. Verzijden, C. Samieri, O. H. Franco, J. F. Korobelnik, C. C. W. Klaver, and C. Delcourt. 2019. 'Mediterranean Diet and Incidence of Advanced

Age-Related Macular Degeneration: The EYE-RISK Consortium', *Ophthalmology*, 126: 381-90.
Mitchell, P., G. Liew, B. Gopinath, and T. Y. Wong. 2018. 'Age-related macular degeneration', *Lancet*, 392: 1147-59.
Mitchell, S., J. Vargas, and A. Hoffmann. 2016. 'Signaling via the NFκB system', *Wiley Interdiscip Rev Syst Biol Med*, 8: 227-41.
Molins, Blanca, Pablo Fuentes-Prior, Alfredo Adán, Rosa Antón, Juan I. Arostegui, Jordi Yagüe, and Andrew D. Dick. 2016. 'Complement factor H binding of monomeric C-reactive protein downregulates proinflammatory activity and is impaired with at risk polymorphic CFH variants', *Scientific Reports*, 6: 22889.
MONSINJON, TIPHAINE, PHILIPPE GASQUE, PHILIPPE CHAN, ALEXANDER ISCHENKO, JENNIFER J. BRADY, and MARC FONTAINE. 2003. 'Regulation by complement C3a and C5a anaphylatoxins of cytokine production in human umbilical vein endothelial cells', *The FASEB Journal*, 17: 1003-14.
Mooijaart, S. P., K. M. Koeijvoets, E. J. Sijbrands, M. R. Daha, and R. G. Westendorp. 2007. 'Complement Factor H polymorphism Y402H associates with inflammation, visual acuity, and cardiovascular mortality in the elderly population at large', *Exp Gerontol*, 42: 1116-22.
Moon, M. R., A. A. Parikh, T. A. Pritts, J. E. Fischer, S. Cottongim, C. Szabo, A. L. Salzman, and P. O. Hasselgren. 1999. 'Complement component C3 production in IL-1beta-stimulated human intestinal epithelial cells is blocked by NF-kappaB inhibitors and by transfection with ser 32/36 mutant IkappaBalpha', *J Surg Res*, 82: 48-55.
Morgan, B. P. 2016. 'The membrane attack complex as an inflammatory trigger', *Immunobiology*, 221: 747-51.
Natarajan, K., S. Singh, T. R. Burke, Jr., D. Grunberger, and B. B. Aggarwal. 1996. 'Caffeic acid phenethyl ester is a potent and specific inhibitor of activation of nuclear transcription factor NF-kappa B', *Proc Natl Acad Sci U S A*, 93: 9090-5.
Nowak, J. Z. 2014. 'AMD--the retinal disease with an unprecised etiopathogenesis: in search of effective therapeutics', *Acta Pol Pharm*, 71: 900-16.
Oeckinghaus, A., M. S. Hayden, and S. Ghosh. 2011. 'Crosstalk in NF-κB signaling pathways', *Nature immunology*, 12: 695-708.
Ogura, S., R. Baldeosingh, I. A. Bhutto, S. P. Kambhampati, D. Scott McLeod, M. M. Edwards, R. Rais, W. Schubert, and G. A. Lutty. 2020. 'A role for mast cells in geographic atrophy', *Faseb j*, 34: 10117-31.
Okubo, A., R. H. Rosa, Jr., C. V. Bunce, R. A. Alexander, J. T. Fan, A. C. Bird, and P. J. Luthert. 1999. 'The relationships of age changes in retinal pigment epithelium and Bruch's membrane', *Invest Ophthalmol Vis Sci*, 40: 443-9.
Paeng, S. H., W. K. Jung, W. S. Park, D. S. Lee, G. Y. Kim, Y. H. Choi, S. K. Seo, W. H. Jang, J. S. Choi, Y. M. Lee, S. Park, and I. W. Choi. 2015. 'Caffeic acid phenethyl ester reduces the secretion of vascular

endothelial growth factor through the inhibition of the ROS, PI3K and HIF-1α signaling pathways in human retinal pigment epithelial cells under hypoxic conditions', *Int J Mol Med*, 35: 1419-26.
Pangburn, M. K., and H. J. Müller-Eberhard. 1983. 'Initiation of the alternative complement pathway due to spontaneous hydrolysis of the thioester of C3', *Ann N Y Acad Sci*, 421: 291-8.
Parente, Raffaella, Simon J. Clark, Antonio Inforzato, and Anthony J. Day. 2017. 'Complement factor H in host defense and immune evasion', *Cellular and Molecular Life Sciences*, 74: 1605-24.
Pauleikhoff, D., C. A. Harper, J. Marshall, and A. C. Bird. 1990. 'Aging changes in Bruch's membrane. A histochemical and morphologic study', *Ophthalmology*, 97: 171-8.
Peng, Q., K. Li, S. H. Sacks, and W. Zhou. 2009. 'The role of anaphylatoxins C3a and C5a in regulating innate and adaptive immune responses', *Inflamm Allergy Drug Targets*, 8: 236-46.
Reichhardt, M. P., and S. Meri. 2018. 'Intracellular complement activation-An alarm raising mechanism?', *Semin Immunol*, 38: 54-62.
Ricklin, Daniel, George Hajishengallis, Kun Yang, and John D. Lambris. 2010. 'Complement: a key system for immune surveillance and homeostasis', *Nature immunology*, 11: 785-97.
Ripoche, J., A. J. Day, T. J. Harris, and R. B. Sim. 1988. 'The complete amino acid sequence of human complement factor H', *The Biochemical journal*, 249: 593-602.
Roskoski, Robert. 2012. 'ERK1/2 MAP kinases: Structure, function, and regulation', *Pharmacological Research*, 66: 105-43.
Rutar, Matt, Riccardo Natoli, R. X. Chia, Krisztina Valter, and Jan M. Provis. 2015. 'Chemokine-mediated inflammation in the degenerating retina is coordinated by Müller cells, activated microglia, and retinal pigment epithelium', *Journal of Neuroinflammation*, 12: 8.
Saddala, Madhu Sudhana, Anton Lennikov, Anthony Mukwaya, and Hu Huang. 2020. 'Transcriptome-Wide Analysis of CXCR5 Deficient Retinal Pigment Epithelial (RPE) Cells Reveals Molecular Signatures of RPE Homeostasis', *Biomedicines*, 8: 147.
Salesse, C. 2017. '[Physiology of the visual retinal signal: From phototransduction to the visual cycle]', *J Fr Ophtalmol*, 40: 239-50.
Sarma, J. V., and P. A. Ward. 2011. 'The complement system', *Cell Tissue Res*, 343: 227-35.
Schmidt, C. Q., A. P. Herbert, D. Kavanagh, C. Gandy, C. J. Fenton, B. S. Blaum, M. Lyon, D. Uhrín, and P. N. Barlow. 2008. 'A new map of glycosaminoglycan and C3b binding sites on factor H', *J Immunol*, 181: 2610-9.
Schraufstatter, I. U., R. G. Discipio, M. Zhao, and S. K. Khaldoyanidi. 2009. 'C3a and C5a are chemotactic factors for human mesenchymal stem cells, which cause prolonged ERK1/2 phosphorylation', *J Immunol*, 182: 3827-36.

Schulze-Osthoff, K., D. Ferrari, K. Riehemann, and S. Wesselborg. 1997. 'Regulation of NF-kappa B activation by MAP kinase cascades', *Immunobiology*, 198: 35-49.

Seddon, Johanna M., Jennifer Cote, Nancy Davis, and Bernard Rosner. 2003. 'Progression of Age-Related Macular Degeneration: Association With Body Mass Index, Waist Circumference, and Waist-Hip Ratio', *Archives of Ophthalmology*, 121: 785-92.

Strauss, O. 2005. 'The retinal pigment epithelium in visual function', *Physiol Rev*, 85: 845-81.

Streilein, J. W. 2003. 'Ocular immune privilege: the eye takes a dim but practical view of immunity and inflammation', *J Leukoc Biol*, 74: 179-85.

Sugita, S., Y. Kawazoe, A. Imai, Y. Usui, Y. Iwakura, K. Isoda, M. Ito, and M. Mochizuki. 2013. 'Mature dendritic cell suppression by IL-1 receptor antagonist on retinal pigment epithelium cells', *Invest Ophthalmol Vis Sci*, 54: 3240-9.

Tak, Paul P., and Gary S. Firestein. 2001. 'NF-κB: a key role in inflammatory diseases', *The Journal of Clinical Investigation*, 107: 7-11.

Thau, L., E. Asuka, and K. Mahajan. 2021. 'Physiology, Opsonization.' in, *StatPearls*

Tóbon-Velasco, J. C., E. Cuevas, and M. A. Torres-Ramos. 2014. 'Receptor for AGEs (RAGE) as mediator of NF-kB pathway activation in neuroinflammation and oxidative stress', *CNS Neurol Disord Drug Targets*, 13: 1615-26.

Tolba, M. F., H. A. Omar, S. S. Azab, A. E. Khalifa, A. B. Abdel-Naim, and S. Z. Abdel-Rahman. 2016. 'Caffeic Acid Phenethyl Ester: A Review of Its Antioxidant Activity, Protective Effects against Ischemia-reperfusion Injury and Drug Adverse Reactions', *Crit Rev Food Sci Nutr*, 56: 2183-90.

Toomey, C. B., L. V. Johnson, and C. Bowes Rickman. 2018. 'Complement factor H in AMD: Bridging genetic associations and pathobiology', *Prog Retin Eye Res*, 62: 38-57.

van Lookeren Campagne, M., J. LeCouter, B. L. Yaspan, and W. Ye. 2014. 'Mechanisms of age-related macular degeneration and therapeutic opportunities', *J Pathol*, 232: 151-64.

van Lookeren Campagne, M., E. C. Strauss, and B. L. Yaspan. 2016. 'Age-related macular degeneration: Complement in action', *Immunobiology*, 221: 733-9.

Vaughan, Douglas E., Rahul Rai, Sadiya S. Khan, Mesut Eren, and Asish K. Ghosh. 2017. 'Plasminogen Activator Inhibitor-1 Is a Marker and a Mediator of Senescence', *Arteriosclerosis, thrombosis, and vascular biology*, 37: 1446-52.

Venkatesha, R. T., E. Berla Thangam, A. K. Zaidi, and H. Ali. 2005. 'Distinct regulation of C3a-induced MCP-1/CCL2 and RANTES/CCL5 production in human mast cells by extracellular signal regulated kinase and PI3 kinase', *Molecular immunology*, 42: 581-7.

Wakatsuki, Yu, Ari Shinojima, Akiyuki Kawamura, and Mitsuko Yuzawa. 2015. "Correlation of Aging and Segmental Choroidal Thickness Measurement using Swept Source Optical Coherence Tomography in Healthy Eyes." In *PloS one*, e0144156.

Walport, Mark J. 2001. 'Complement', *New England Journal of Medicine*, 344: 1058-66.

Wang, Jay Ching Chieh, Sijia Cao, Aikun Wang, Eleanor To, Geoffrey Law, Jiangyuan Gao, Dean Zhang, Jing Z. Cui, and Joanne A. Matsubara. 2015. 'CFH Y402H polymorphism is associated with elevated vitreal GM-CSF and choroidal macrophages in the postmortem human eye', *Molecular vision*, 21: 264-72.

Weismann, D., K. Hartvigsen, N. Lauer, K. L. Bennett, H. P. Scholl, P. Charbel Issa, M. Cano, H. Brandstätter, S. Tsimikas, C. Skerka, G. Superti-Furga, J. T. Handa, P. F. Zipfel, J. L. Witztum, and C. J. Binder. 2011. 'Complement factor H binds malondialdehyde epitopes and protects from oxidative stress', *Nature*, 478: 76-81.

Wong, W. L., X. Su, X. Li, C. M. Cheung, R. Klein, C. Y. Cheng, and T. Y. Wong. 2014. 'Global prevalence of age-related macular degeneration and disease burden projection for 2020 and 2040: a systematic review and meta-analysis', *Lancet Glob Health*, 2: e106-16.

Wu, Jin, You-Qiang Wu, Daniel Ricklin, Bert J. C. Janssen, John D. Lambris, and Piet Gros. 2009. 'Structure of complement fragment C3b-factor H and implications for host protection by complement regulators', *Nature immunology*, 10: 728-33.

Xu, D., J. H. Young, J. M. Krahn, D. Song, K. D. Corbett, W. J. Chazin, L. C. Pedersen, and J. D. Esko. 2013. 'Stable RAGE-heparan sulfate complexes are essential for signal transduction', *ACS Chem Biol*, 8: 1611-20.

Yamada, Yuko, Kazuko Ishibashi, Kazuki Ishibashi, Imran A. Bhutto, Jane Tian, Gerard A. Lutty, and James T. Handa. 2006. 'The expression of advanced glycation endproduct receptors in rpe cells associated with basal deposits in human maculas', *Experimental eye research*, 82: 840-48.

Yang, Ping, James J. Peairs, Ryotaro Tano, and Glenn J. Jaffe. 2006. 'Oxidant-mediated Akt Activation in Human RPE Cells', *Investigative Ophthalmology & Visual Science*, 47: 4598-606.

Yang, Ping, Jillian Tyrrell, Ian Han, and Glenn J. Jaffe. 2009. 'Expression and Modulation of RPE Cell Membrane Complement Regulatory Proteins', *Investigative Ophthalmology & Visual Science*, 50: 3473-81.

Zhou, R., and R. R. Caspi. 2010. 'Ocular immune privilege', *F1000 Biol Rep*, 2.

Zhou, Ti, Yang Hu, Ying Chen, Kevin K. Zhou, Bin Zhang, Guoquan Gao, and Jian-xing Ma. 2010. 'The pathogenic role of the canonical Wnt pathway in age-related macular degeneration', *Investigative Ophthalmology & Visual Science*, 51: 4371-79.

9 Eigenanteilserklärung

EBERHARD KARLS
UNIVERSITÄT
TÜBINGEN

Erklärung zum Eigenanteil der Dissertationsschrift

Die vorliegende Arbeit wurde am Forschungsinstitut für Augenheilkunde (FIA) der Universitäts-Augenklinik am Universitätsklinikum Tübingen unter Betreuung von Prof. Dr. rer. nat. Marius Ueffing durchgeführt.

Die anfängliche Planung und Konzeption der Experimente erfolgte gemeinsam mit Dr. Angela Armento (Betreuerin) und Prof. Dr. Marius Ueffing (Doktorvater). Die Einarbeitung in alle labortechnischen Methoden erfolgte durch Dr. Angela Armento und Dr. Inga Sonntag.

Sämtliche Versuche (wie bspw. die Arbeit in der Zellkultur, Proteinaufbereitung und Western Blot, RNA Aufbereitung und qPCR, Viability und Zytokin Assays) wurden nach der Einarbeitung von mir eigenständig durchgeführt, ebenso die Datenauswertung und -interpretation.

Die statistische Auswertung erfolgte nach einer Beratung durch das Institut für Biometrie eigenständig durch mich.

Ich versichere, das Manuskript selbständig verfasst zu haben und keine weiteren als die von mir angegebenen Quellen verwendet zu haben.

Tübingen, den 10.06.2021

10 Acknowledgement

My sincere thanks to Prof. Dr. Marius Ueffing for providing the subject of this doctoral thesis and the opportunity to do it in his lab. During the entire time, he was always available to offer helpful advice and support and accompanied this project in an excellent and supportive manner.
Special thanks also to Dr. Angela Armento, who supervised me exceptionally well throughout my dissertation and supported me at all times. Thank you for showing me everything in the lab, for teaching me all the methods and for being such a great and highly motivated discussion partner. Without your mentorship and your experience in the field, this work would not have been possible this way!
I am also very thankful to Prof. Dr. Simon Clark for his scientific input and highly constructive feedback on this thesis.
Another big thank you goes to Dr. Inga Sonntag, who, together with Dr. Angela Armento, helped me acquire all the necessary lab skills and always proved to be an encouraging and supportive person to reach out to – thanks a lot!
Many sincere thanks also to Aparna Murali PhD and Dr. med. David Merle for their pleasant company and support during my time in the lab.
A big extra thank you to the whole AG Ueffing for kindly including me into the team and making me feel welcome from day one. Thank you for the great time!
I would also like to thank the Institute for Clinical Epidemiology and Applied Biometry at the University of Tübingen for their consulting advice in the field of statistics.
Finally, I would also like to thank my dear parents and family, who accompanied this doctoral thesis from the idea to completion with their encouragement and support.